AD_____

Award Number: DAMD17-00-1-0277

TITLE: Protease Activated Receptors (PARs) in the Malignant Invasion Process

PRINCIPAL INVESTIGATOR: Rachel Bar-Shavit, Ph.D.
Beatrice Uziely, M.D.

CONTRACTING ORGANIZATION: Hadassah Medical Organization
Jerusalem, Israel 91120

REPORT DATE: June 2002

TYPE OF REPORT: Annual

PREPARED FOR: U.S. Army Medical Research and Materiel Command
Fort Detrick, Maryland 21702-5012

# REPORT DOCUMENTATION PAGE

*Form Approved*
*OMB No. 074-0188*



| 1. AGENCY USE ONLY (Leave blank) | 2. REPORT DATE | 3. REPORT TYPE AND DATES COVERED |
|---|---|---|
| | June 2002 | Annual (1 Jun 2001 - 31 May 2002) |

**4. TITLE AND SUBTITLE**
Protease Activated Receptors (PARs) in the Malignant Invasion Process

**5. FUNDING NUMBERS**
DAMD17-00-1-0277

**6. AUTHOR(S)**
Rachel Bar-Shavit, Ph.D.
Beatrice Uziely, M.D.

**7. PERFORMING ORGANIZATION NAME(S) AND ADDRESS(ES)**
Hadassah Medical Organization
Jerusalem, Israel 91120

**E-Mail:** barshav@md.huji.ac.il

**8. PERFORMING ORGANIZATION REPORT NUMBER**

**9. SPONSORING / MONITORING AGENCY NAME(S) AND ADDRESS(ES)**
U.S. Army Medical Research and Materiel Command
Fort Detrick, Maryland 21702-5012

**10. SPONSORING / MONITORING AGENCY REPORT NUMBER**

**11. SUPPLEMENTARY NOTES**
Report contains color.

**12a. DISTRIBUTION / AVAILABILITY STATEMENT**
Approved for Public Release; Distribution Unlimited

**12b. DISTRIBUTION CODE**

**13. ABSTRACT** *(Maximum 200 Words)*

Protease Activated Receptors (PARs) are G-protein - coupled receptors consisting of four family members, all which are activated via proteolytic cleavage. Our data stems from prior observations indicating that thrombin receptor, PAR1 plays a central role in breast carcinoma invasion and metastasis. The mammary gland provides a powerful tool to study developmental and pathological (breast tumor progression) aspects of the gland. We prepared now mice carrying an MMTV LTR – driven *Par-1* transgenes specifically overexpressed in the mammary glands. Analysis of whole mount glands of virgin *hPar1* +/- mice, showed enhanced complexity of alveolar side branching as compared with normal virgin glands. A striking ductal side branching, budding from preexisting ducts was observed in *hPar1* overexpressing glands of pregnant mice. This phenotype is precociously reminiscent of the effect of several oncogenes in the mouse breast. Syk, a tandem SH2 tyrosine kinase protein widely expressed in hematopoeitic cells has been recently assigned as a potent tumor suppressor gene in human breast carcinoma. We set-out to analyze the interrelation between the breast invasive phenotype and Syk, more specifically, the mutual interactions between *hPar1* and Syk. The recruitment of new blood vessels is a prerequisite for tumor growth and metastasis. While recently it has been shown that PAR1 plays a critical role in endothelial cell embryonic development rescuing *Par 1* -/- mice from bleeding to death - its role in tumor angiogenesis is unknown. We have addressed this issue by applying the Matrigel plug assay and investigated whether *hPar1* can elicit tumor angiogenesis *in vivo*. Our approach involving the combined analyses of tissue specific *hPar1* transgenes, biopsy specimens and established cell lines may help elucidate the involvement of PAR1 in tumor metastasis and angiogenesis.

| 14. SUBJECT TERMS | 15. NUMBER OF PAGES |
|---|---|
| breast cancer, protease activated receptors (PARs), integrins, mammary glands | 117 |
| | 16. PRICE CODE |

| 17. SECURITY CLASSIFICATION OF REPORT | 18. SECURITY CLASSIFICATION OF THIS PAGE | 19. SECURITY CLASSIFICATION OF ABSTRACT | 20. LIMITATION OF ABSTRACT |
|---|---|---|---|
| Unclassified | Unclassified | Unclassified | Unlimited |

# Table of Contents

TITLE:**Protease Activated Receptors (PARs) in the Malignant Invasion Process**

# *Statement of Work*

The critical issue in malignant tumor progression is the turning point for the acquisition of the ability to invade and establish new metastatic colonies throughout the body. We have identified novel molecular targets belonging to the Protease Activated Receptor (PAR) family, and assigned thrombin receptor (PAR1) as a cellular probe with a central role in breast carcinoma invasion and metastasis (*Nature Medicine* 4: 909-914, 1998). Elucidation of the involvement of other PAR family members in malignant carcinoma metstasis may help develop an individually based therapy program according to the specific and spatial profile obtained for each patient. A direct correlation has been established between the levels of PAR1 expression and the invasive properties of various types of carcinomas (i.e., breast, ovary, colon, bladder prostate as also melanoma) both *in vitro* in a collection of cell lines and *in vivo* in biopsy specimens. Furthermore, the criteria of genes that are part of the invasive program are demonstrated in a physiological invasion system of the placenta where PAR1 is exclusively expressed during the time-limited invasion period and completely shuts-off thereafter. Nonetheless, PAR1 has been recently assigned as a novel oncogene based on a screen for cDNAs capable of foci formation and transformation in NIH 3T3 cells. The transforming activity of *Par1* is due to the ectopic overexpression of the receptor rather than an inserted mutation. This, stands in a good agreement with our observations on *Par1* overexpression in breast biopsy specimens and differentially metastatic breast cell lines.

The mammary gland provides a powerful tool to study developmental and pathological (i.e., tumor breast) aspects of the gland. Our major effort is centered around preparing mice carrying an MMTV LTR-driven *Par1* transgenes over expressed directly in the mammary glands. Analysis of the whole mount glands of virgin *hPAR1* +/- mice showed enhanced complexity of the alveolar side branching as compared to normal age-matched wild type mice. A striking ductal side branching, budding from preexisting ducts was observed in *hPar1* +/- pregnant mice as compared to wild type counterparts. This phenotype is precociously reminiscent of the role played by several well described oncogenes in breast tumorigenicity.

One consequence of the mechanism by which the PAR1 is activated is the release of an N-terminal peptide from the receptor - cell surface. Therefore, the mirror image reflection in the body fluids, of the overexpressed, activated PAR1 in carcinoma progression, is the released PAR1 peptide. We have developed means to detect the released activated PAR1 fragment/s. This is intended to be

carried out by immunodetection in body fluids of breast cancer patients via the utilization of monoclonal antibodies raised against the cleaved peptide. The monoclonal antibodies are raised against several discrete and overlapping epitope regions along the released 41 amino acid fragment. Currently, we have developed 3 of the 5 planned monoclonal antibodies for the early detection in body fluids (e.g., plasma and/or urine) of breast cancer patients.

Syk, a tandem SH2 tyrosine kinase protein widely expressed in hematopoeitic cells has been recently assigned as a potent tumor suppressor gene in human breast carcinoma. Analysis of Syk expression levels in either human biopsy specimens or a panel of well established breast cancer cell lines revealed an inverse correlation between Syk expression levels and malignancy. While the loss of Syk seems associated with malignant features such as increased motility and invasion, the role of oncogenic transformation in the regulation of Syk has not been studied. The delicate balance between tumor suppressor gene activation and oncogenic transformation may nonetheless provide a key determinant in the molecular decision leading to the acquisition of progression toward malignancy. Since Syk exerts its tumor suppression activity only *in vivo* in animals or in three-dimensional Matrigel cultures, but not in a plastic 2D culture dish, it is likely that the signals conveyed by the extracellular matrix environment are critical for the activation of Syk. During our studies on the role of *hPar1* in breast carcinoma invasion and metastasis we set-out to analyze the interrelation between the breast invasive phenotype and Syk, more specifically the mutual interactions of *hPar1* and Syk.

The recruitment of new blood vessels is a prerequisite for tumor growth and metastasis. While it has been shown that *Par1* plays a critical role in vascular embryonic development, rescuing *Par1*-/- mice from bleeding to death after re-expression of *Par1* directly in endothelial cells, its role in tumor angiogenesis is unknown. We have demonstrated now that *Par1* gene expression plays a central role in the induction of blood vessel recruitment in animal models *in vivo,* as determined by the "Tet-on" *Par1* inducible prostate system and by the Matrigel micropocket assay. *Par1* induced angiogenesis is mediated via the increased expression of vascular endothelial growth factor splice forms; VEGF121, VEGF145, VEGF165 and VEGF189 or but not VEGF 206. Elucidation of the molecular mechanism of PAR1 in tumor invasion indicates that activation of PAR1; in-fact, induced integrin-mediated adhesion to various extracellular substrata. This takes place, via the "inside-out" signaling and formation of focal adhesion contact sites. We propose, that PAR1 regulate at least in part, the extent and type of the tumor interaction with the extracellular microenvironment by determining specific (yet to be determined) integrin/s activation. Our approach involving the combined analyses of tissue specific over expression of *Par1* transgenes, biopsy specimens and established clones of transfected cell lines (i.e., of full length, antisense or truncated forms) may help elucidate the regulation of PAR1 in tumor metastasis and angiogenesis. PARs family may prove helpful in planning appropriate therapeutic medicaments, a task

which is beyond the scope of the present report. PAR family nonetheless, might be beneficial for future application in gene therapy.

## Originally we have proposed the following specific aims:

**Task 1 a&b: To determine the involvement of PAR family members (PAR1 - PAR4) in breast carcinoma**

- Determine the expression profile of PAR family members (1-4) in breast carcinoma metastasis (5 months)
- *In situ* hybridization analysis in paraffin sections (6-15 months)
- PAR (1-4) expression during normal physiological invasion of the placenta (7-15 month)
- To establish extravillous trophoblast (EVT) cultures for the modulation of the invasive phenotype by PAR family ( 14-18 month)
- Computer analysis and evaluation of the level of *In situ* hybridization analysis (16-18 month)

**Task 2a: To modulate the malignant cell metastatic behavior by PAR1**

- Transfections /selections of the full length PAR1 in non invasive MCF-7 and ZR-75 breast carcinoma cells.
- Tetracyclin (TeT) "on-off" regulation in tissue cultures (19-24 month)
- Animal models for metastasis using the Tet "on-off" PAR1 system. Analysis of the fate of metastatic foci in the presence of PAR1 gene /following activation (25 - 30 month)
- The fate of metastatic foci (i.e for possible regression) upon turning off PAR1 expression (27-36 month)

**Task 2b: To study the molecular mechanism underlying PAR1 invassiveness**

- Characterization of PAR1 transfected clones: The level of PAR1 mRNA and proteins (6-12 month)
- Modulation of the invasive phenotype by PAR1 ( in PAR1 transfected clones)(13-18 month)
- Integrin profile and function in the overexpressing PAR1 clones (19-25 month)
- To elucidate focal adhesion plaque formation and integrin signaling in PAR1 overexpressing clones (26-36 month)
- Chimeras of PAR1 transfection of either the extracellular deficient portion or the cytoplasmic portion, and the assembly of focal adhesion plaque formation (24-36 month)
- ==========

# Body of report & Key research accomplishment

## Introduction

The molecular decision leading to the acquisition of invasive/metastatic potential is a key determinant in tumor progression. A critical event in malignant tumor development is the acquisition of the ability to invade through basement membrane and reemerge from blood vessels to establish new metastatic colonies at distant sites. This task is accomplished via a well orchestrated and sequential actions of enzymes that actively remodel targeted and discrete locations of the basement membrane microenvironment. Proteolytically Activated Receptor 1 (PAR1) plays a central role in the malignant and physiological invasion processes (1, see also Figs. 1-4). The seven transmembrane G-coupled thrombin receptor (PAR1) is the first example of a novel PAR family possessing a unique mode of activation. Members of the family may be viewed as polypeptide receptors that contain their own internal ligand, exposed following proteolytic cleavage (2-4). To date, four such cleavable receptors have been described (5, 6). It is certainly possible that these receptors mediate responses to other proteases or even peptide ligands *in vivo*. Thus the full repertoire of protease signaling through PARs remains to be defined. This family provides a powerful tool to respond towards a wider range of concentrations, possibly for different rates of signaling. Most importantly, it may provide a framework to define the role of distinct PARs in angiogenesis and tumor metastasis.

## Oncogenic properties of *hPar1*

PAR1 has recently been reported as an oncogene, promoting transformation in NIH 3T3 cells. In addition to its potent focus forming activity the constitutive overexpression of PAR1 in NIH-3T3 cells promoted the loss of anchorage - and serum dependent growth. PAR-1 activity was found directly linked to Rho A, an activity which is inhibited by pertussis toxin and is mediated via the Gα13 subunit (7). The oncogenic function of PAR1 is especially significant in light of our observations that PAR1 is over expressed in series of biopsy specimens of breast (1), colon, prostate, ovary carcinomas and melanoma (8, 9) as well as in a collection of differentially metastatic cell lines (1, 8). The oncogenic property of PAR1 may provide further valuable insight highlighting novel mechanisms involved in PAR family and cellular transformation.

## Body of Report

## Molecular basis of PAR1 induced tumor invasion (8)

The molecular mechanism of PAR1 induced tumor invasion and metastasis was next addressed. PAR1 is capable of modulating the invasive behavior of the cells by either conferring metastatic properties of non invasive melanoma cells (as evaluated by formation of metastatic foci, *in vivo* and migration through Matrigel, *in vitro* ) (Figs 6, 7). Alternatively, a marked reduction in the invasion

properties of A375-SM cells, highly metastatic melanoma was observed, following transfection with a PAR1 antisense probe (a plasmid composed of part of the promoter and the start initiation region of the protein; consisting of 462 bp; Fig. 8).

It appears that PAR1 increases the invasive properties of tumor cells primarily by the increased adhesion to extracellular matrix components. This preferential adhesion is accompanied by cytoskeletal reorganization of F-actin stress fibers toward migration favoring morphology. Although a correlation has been made between specific integrins and metastatic behavior *in vivo*, little is known about how the molecular events that regulate tumor cell motility and invasion. The signaling pattern of the major focal adhesion plaque proteins; focal adhesion kinase (pp125 FAK) and paxillin have been analyzed in our stable transfected clones of *Par1*/SB-2 cells. For this, we have performed immunoprecipitation analysis using antibodies directed to FAK and paxillin (Transduction Laboratories, Inc. Lexington KN), detected by anti phosphotyrosine antibodies (4G10, *Upstate Biotechnology Inc*). The assays have been performed in *Par1* expressing stable clones of SB-2 cells, following activation of the receptor either by thrombin or TRAP (thrombin receptor activating peptide). As one can see in Figure 9a, the activation of PAR1 induced markedly the phosphorylation of paxillin and FAK. The characterization of focal adhesion complex (FAC) assembly was carried out in parallel, following the immumo-fluorescent staining with monoclonal antibodies toward FAC proteins, such as: vinculin, paxillin and a polyclonal antibody to pp125FAK. Our data point to the formation of focal adhesion contacts that were observed in all the cell types examined. However, activated PAR1 transfectants exhibited larger and more distinct complexes as detected either by staining of FAK and paxillin (Figure 9c). Integrin levels were detected by using a battery of antibodies directed to $\alpha v\beta 3$, $\alpha 5\beta 1$ and $\alpha v\beta 5$ integrin followed by FITC-labeled second antibodies evaluated by fluorescent activated cell sorter (FACS) analysis to monitor cell surface levels of expression. As shown in Figure 10a, no difference was observed in the non metastatic ligand activated SB-2 or the PAR1 stable transfected cells following activation (Figure 10a).

Adhesive interactions critically influence the organization of the cytoskeleton. Reciprocally, the cytoskeleton affects the organization and function of integrins. This is believed to be one of the means by which soluble growth factor (GF) receptors cooperate with adhesive receptors to synergize and promote cellular response. To further explore the effect of PAR1 activation on cytoskeletal re-organization and focal contact assembly, we have plated cells on glass cover slips and treated them with thrombin or TRAP for various time periods. Cells were then permeabilized, fixed and stained with

FITC-labeled phalloidin to detect filamentous actin (F-actin). Cytoskeletal reorganization were observed soon as 15 minutes after activation. PAR1 transfectants displayed a transition from elongated spindle-like shape to spread, jelly-fish-like structures, followed by the rounding of the cell and the appearance of a ring-like bundle of actin filaments 90 min after activation. These observed changes occurred more rapidly and were more dramatic in PAR1 over-expressing cells as compared to their non-transfected counterparts.

In order to determine which of the integrins participate in the induction of the cytoskeleton signaling events in response to PAR1, we have used immunofluorescent visualization of the cell surface integrins, before and after activation of PAR1. While $\alpha5\beta1$ and $\alpha v\beta3$ are distributed in a diffused manner over the cell surface, $\alpha v\beta5$ (Fig. 10b, D) was localized to distinct sites of focal contacts. However, the detection of $\alpha v\beta5$ within discrete focal contacts occurred only in the activated PAR1 over-expressing cells, but not in the parental cells (Fig. 10b, A), or in the mock transfectants. These data further suggest that $\alpha v\beta5$ integrin is responding to the signals conveyed by activated PAR1, specifically recruited to the focal contact sites and plays a major role during the re-organization of the cytoskeleton. Additional support of the above data comes from reciprocal co-precipitation experiments: $\alpha v\beta5$ and $\alpha v\beta3$ were immuno-precipitated, separately, from lysates of treated or non-treated PAR1 transfectant cells, and the blotted membranes were probed with anti-paxillin mAb. Paxillin was found to co-precipitate with $\alpha v\beta5$ and also with $\alpha v\beta3$ (see reference 8; Appendix). In PAR1 transfectants, the precipitated paxillin level was apparently higher upon receptor activation then in non activated cells and only basal levels were detected in the parental cells, regardless of the cell activation state. However, the detected levels of paxillin co-precipitated with $\alpha v\beta3$ were only basal and were not affected by thrombin activation in any of the cell types. In addition, paxillin and FAK were specifically immuno-precipitated from cell lysates of PAR1 transfectants or parental SB-2 cells. The blotted membrane was probed with anti-$\alpha v\beta5$ mAb. As expected, higher levels of $\beta5$ subunit were detected in PAR1 transfected cells upon activation, as compared to the parental cells (Fig. 11). When anti-$\alpha v\beta3$ was used to probe the same blot, no $\beta3$ subunit was detected (data not shown). These data show that $\alpha v\beta5$ and the typical signaling molecules, paxillin and FAK are in tight association and thus co-precipitate. This association is likely to befall within focal adhesions rather in other cellular compartments. It appears to be labile and to occur in response to PAR1 activation, indicating the presence the $\alpha v\beta5$ integrin within newly assembled focal contacts. These data do not exclude the presence of $\alpha v\beta3$ on the cell surface. However, $\alpha v\beta3$ integrin

probably does not cooperate with PAR1 specific signaling to induce the cellular responses that are described here.

To conclude, our studies propose that activation of PAR1 may lead to a novel cooperation with the αvβ5 integrin, cytoskeletal re-organization and the assembly of FAC formation to promote migration and tumor cell invasion.

## *hPar1* Overexpressing Transgenic Mice: Role in Mammary Gland Morphogenesis

The mouse model provides a powerful system to study mammary gland development. Largely, the functional progression of a mammary gland proceeds in distinct stages that are fundamentally defined by the hormonal status of the animal. At the onset of puberty, about 4 weeks of age, large club shaped terminal end buds (TEB) appear (9) consisting a simple system of branching ducts that begin growing out from the nipple area into a pad of fatty connective tissue that underlies the skin. The ducts then elongate, through a balanced process between proliferation and apoptosis and bifurcate until they reach the edge of the fat pad, in puberty (9, 10). During early pregnancy the mammary gland develops largely under the control of the female reproductive hormones such as; estrogen, progesterone, and prolactin (10). Subsequently with the recurrent estrous cycles the ductal system increases in level of complexity forming a network of ductal side branches that sprout from preexisting ducts. During pregnancy, epithelial growth takes place, involving the extensive proliferation and side branching into a tree of lobualveolar units. The epithelial cells commence into terminal differentiation and begin to secrete milk – at lactation. Finally, during involution the majority of the epithelial network regresses in size through apoptosis and tissue remodeling to a structure that resembles the gland of a nulliparous female. Needless to point out that the mechanism that enables the delicate regulation of factors involved in this complexed morphogenetic events is still poorly understood. The ability to delete or overexpress targeted genes in the mouse genome allowed the identification of genes involved in mammary gland development and assisted in elucidating the molecular mechanism of mammary gland progression. For example, targeted gene deletion (knock out) experiments enabled the dissection of the role of individual hormones in the mammary gland development. Studies on estrogen receptor α (ER α) deleted mice revealed that estrogen is required for ductal outgrowth (11). This role, affecting ductal outgrowth is confined to ER in the stroma but not in the epithelium (12). On the other hand, ductal side branching and alveologenesis, is attributed to

the effect of progesterone. The elucidation of the role of progesterone is complicated by the fact that in the mammary epithelium, synthesis of progesterone receptor (PR) depends on estrogen that is elevated (as also progesterone) during puberty and pregnancy. Both, exogenous administration of estrogen and progesterone to PR-/- inactivated mice, as well as tissue recombination techniques revealed an essential role for progesterone in ductal side-branching (13). While in the absence of PR from the mammary epithelium, ductal side branching fails to occur, it can be overcome by the ectopic expression of the proto-oncogene Wnt-1 (14, 15). Wnts encode a family of secreted glycoproteins that carry short range signals between cells and bind to members of the Frizzled family of seven - transmembrane receptors. A good candidate for side branching was assigned to Wnt-4, weakly expressed in the virgin gland and its expression is increased early in pregnancy (15, 16). The increased Wnt-4 expression during pregnancy was elegantly demonstrated by Brisken et al., suggesting that progesterone signaling is required for the induction of Wnt-4 expression (14). Altogether, five of the ten mouse Wnt genes; Wnt-4, -5a, -5b, -6 and -7b are expressed in the mammary gland (17). While Wnt-4 plays a role in ductal side branching and kidney development (18) the individual roles of other Wnts are yet to be elucidated. Moreover, whether PAR1 plays a role in mammary side branching via wnts needs to be addressed.

During pregnancy, prolactin is essential for the expansion and differentiation of the lobuloalveolar system. After parturition, prolactin acts in synergy with insulin and glucocorticoids, to induce terminal differentiation and milk production. Binding of prolactin to its cognate receptor (PRLR) induces dimerization and results in the recruitment and activation of Janus-2 kinase (Jak-2). This in turn leads to receptor phosphorylation and finally translocation to the nucleus where transcriptional activation of targeted genes, including those encoding several milk proteins - takes place (19). Targeted disruption of genes in prolactin signaling pathway has highlighted prolactin importance in mammopoiesis and lactogenesis. Prolactin deficient mice exhibit curtailed ductal branching with the arrest of mammary organogenesis at puberty (19). Likewise, PRLR $^{+/-}$ females exhibit impaired differentiation of lobualveolar units and an inability to lactate (20, 21).

We have prepared transgenic mice carrying an MMTV-LTR driven *hPar1*, specifically over expressed in the mammary glands (Figs. 12, 13). The full length *hPar1* (1.4 kb) was inserted between Hind III and EcoR1 immediately following the MMTV promoter (Fig. 15). A *hPar1* containing fragment was next digested using HgaI and EcoR1 to generate the appropriate DNA fragment for

injection. DNA injected to the fertile eggs was inserted into 11 C57Bl/CB6/F1 mothers. Of these, 60 pups were obtained and screened for *hPar1* by analyzing the genomic DNA isolated from tails and by PCR. Six mice were found positive and termed Fo - founders. Following mating with wild type control mice, 76 additional pups were obtained, of which 11 were found positive (as evaluated by both PCR and southern blot analysis). These heterozygus mice -/+ were mated ($F_o + F_1$) resulting with additional 55 pups. We currently are heavily involved in testing and characterizing *hPar1* homozygous +/+ mice, as determined by southern blot analysis (see Fig. 16). When different organs of the mouse were tested by RT-PCR for the expression of *hPar1* indeed, the only positive expression was obtained in the mammary glands but none in other organs such as; ovary, brain, colon, heart, kidney, lung, spleen, salivary gland or liver (see Fig, 17). Whole - mount histological evaluation of the growing branch ends showed smaller buds and represented a higher level of ductal complexity in the virgin *hPar 1*+/- overexpressing mice, especially highlighted in the pregnant *hPar 1*+/- mice. These mammary glands exhibited grossly hyperplastic features as compared with the non transgenic littermates (Fig. 14). *In situ* hybridization analysis on sections of virgin mammary glands and during early pregnancy, showed high and abundant levels of *hPar1* at the luminal phase of the mammary epithelium (Fig. 15, I& II). Likewise, quantitative analysis of RT-PCR showed high levels of *hPar1* expression at 5, 8 and 13 weeks of virgin *hPar1*+/- as also elevated *hPar1* levels in pregnant mice (P4d, P8d, P12d).

Since Wnt-4 has been recently assigned (15) as a major candidate playing a role in ductal side branching of the mouse mammary gland, we wondered whether in *hPar1* transgenic mice the enhanced ductal side branching is mediated via Wnts. To address this issue we have analyzed the expression levels of mouse Wnts during normal mammary gland development as compared to *h Par1*+/- (or *hPar1*+/+ once we establish a homozygous line of mice). The levels in virgin mice is compared to the expression during pregnancy, post partum and after weaning. The wnts tested included the family members: wnt 4 wnt 5a, Wnt 5b, Wnt 6, Wnt 7a and Wnt 7b.

Our preliminary data indicate that in the *hPar*+/- overexpressing glands, Wnt-4 expression is induced markedly as compared to normal mice, demonstrated by RT-PCR (especially at 5 &13W virgin and during pregnancy P4d, P8d & P12d). Immunohistochemical staining showed a high level of staining in the epithelial compartment of *hPar1*+/- essentially at 13W virgin mice, P4d and P8d mice (Figs. 16&17 ) as compared to the localization and expression of *h Par* 1+/- in the mammary glands during this time-period. No such effect was observed when Wnt 5a - 5b, -6 or –7a were analyzed as

shown by RT-PCR (Fig. 16). Wnt 7b however, showed induced expression in pregnancy (at day 4 and 8 but not at day 12) and in the virgin at 5 and 13 weeks as compared with normal age-matched mice (Fig. 16). Mammary gland morphogenesis proceeds in distinct steps, beginning with a fetal mammary analge that undergoes ductal elongation and branching (22). Early to mid-pregnancy the expression of β-casein, the major milk protein is synthesized. Indeed, when total RNA was extracted from the *hPar1* +/- mammary glands at various time points along the mammary development of virgin and pregnant mice, enhanced β-casein synthesis was observed early in pregnancy of *hPar1*+/- transgenic mice as compared to wild type, and levels-off thereafter (Fig. 18).

Next we have addressed the possibility whether *hPar1* +/- overexpression in the mammary gland induces (in addition to ductal side branching) also alveologenesis (i.e., proliferation in the lobulo-alveolar structures). The prospect of higher ductal network complexity as a result of enhanced alveoli proliferation rate or alternatively an inhibited apoptois process – was examined. To address this issue, the status of epithelial proliferation was assessed in situ by immunostaining using antibodies to the "proliferating cell nuclear antigen" (PCNA). TUNEL assay was employed for the evaluation of apoptosis. The proliferation index is defined rather as the number of PCNA – positive nuclei of alveolar epithelial cells per total nuclei. Our data show that indeed, the proliferation of alveolar bud epithelium was significantly enhanced in *hPar1*+/- overexpressing mice as compared to wild type counterparts. Enhanced PCNA activity was observed at 5W *hPar1*+/- mice, declined at weeks 8 and 10 and was induced back again at 13W virgin mice. In contrast to alveolar epithelium, the proliferation of the ductal epithelium was comparable between the *hPar1*+/- and wild type age matched counterpart. During pregnancy, although active on-going alveoli proliferation takes place in *w.t.* mice a higher, enhanced PCNA staining is observed at *hPar1*+/- mice along pregnancy (at P4d, P8d and P12d; see Fig. 19). On the other hand, low basal apoptosis levels were obtained and there was no significant differences in apoptosis rates, measured by TUNEL assay (data not shown). Overall, we conclude that *hPar1*+/- transgenic mammary glands exhibit enhanced alveoli proliferation as also ductal side branching, ultimately leading to a higher ductal network complexity.

The TNF receptor family RANK ( receptor activator of NFκB) is activated by its ligand RANKL, and plays an important role in bone remodeling, inducing differentiation and activation of osteoclasts, and hence the morphogenesis of bone matrix. Surprisingly, it has been recently demonstrated that RANK plays a significant role in mammary gland development involving mainly in

the survival and proliferation of the alveolar epithelial cells. Mice lacking RANKL or its receptor RANK fail to form lobulo-alveolar mammary structures during pregnancy and resulting in death of the newborns (23). Since *hPar1*+/- mice show enhanced alveoli proliferation we have evaluated the levels of RANK and RANKL in our *hPar1*+/- transgenic mammary glands as an additional indicator for lobulo-alveolar proliferation index. RT-PCR (Fig. 18) as well as Northern blot analysis (data not shown) revealed that RANK levels were induced in *hPar1*+/- mammary glands especially at 18days of pregnancy and during lactation, as compared to the wild type age matched counter parts. These data support and strengthen our observations that *hPar1* overexpressing mice in addition to ductal side branching, are involved in lobulo-alveolar proliferation and the enhanced expression of RANK and RANKL. Collectively, these data provide additional support for the involvement of *hPar1* in mammary gland hyperplasia and oncogenesis. *hPar1* thus, joins the list of novel oncogenes with a similar effect, inducing the mammary gland network complexity.

## Pattern of expression and tissue localization of Syk; a tumor suppressor gene - in normal mammary gland development

Analysis of Syk expression levels in either human biopsy specimens or a panel of well established breast cancer cell lines revealed an inverse correlation between Syk expression and malignancy (24-27). However, the pattern of Syk expression during normal mammary gland development has not been addressed. We have performed immunohistostaining analysis on paraffin embedded sections of mammary gland sections during different developmental age. Surprisingly, Syk expression was high and abundant in the mammary gland epithelial cells of 5 weeks virgin mice. Syk expression declined dramatically thereafter at weeks 8 and 10 with little or nearly no Syk expression (Fig. 20 ) and was induced back again at week 13 virgin mice as also during pregnancy (Pday4 and Pday14; Fig. 20). It appears that Syk expression levels during the normal mammary gland development mimics the pattern obtained for PCNA staining in *w.t.* mice as an index for mammary gland alveoli - proliferation. This pattern of Syk expression was re-affirmed by RT-PCR and immunoblot analysis (data not shown). What is the role of Syk during normal mammary gland development remains yet fully to be determined.

# Regulation of Syk, a tumor suppressor gene during breast cancer oncogenic transformation: Modulated expression and means of activation by *hPar1*

Syk, a tandem SH2 tyrosine kinase protein widely expressed in hematopoeitic cells (24) has been recently assigned as a potent tumor suppressor gene in human breast carcinomas (25-27). Analysis of Syk expression levels in either human biopsy specimens or a panel of well established breast cancer cell lines revealed an inverse correlation between Syk expression levels and malignancy. High expression levels are detected in the normal mammary gland tissues as well as in nearly normal and benign cell lines. No Syk expression was detected in the invasive pathological breast tissue specimens and the highly metastatic cell lines (25). Oncogenic transformation of breast epithelial cells provides a powerful system to study the molecular mechanism and signal transduction pathways involving malignant breast cancer progression. These may include Ras and Src; which are signaling oncogenes or *Par1* (*Protease Activated Receptor*-1) a membrane associated G-protein coupled receptor. The full length thrombin-receptor; PAR1, has been recently assigned as an oncogene based on a screen for cDNAs whose expression causes foci formation in NIH3T3 cells. The transforming activity of *Par1* seems to be due to the ectopic overexpression of the receptor rather than to an activating mutation although, *Par1* mutant (that could not be cleaved by thrombin) was impaired in its transforming activity insinuating that *hPar1* signaling events are essential (28).

While the loss of Syk seems associated with malignant features such as increased motility and invasion, the role of oncogenic transformation in the fate of Syk expression and activation has not been studied. The delicate balance between tumor suppressor gene activation and oncogenic transformation may nonetheless provide a key determinant in the molecular decision leading to the acquisition of progression toward malignancy. The loss of Syk, however, is only one determinant in the multistep process of breast tumor development. Expression of Syk on the other hand, is not sufficient for its full biological response. Since Syk exerts its tumor suppression activity only *in vivo* in animals or in three-dimensional Matrigel cultures, but not on a plastic 2D culture dish, it is likely that the signals conveyed by the extracellular matrix environment are critical for the activation of Syk. During our studies on the role of *hPar1* in breast carcinoma invasion and metastasis we set-out to analyze the interrelation between the breast invasive phenotype and Syk; more specifically the mutual interactions of *hPar1* and Syk.

Human mammary epithelial cells form acini-like structures containing a single layer of polarized, growth - arrested cells when grown within a Matrigel environment; (matrix rich in collagen type IV and laminin derived from the Englebreth-Holm Swarm; EHS tumor) (29). The epithelial cells within the acini in cultures as also *in vivo* deposit collagen type IV and secrete sialomucin in their basal and apical surfaces, respectively. They also have a typical apico-basal distribution of polarity markers such as ZO-1, E-cadherin and $\alpha 6\beta 4$ integrins. These indicate that the acinar structures formed in culture closely mimic the acini in the adult breast. Three-dimensional acinar structures were generated by plating MCF-10A cells on an exogenous basement membrane matrix (Matrigel). After 10-12 days in culture, each cell formed an acinus containing 20-40 cells (Fig. 21). Confocal immunofluorescence analyses of acini labelled with 4', 6-diamidino-2-phenylinidole (DAPI) revealed that the acinar units had basally localized nuclei and a hollow lumen. Immunostaining for basal surface markers such as collgen type IV (data not shown) and cell-cell junction markers as β-catenin and E-cadherin (Fig. 21), indicated that the acinar structures consisted of polarized epithelial cells (30). In contrast, these cells exhibited highly invasive phenotype of disorganized intrusion structures (Fig. 22a), when infected with an adeno virus carrying activated Ras oncogene V12Ras, or when an invasive breast cancer cells highly expressing *hPar1* were plated, under similar conditions.

One of the major candidates playing a central role in the migratory invasive phenotype of the cells - is Focal Adhesion Kinase (FAK). FAK is known to enhance cell migration through focal adhesion turnover because fibroblasts from FAK - deficient mice exhibit markedly reduced cell migration and large focal adhesions (31). It has been also documented that overexpression of FRNK (FAK Related Non Kinase fragment), a C-terminus fragment representing FAK, with dominant negative properties in endothelial or chicken embryo cells, respectively, reduced cell migration and proliferation (32, 33). When we have transfected FRNK (in a pcDNA3.1 plasmid, kindly provided by Dr. David Schlaepefer, The Scripps La Jolla, CA) to the cells that express high *hPar1* levels, the following properties were observed. Cells transfected with FRNK showed good expression levels as indicated by an HA-tag FRNK antibodies. Furthermore, when the phosphorylation levels of FAK were analyzed, as compared to non transfected parental cells, a dose dependent inhibition was observed at a concentration that correlated with the expression levels of FRNK (Fig. 22 b, c). When the FRNK transfected cells were then plated on a Matrigel 3D cultures, and the morphogenesis of these cells were compared to the parental highly invasive cells - a nearly well organized spheroids structures were obtained (Fig. 22a,

bottom panel). This however, was not the case when highly invasive *hPar1* expressing cells were plated on Matrigel, showing a typical invasive phenotype.

These preliminary observations indicate that *hPar1* invasive phenotype can be abrogated when a dominant negative form of FAK; FRNK is overexpressed. Altogether these data provide additional support to our previous studies demonstrating that part of the molecular mechanism of *hPar1* invasiveness is mediated via integrin activation and formation of focal adhesion contact sites (1, 8).

As mentioned above, when we have screened a set of differentially invasive breast cancer cell lines for the levels of Syk expression-high levels of Syk were observed in MCF-7 breast carcinoma cells or in the nearly normal fibrocystic MCF10A cells. No Syk expression however, was observed when clones of MCF7 cells stabley expressing a full length of *hPar1*, MCF10A expressing V12Ras or the highly invasive cell line MDA 435 were analyzed (Fig. 23b). It appears therefore, that the loss of Syk, a tumor suppressor gene takes place, as part of the invasive properties of breast cancer cells. What are the molecular mechanisms involved in the silencing of SYK gene during invasion is of interest. Is it mediated via hypermethylation in the Syk promoter as reported for the highly invasive MDA 435 breast carcinoma cells (26). In this regard we are currently studying whether *hPar1* overexpression leads to a similar hypermethylation of SYK promoter.

While exploring the role of Syk in breast cancer invasion and metastasis we introduced Syk to the highly invasive, high *hPar1* expressing cells (3TB breast carcinoma). This was carried out by infection with the Syk virus that was prepared by the cloning of Syk into a viral vector pLHCX (the Moloney Murine leukemia virus, MoMuLV) and following the appropriate packaging in adequate cells (293-GPG cells)(studies in collaboration with J.S. Brugge, Dept. of Cell Biology, Harvard Medical School, Boston , MA ). These cells when plated in a Matrigel environment mimicking the 3D cultures, exhibited distinct circular phenotype following activation of PAR1. This was not the case in Syk-3TB cells prior to PAR1 activation, exhibiting still an invading phenotype (Fig. 24a). Thus, it is not sufficient to merely overexpress Syk but in-fact, an activation step is essential in order to manifest Syk tumor suppressor effect and the rounded appearance of the cells ( Fig. 24a). Intriguingly this was not the case when parental 3TB breast carcinoma cells were plated under similar conditions. 3TB cells expressing high *hPar1* exhibited a typical invasive phenotype, regardless of PAR1 activation. The "suppression" phenotype obtained following PAR1 activation in Syk-3TB cells, was markedly obtained over a range of a dose dependent concentrations for PAR1 activation (Fig. 24) and in a period of 2-3

days. Concomitantly, we have found that PAR1 activation induced the phosphorylation levels of Syk, reaching maximal stimulation after 30 min and declining by 1 h (Fig. 25). Next, we have examined the signaling pathways in Syk-3TB cells as compared with parental 3TB cells (expressing high levels of *hPar1*).

C Jun N-terminal kinases (JNKs) are members of the MAPK family that are activated in response to growth factors, cellular stresses and other stimuli such as UV irradiation and changes in osmolity (34). Substrates for activated JNK include several transcription factors, among of which are : c-Jun, ATF2 and Elk1. JNK phosphorylates a specific domain within each of these molecules and thereby increasing their transcriptional activity. Ample evidence support a pivotal role for GTP-binding proteins in inhibiting the activation of MAPK pathways. In particular, Rac and Cdc42 which belong to the Rho family of small GTPases, and have been shown to lie upstream of the JNK cascades (5, 36). The topology of the signaling path leading to the activation of these GTPases has remained yet elusive. JNK can be activated also via Crk, an adaptor protein consisting of SH2 and SH3 domains. Interestingly, Cas130 a downstream signaling protein following integrin activation which gets phosphorylated after integrin ligation- appears to be a major binding protein of SH2-Crk (37). Thus, Crk may connect additional signaling pathways to the traditional Rac-JNK pathway within a cell (38).

Activation of PAR1 led to JNK1 phosphorylation, maximal phosphorylation levels were obtained 15' following activation, declined gradually thereafter (and reached basal levels after 1h stimulation) (see Fig. 26a). Syk-3TB cells however, when activated in a similar manner were unable to phosphorylate JNK over the same time-period. This result point to the possibility that upon activation of PAR1, Syk conveys an inhibitory effect resulting with abrogation of downstream of JNK phosphorylation. In parallel, when we have analyzed the phosphorylation pattern of cCbl, an immediate substrate of the Syk/ZAP-70 kinases, a dose dependent phosphorylation was observed in the Syk-3TB but not in the 3TB cells (that lack Syk) following PAR1 activation (Fig. 26b). cCbl has been shown to be associated with large number of signaling molecule among of which are: Src, Fyn, Lyn, Syk ZAP-70 and PI3K. It is conceivable that activation of Syk by PAR1 leads to sequential recruitment of molecules ultimately resulting with JNK inhibition downstream. We tentatively suggest, that Syk inhibition of JNK phosphorylation, led to the "suppression phenotype" in 3 D cultures giving rise to a rounded appearing cells, following PAR1 activation.

Due to the distinct biological phenomenon observed in Syk containing cells following PAR1 activation, we have next examined the possibility that PAR1 directly interacts with Syk. For this we have prepared immuno-complexes containing PAR1 and analyzed the expression levels of Syk. We have found that in Syk containing cells, abundant levels of PAR1 were found co-immunoprecipitated. This was carried out by IP of PAR1 and detection of Syk in the immuno complexes obtained (Fig. 27a). The same was true also vise versa, when Syk was first immunoprecipitated, PAR1 levels were found present within the immuno – complexes (data not shown). Thus, we conclude that Syk and PAR1 co-immunoprecipitate as a result of protein – protein associations (Fig. 27a). When a truncated form of PAR1 devoid of the entire cytoplasmic tail used for immunocomplex analysis-no Co-IP of syk and hPAR1 were detected. In parallel, we have prepared GST-C-tail of PAR1, containing Serine (S) 369 /N-terminus and up to residue 425 (T) / COOH. The C-tail was prepared using RT-PCR ( 5' TACTATTACGCTGGATCCTCTGAG-3' and 5' CTGAATTCCTAAGTTAACAGCTT-3'). The DNA fragment obtained was further cut with the appropriate restriction enzymes (BamH1 and EcoR1) and ligated into pGEX2T vector (see scheme). The GST-C-tail was separated on a SDS-gel, indicating that the fusion protein of the C-tail was adequately prepared. Next we have prepared various cell lysates and applied them onto the GST-PAR1 - C-tail in order to determine a specific possible binding protein. The specifically eluted material showed clearly that in lysates of Syk-3T3 cells - Syk was bound to the PAR1 C-tail but not when a control GST- beads were used as a binding column ( Fig. 27c ). No specific proteins were bound when lysates of 3T3 cells were applied under similar conditions (Fig. 27c). When a GST - C-tail of PAR1 was digested and cleaved from the GST beads (for the purpose of possible competition analysis during the Co-IP experiments between PAR1 and Syk), a marked inhibition of Syk levels observed. These results further substantiated and strengthened the basic assumption that Syk and PAR1 are physically co- associated (Fig. 27b). We are currently analyzing whether the N-terminal SH2 or the tandem SH2 domains of Syk are involved directly in the binding to PAR1 cytoplasmic portion. We are also preparing deletion regions of PAR1 cytoplasmic tail in order to determine the minimal size necessary for this direct association between PAR1 and Syk. We plan to insert mutants in specific selected residues of PAR1 cytoplasmic tail, in order to establish the critical amino acids involved in Syk binding. In leukocytes , Syk is activated by binding to diphosphorylated immune receptor tyrosine-based activation motifs (pITAMs) (39). Syk also has been recently demonstrated to directly interact with the C-terminal portion of integrin β3 cytoplasmic tail (40). The possibility that Syk interacts directly with the cytoplasmic region of PAR1 is nonetheless interesting and intriguing. It

may implicate that PAR1, a G-coupled receptor is capable of recruiting Syk kinase to couple tyrosine induced pathways, for a protective tumor suppressing outcome.

## *hParl* and Tumor angiogenesis.

The formation of new blood vessels (vasculogenesis and angiogenesis) is generally low in the adult organism, yet essential during embryonic development, wound healing and the normal cyclical changes that occur in the female reproductive tract. Angiogenesis is a prerequisite for tumor growth and metastasis (41, 42). In-fact, tumor angiogenesis is viewed as a consequence of activation of an angiogenic switch, which allows, based on genetic alterations, the ability to recruit blood vessels from neighboring tissues (43). Tumors are limited in size, and cannot exceed beyond a few cubic millimeters without the innermost cells undergoing necrosis (42). Targeting selective anti tumor vasculature therapies is based on the notion that inhibiting the ongoing tumor neovascularization will be without affecting much the host circulatory system, generally quiescent in nature. Ongoing neovascularization and constant remodeling of the tumor vessels may account for the fact that at any given time, along the tumor growth, a significant fraction of the tumor vessel is poorly structured and represents immaturity. This may account for the lack or incomplete periendothelial, smooth-muscle coating of the vessel that lag behind the initial formation of the endothelial network. VEGF has emerged as the most commonly upregulated angiogenic factor in tumors, as well as its established relevance in embryonic and physiological angiogenesis, rendering the molecule a prime target for antiangiogenic therapy. VEGF exerts its activity by binding to its tyrosine kinase receptors Flt-1 and Flk1/KDR and to the auxiliary receptor neuropilin (44). VEGF also function as a survival factor for the immature blood vessels. These vessels become VEGF independent once they recruit periendothelial cells and undergo maturation. Consequently, a newly formed vascular network will regress if VEGF is prematurely withdrawn. VEGF deprivation may thus lead not only to inhibition of further angiogenesis, but also to regression of preformed tumor vessels (45).

While recently (46) it has been shown that PAR1 plays a critical role in endothelial cell embryonic development rescuing *Par 1* -/- mice from bleeding to death - its function in tumor angiogenesis is unknown. It was unclear whether bleeding in embryos lacking *Par1*, tissue factor as well as other coagulation factors result from impaired hemostasis or damaged blood vessel formation. Griffin et al, (46) provided elegant evidence highlighting the loss of PAR1 that in-fact, does not prevent vessel formation but rather impairs stabilization and maturation of the newly forming vessels, thereby causing

abnormal fragility and ruptures in the vessel wall (46, 47). By initiating PAR1 signaling in endothelial cells, Griffin et al, were able to rescue *Par1* deficient mouse embryos from bleeding to death. These demonstrate that activation of PAR1 and its signaling pathway in endothelial cells is essential for vascular integrity. There are similarities shared between the phenotype of several coagulation factor knock out embryos (i.e., factor V-/-, tissue factor -/- and prothrombin -/-) and *Par1*-/- embryos. Most of them die at midgestation with yolk sac defects and continuous bleeding (48-51). These suggest that tissue factor might contribute either to blood vessel development or hemostasis via its ability to initiate the coagulation cascade in the embryo.

Our studies indicate that *Par1* gene expression plays a central role in the induction of blood vessel recruitment in animal models *in vivo,* as determined by the "Tet-on" *Par1* inducible prostate system and by the Matrigel micropocket assay. *Par1* induced angiogenesis is mediated via the increased expression of vascular endothelial growth factor splice forms; VEGF121, VEGF145, VEGF165 and VEGF189 or but not VEGF 206. Activation of PAR1 induces markedly the expression levels of functional VEGFs as determined by Northern blot analysis, endothelial tube alignment in a 3 dimensional collagen gel, as well as bovine aortic endothelial cell proliferation *in vitro*. Since neutralizing anti VEGF antibodies potently inhibited *Par1* induced endothelial cell proliferation, we conclude that functional VEGF expression and secretion is at least partly regulated by *Par1*. The *Par1* induced VEGF expression is inhibited by specific PKC, Src and PI3K inhibitors (i.e., Calphostin C, PP-2 and Wortmanin, respectively), suggesting the participation of these signaling enzymes in the process. In parralel, we show that oncogenic transformation of genes shown to be part of PAR1 signaling machinery - is sufficient to increase VEGF expression. While NIH3T3 cells do not express VEGF, transfection of the cells with the activated forms of either *src* or *vav* results in a marked increase in the expression of VEGF. On the other hand, only a slight increase in VEGF isoform expression is observed when the cells are transfected with *ras* and the non - transforming proto-oncogene *vav* transfected cells and very little or none in the SH2 mutants of the *vav* oncogene transfected cells. Altogether we show here, the *in vivo* induction of *Par1* tumor angiogenesis by the use of either *Par1* transfected Matrigel plug assay or the "Tet-on" *Par1* inducible system. This process is mediated by the induction of four VEGF splice forms. We provide herewith additional evidence supporting the novel notion that initiation of cell signaling either by activating PAR1 or in the presence of activated forms of *ras, src* and *vav* is sufficient to induce VEGF and hence angiogenesis.

## PAR1 promotes tumor angiogenesis *in vivo*

For this, we have applied Matrigel plug assay to evaluate whether *Par1* can recruit blood vessels *in vivo*. Stable *Par1* transfected, non metastatic SB-2 melnaoma cells were mixed at $4^0$C with Matrigel (reconstituted basement membrane (BM) preparation extracted from EHS mouse sarcoma) and injected *s.c.* into BALB/c mice. Similarly treated mock-transfected SB-2 cells expressing no *Par1* served as control. Upon injection, the liquid Matrigel rapidly formed a solid gel plug that served not only as an inert vehicle for PAR1 producing cells, but in-fact maintained the natural interactions existing between tumor cells and the surrounding extracellular matrix (ECM). As shown in Fig. 28 a pronounced angiogenic response was induced by Matrigel embedded over expressing *Par1* cells as compared with little or no neovascularization exerted by the mock- transfected cells expressing no *Par1*. The angiogenic response was reflected by a network of capillary blood vessels attracted toward the Matrigel plug containing *Par1* overexpressing cells while very little or no vascular response was obtained by the control mock- transfected SB-2 cells. Highly pronounced blood vessel recruitment was observed especially in the Matrigel embedded with cells that were initially PAR1 activated, prior to mixing with the Matrigel liquid pellet (Fig. 28, I). The differential amount of blood vessels obtained is shown in sections of the Matrigel plug stained for collagen (Mallory's staining), allowing the evaluation blood vessels (red) in different areas per section. A striking difference is obtained in activated PAR1 transfected cells as compared to non transfected or mock-transfected activated cells (Fig. 28, II). Evaluation of the blood vessels, as counted in each Matrigel section and following the various treatments is demonstrated (Fig. 28, III).

## Inducible *Par1* expression in rat prostatic carcinoma increases tumor mass and angiogenesis.

Differential expression of *Par1* in the Dunning rat prostate carcinoma cell variants was observed by RT-PCR. Low levels of *Par*1 in AT2.1 and high levels in AT3.1 (Fig. 29 I, A) which is more motile and tumorigenic than AT2.1 (52). In order to establish the exclusive effect of *Par1* expression on prostate tumor progression, AT2.1 cells were transfected with human *Par1* cDNA under the control of a tetracyclin-inducible promoter (Fig. 29II). Two highly inducible clones, AT2.1/Tet-On/ *h*PAR1 clones 4 and 10, were isolated, in which *h*PAR1 expression was strongly induced by a tetracycline analog Doxorubicyn (Dox) as determined by Northern blot analysis. PAR1 expression was nearly non detectable in the absence of Dox. Upon the addition of Dox the levels of the 4.1 kb *Par1* mRNA were increased substantially (Fig. 29 II, D &F). AT2.1 cells, mock transfected with the pTet-On vector but

without PAR1, did not express any detectable *Par1* levels either in the presence (Fig. 29 II, lane B) or in the absence of Dox (Fig. 29 II, lane A). The optimal dose of Dox necessary to induce PAR1 expression was 1-2 μg/ml (not shown). *Par1* mRNA could be detected as early as 4-6 h, and reached maximum levels at 20-24 h after Dox treatment (not shown). When AT2.1/Tet-On/*h*PAR1 clone 4 cells and mock transfected cells were injected s.c. into rats and fed Dox in their drinking water (over 2 weeks period) – a marked tumor growth was visualized. As one can note, (Fig. 29 III) in the absence of Dox, AT2.1 clone 4 tumors grew to a tumor mass of 0.35 gr. Once PAR1 expression was induced by Dox, the tumor mass increased to an estimated ~ 1.35gr a 3.8 fold increase. On the other hand, mock transfected tumor cells grew to a tumor size of 0.55gr as compared to AT2.1 non transfected cells of (0.35 gr) regardless whether the animals were fed Dox or not (Fig. 29, IV). This demonstrates that Dox in itself has no significant effect on tumor growth *in vivo*. AT2.1/Tet-On/*h*PAR1 cells following Dox treatment resulted also in a highly reddish appearing tumors (Fig. 29 III, A) as compared to a pale looking one in the absence of Dox (29 III, B). We conclude therefore, that the regulated induction of *Par1* gene enhanced markedly two critical determinants in tumor progression; tumor size and angiogenesis.

## *hPar1* expressing cells induce functional VEGF

Next we analyzed the expression levels of VEGF in stable *Par1* transfected melanoma cells. While non expressing *Par1* cells did not show any VEGF expression, stable transfectants overexpressing *Par1* exhibited distinct induction in VEGF 165 levels as obtained by Northern blot analysis (Fig. 30I). Parental SB-2 or mock transfected cells (30I, A&B respectively) showed no detectable levels of VEGF, as compared with *Par1* transfected clones (Clone 13 and Mix L) showing substantial increase in VEGF165 levels ( Fig. 30 I, respectively). Activation of PAR1 either by thrombin or TRAP elicited a higher level of VEGF as compared with non transfected *Par1* and a house keeping gene - β-actin (Fig. 30II). Maximal induction was obtained 8 hrs following treatment by TRAP (Fig. 30b, lane G), at a concentration of 100 and 50 nM which was reduced markedly thereafter (Fig. 24III, lanes B-F). Similar pattern was obtained also for VEGF 145 but not for VEGF 189 (slightly expressed only after PAR1 activation for 8h) as detected by Northern blot analysis (Fig. 30II). In-fact, by the use of primers designed to the start site of the gene (exon 1) and to the gene end point ( exon 8), we could detect by RT-PCR the different splice forms induced by *Par1*. As one can note, *Par1* induced markedly VEGF 121, VEGF 145 , VEGF 165, very little of VEGF 189 and none of VEGF 206. No VEGF isoforms were detected in either the absence of *Par1* (SB-2), mock transfectants (SB-2 vector) or non

metastatic cells (MCF7) (Fig. 30IV). Activation of PAR1 (TRAP, 8h) increased substantially also the level of VEGF 189, similar to the pattern obtained in the highly metastatic cells (MDA 435). Next, we wondered whether the induced VEGF mRNA levels by *Par1* gene leads to a functionally active VEGF protein. For this purpose we have collected conditioned medium of *Par*1 transfected cells either prior or following PAR1 activation, as well as mock transfected and non transfected cells. Endothelial tube forming assay, embedded in a 3 dimensional collagen (type I) mesh was then performed and the extent of tube forming network was evaluated following the application of the variably treated conditioned medium. While low activity of vascular branching is obtained in non treated control conditioned medium (Fig. 31 I A-C) a more complex appearing network was obtained following *Par1* expressing cell conditioned medium and activated PAR1 conditioned medium ( Fig. 31 I, D-F)). Concomitantly, the rate of bovine aortic endothelial cell (BAEC) proliferation was found maximal in *Par1* transfected (Cl13) cells activated via TRAP (8 hours) as compared to highly invasive (MDA 435) cell conditioned medium (Fig. 31 III). When neutralizing anti VEGF antibodies were applied during the proliferation assay, a significant inhibition was obtained, maximal at a 1:100 dilution of the antibodies showing reduced inhibition at lower concentrations. These data clearly point out the fact that activated PAR1 expressing cells exhibit high levels of functional VEGF that when specifically inhibited by anti VEGF antibodies, the proliferation was abolished nearly completely, in a dose dependent manner (Fig. 31 III).

## VEGF induction by *Par1* is mediated via PKC, PI3K and Src

Addition of PMA increased VEGF levels in *Par1* expressing cells (Cl13), maximally obtained at a concentration range of 500ng/ml - 100 ng/ml (Fig. 32I). Calphostin C, a potent PK C inhibitor, when applied at concentrations of 500ng/ml and up, potently inhibited this induction (Fig. 32II). No effect was observed when Calphostin C at a lower concentration (5 ng/ml) was applied. These data point out the involvement of PKC in a the *Par1* induced VEGF levels. In parallel, the addition of Wortmannin, a PI3K inhibitor resulted with the effective dose dependent inhibition of activated PAR1 induced VEGF levels (Fig. 32III). The involvement of Src in *Par1* induced VEGF is shown by the application of PP-2, a Src potent inhibitor. When PP-2 was briefly applied to the cells prior to PAR1 activation - inhibition of VEGF induction (Fig. 32IV ) was obtained. Altogether these data point to the central roles of PKC, Src and PI3K in the signaling machinery of PAR1 induced VEGF level.

## Transfection of NIH 3T3 cells by the oncogenes v-Ha-Ras, V-Src and Vav induce VEGF splice forms but not by *vav* proto-oncogene or an SH2-mutant of Vav.

To examine the effect of oncogene transformation in NIH 3T3 cells on VEGF expression, mRNA was assayed in the transformed and control cells (Fig 33I). For this we have utilized NIH3T3 cells transfeced with the active forms of either *ras* or *src* oncogenes as compared with NIH3T3 mock transfectants. NIH3T3 overexpressing *src* or *ras* oncogenes exhibited an activated state of signaling in the cells. Likewise, when NIH3T3 cells were also transfected with wild type (wt) *vav* (K62) protooncogene, the *vav* oncogene (K49) and a mutant introduced in the SH2 region of the vav oncogene [i.e., a mutants carrying either a substitution of tryptophan 622 to arginine (W622R; K70-9) and a mutant carrying a substitution of arginine 647 to leucine (R647L; K70-12)]. Whereas the W622R mutant exhibits a greatly reduced transforming potential as compared to the *vav* oncogene, R647L mutant retained the transforming potential of the oncogene. Interestingly, although all the *vav* SH2 mutant proteins were constitutively phosporylated on tyrosine they fail to bind to tyrosine phosphorylated proteins regardless of their transforming potential (53). As shown in Fig. 33 (I&II), a marked induction in VEGF expression was observed in the Src transfected cells as also in the Vav oncogene. A slight induction however observed in the Ras transfected cells or the proto-oncogene *vav* (Fig. 33 wt and vav onc, respectively) , while none in the control NIH3T3 cells (Fig. 33I) or the SH2 mutant (W622R; K70-9) of Vav (Fig. 33; NIH3T3, vavSH2; respectively). Low VEGF levels was obtained in the SH2 mutant that still maintain its transforming capability (53) (R647L;K-70-12, data not shown). These results are in correlation with the notion that cell transformation is sufficient to induce VEGF level of expression. The transformation is found in a linear association with the activation of the signaling cascade in the cells, since a mutant version of *vav* SH2 (W622R; K70-9) no longer allowed cell transformation and abrogated the association of adaptor proteins in the cells. By performing an RT-PCR assay using primers directed to exon 1 and exon 8 of VEGF gene, we substantiated the data regarding the expression of various VEGF splice forms. As shown in a representative experiment (Fig. 33III), while the NIH 3T3 cells do not express VEGF, *src* transfected NIH 3T3 exhibited all 4 splice forms; $VEGF_{121, 145, 165}$, very little $_{189}$ but not $VEGF_{206}$. The VEGF forms obtained by *src* transformed NIH3T3 were compared with *Par1* transfected / activated cells (TRAP for 8h) - and a negative control of parental SB-2 cells (Fig. 33 III).

# The Involvement of PAR Family in Malignant Carcinoma Progression: Biopsy specimens

## Breast carcinoma

We have previously demonstrated that PAR1 plays a significant role in breast carcinoma metastasis (1). This was shown by a direct correlation between the levels of PAR1 expression and the invasion properties of breast carcinoma both *in vitro* in a collection of cell lines (Northern and Western blot analyses) and *in vivo* in biopsy specimens (*in situ* hybridization analysis). Our data *(Nature Medicine,* 1), performed on paraffin embedded sections taken from patients representing a broad range of different stages of the disease showed the following: abundant distribution of PAR1 in sections of IDC, confined to the carcinoma cells of the primary tumors, representing high level of metastasis (Figure 3; B,C). Weaker positive staining was obtained in *high grade* DCIS of comedo type (as above Figure 3; E,F). In contrast, very little or no staining was observed in *low grade* DCIS of the solid type, and no staining in AIDH (as above-Figure 3; E,F) and in the normal duct lobular units (as above-Figure 3; A,D). Overall, this pattern points to a high level of PAR1 expression in IDC, lower level in cases of DCIS, in particular in the high grade of the comedo type of lesions. In contrast, weak to no PAR1 expression was observed in *low grade* DCIS of the *solid type*. Normal tissues obtained from reduction mammoplasty specimens did not exhibit any staining of PAR1. PAR1 antisense transfection showed effective inhibition of the invasion properties of highly metastatic breast carcinoma cells (1). The possible association of other PAR family members, may help develop an individually based therapy program according to the specific and spatial profile obtained for each patient. *In situ* hybridization analysis using PAR3 riboprobes on paraffin biopsy specimens of sections taken from patients representing a broad range of different stages of the disease showed essentially similar data as reported for PAR1 (Fig. 5). We therefore conclude that in addition to PAR1 also PAR3 is over expressed in a direct correlation to malignant carcinoma progression.

# Team Involved in PARs and Breast Carcinoma Invasion and Metastasis

The team includes Ph.D. students, an experienced laboratory research assistant as well as professional personnel (among of which are: Oncologist, Gynecologist and Pathologist) who can share responsibilities with the PIs.

* **Bar-Shavit, Rachel Ph.D. PI / Team Leader**

- **Uziely, Beatrice, M.D. /Oncologist**
- **Grisaru-Granovsky, Sorina, M.D. /Gynecologist,**
  **Project: Physiological invasion processes of placenta, Ovary varcinomas**
- **Galina Pizov, M.D. /Pathologist**

- ***Sharona Cohen Even-Ram*** Ph.D. student (currently a PostDoc, K. Yammada, NIH)

- ***Maoz Miriam, M.Sc.*** / Research Assistant. Involved in various aspects of the project

- ***YongJun Yin Ph.D. student*** - project: PAR1 transgenic mice, Angiogenesis

- ***Salah, Zaidoun Ph.D. student*** - project: PAR1 "TET – On" inducible system, solid tumors and androgen hormone regulation of PAR1

- ***Cohen Irit, Ph.D. student*** – Characterization of PAR1 in breast clones : truncated PAR1, full length PAR1 and antisense PAR1

# Major achievements and Concluding Remarks

**Tasks I & II:** Both these aims in-fact are involved and used invariably throughout our research experimental models, among of which are; cell transfectants (inducible tetracycline regulated systems or transfected cells of breast and melanomas ; either full length PAR1, PAR1 antisense and truncated forms). Part of the molecular mechanism of PAR1 in tumor invasion and metastasis has been illustrated in stable PAR1 transfectants (see Appendix 1). Activation of PAR1 leads to focal adhesion contact formation and integrin signaling. PAR1 directly cross-talks with integrin $\alpha v\beta 5$ and initiates thereby integrin activation in a manner that is termed "inside- out".

**-The involvement of protease-activated receptors (PARs) in normal and pathological human trophoblast invasion** (see first annual report-June 2001). This manuscript focuses on establishing a role for PAR1 & PAR3 in the physiological and pathological malignancies of the placenta.

* **The major effort during the recent year was centered around preparing *hPar1* transgenic mice specifically in the mammary glands.** Transgenic *hPar1* were generated showing a phenotype of ductal side branching and increased alveoli proliferation. We have established transgenic PAR1 over expressing mice driven by LTR - MMTV promotor (directed to the mammary glands). Genomic DNA analysis of *hPar1* expression levels was carried out to detect heterozygous expressing mice (Southern blot and PCR analysis). U till now (the screen still continues) ~12 homozygous mice-found. The expression of *hPar1* was confined to the mammary glands and not in any other organs tested. These heterozygous mice exhibit phenotype of high side branching ducts as compared to age matched controls. The complexity of the side branching is pronounced especially in the pregnant mice pointing to the possible involvement of the female hormone system in the process. These glands exhibit hyperplastic phenotype. We are currently evaluating our homozygous mice. Major conclusions: The *hPar1* transgenic mice mammary gland hyperplasia is mediated in part by induction of wnt-4 in ductal side branching. High proliferation levels of alveoli as determined by PCNA staining. *hPar1* induces RANK and RANKL levels. The TNF receptor family RANK ( receptor activator of NFκB) is activated by its ligand RANKL, and plays an important role in mammary gland alveoli proliferation. Whether *Par1* plays a role in the developmental process of the mammary glands is being currently studied. ***Manuscript in preparation.***

* **Oncogenic transformation induces tumor angiogenesis: A role for PAR1 activation** (see Appendix 2). This task was carried out in parallel as a second major aspect of the project. We demonstrate here that *hPar1* gene expression plays a central role in the induction of blood vessel

recruitment in animal models in vivo, as determined by the "Tet-on" *Par1* inducible prostate system and by the Matrigel micropocket assay. Par1 induced angiogenesis is mediated via the increased expression of vascular endothelial growth factor splice forms; VEGF121, VEGF145, VEGF165 and VEGF189 or but not VEGF 206. Activation of PAR1 induces markedly the expression levels of functional VEGFs as determined by Northern blot analysis, endothelial tube alignment in a 3 dimensional collagen gel, as well as bovine aortic endothelial cell proliferation in vitro. Since neutralizing anti VEGF antibodies potently inhibited *Par1* induced endothelial cell proliferation, we conclude that functional VEGF expression and secretion is at least partly regulated by *Par1*. The Par1 induced VEGF expression is inhibited by specific PKC, Src and PI3K inhibitors (i.e., Calphostin C, PP-2 and Wortmanin, respectively), suggesting the participation of these signaling enzymes in the process. In parralel, we show that oncogenic transformation of genes shown to be part of PAR1 signaling machinery - is sufficient to increase VEGF expression. While NIH3T3 cells do not express VEGF, transfection of the cells with the activated forms of either src or vav results in a marked increase in the expression of VEGF. On the other hand, only a slight increase in VEGF isoform expression is observed when the cells are transfected with ras and the non - transforming proto-oncogene vav transfected cells and very little or none in the SH2 mutants of the vav oncogene transfected cells. Manuscript submitted.

** **Interactions of syk, a tumor suppressor gene in breast carcinoma and *hPar1* oncogene**. Analysis of Syk expression levels in either human biopsy specimens or a panel of well established breast cancer cell lines revealed an inverse correlation between Syk expression levels and malignancy. High expression levels are detected in the normal mammary gland tissues as well as in nearly normal and benign cell lines. No Syk expression was detected in the invasive pathological breast tissue specimens and the highly metastatic cell lines. Since Syk exerts its tumor suppression activity only *in vivo* in animals or in three-dimensional Matrigel cultures, but not on a plastic 2D culture dish, it is likely that the signals conveyed by the extracellular matrix environment are critical for the activation of Syk. During our studies on the role of *hPar1* in breast carcinoma invasion and metastasis we set-out to analyze the interrelation between the breast invasive phenotype and Syk; more specifically the mutual interactions of *hPar1* and Syk. Our data show an intriguing biological phenomenon of Syk expressing malignant breast cells following activation of PAR1. We have addressed the signaling molecular pathways of Syk expressing cells versus non Syk cells following PAR1 activation. By the use of **GST-C-tail PAR1**, we demonstrate a novel association between Syk and PAR1 c-tail. This was demonstrated

by a set of experiments of Co-immunoprecipitations , specific competitions in the presence of PAR1 C-tail and purification of bound Syk on GST-C-tail PAR1. These studies are likely to yield intriguing data regarding breast malignancy its suppression by a specific breast tumor suppressor gene.

***We have established an inducible system of PAR1 expression in prostate cell lines. Upon injection of thee cells *s.c.* to rats and addition of Dox to their drinking water, increased tumor mass and reddish tumors are obtained as compared to non-Dox fed rats (see Fig. 29). Blood vessel counts showed at least 3 times higher levels of blood vessels.

The expression and localization of PAR1 and PAR3 has been evaluated in a collection of biopsy specimens of different types of carcinomas (such as: colon, breast, ovary, prostate and melanoma).

## Reportable outcome:

- A manuscript entitled: **Tumor cell invasion is promoted by activation of Protease Activated Receptor-1 in cooperation with the αvβ5 integrin** (see appendix 1, JBC , vol. 276, pp. 10952-10962, 2001). This paper demonstrates in part, the molecular basis of PAR1 involvement in tumor invasion and metastasis. While the observations at large were made in melanoma non metastatic stable PAR1 transfectants, we have established PAR1 expressing clones in breast carcinomas and intend to explore in depth the mechanism in these cells. We are likely to benefit and inspired by our data obtained and shown in manuscripot (appendix 1).

- **A manuscript submitted to FASEB J entitled: Oncogenic transformation induces tumor angiogenesis: A role for PAR1 activation** (see Appendix 2). We demonstrate here that *Par1* gene expression plays a central role in the induction of blood vessel recruitment in animal models in vivo, as determined by the "Tet-on" *Par1* inducible prostate system and by the Matrigel micropocket assay. *Par1* induced angiogenesis is mediated via the increased expression of vascular endothelial growth factor splice forms; VEGF121, VEGF145, VEGF165 and VEGF189 or but not VEGF 206. We have generated *hPar1* overexpressing mice directly expressed in the mammary glands.

- **The phenotype of *hPar1* transgenes in the mammary gland and its mechanism of action has been addressed.** Manuscript in preparation.

- **The pattern of Protease Activated Receptors (PARs) expression during early trophoblast development .** Manuscript submittet to J pathology

Human fetal development depends on the ability of the embryo to gain access to maternal circulation. Thus, specialized stem cells of the newly formed placenta, named trophoblast invade the uterus and its arterial network to establish an efficient feto-maternal molecular exchange. To accomplish this task, trophoblast differentiation during the first trimester of pregnancy, involves cell proliferation, invasion and extracellular matrix (ECM) remodeling. Trophoblast invasion shares many features with tumor cell invasion, with the distinction that it is strictly spatially and temporally controlled. We have previously demonstrated that PAR1, the first member of the Protease Activated Receptor (PAR) family, plays a central role in tumor cell invasion. Therefore, in the present study we examined the pattern of expression of PAR1 and other PAR family candidates, during early human placental development. We show that PAR1 and PAR3 were highly and spatially expressed between $7^{th}$ and $10^{th}$ weeks of gestation but not at $12^{th}$ week and thereafter. Over-invasive trophoblasts may appear occasionally and cause a trophoblastic disease known as Complete Hydatidiform Mole (CHM). Likewise, high expression levels of PAR1 and PAR3 were observed in the cytotrophoblasts of CHM biopsy specimens as compared to none in the normal age-matched placenta. Together, our data suggest the involvement of PAR1 and at least PAR3 in the restricted and unrestricted pathological trophoblast invasion process.

## In conclusion:

- We have elucidated in part the molecular basis of PAR1 during the invasion process (JBC 276, 10952-10962, 2001). Appendix 1

- PAR1 and PAR3 play a role in physiological invasion process , as shown in placenta cytotrophoblast during the 1st trimester of pregnancy.

- PAR1 antisense effectively inhibits tumor invasion via Matrigel coated filters. Appendix 1,

- PAR1 overexpression induce markedly angiogenesis in animal models *in vivo:* ellucidation of a molecular pathway. Appendix 2

- *hPar1* transgenic mice have been established directly overexpressed in the mammary gland. These glands show a high levels of ductal and alveoli complexity. The molecular mechanism is currently being evaluated. Manuscript in preparation.

- PAR1 is regulated by the Androgen hormones: Identification of the androgen domain/s in *hPar1* promoter.

- PAR1 and PAR3 are overexpressed in a collection of biopsy specimens in a direct correlation with the aggressiveness of the disease (i.e., breast, prostate, ovary, colon and melanoma).

- Generation of monoclonal antibodies for the detection of the released PAR1 N-terminal peptides in body fluids.

## References


1. Even-Ram, S., Uziely, B., Cohen, P.,Ginzburg, Y., Reich, R. Vlodavsky, I. and Bar-Shavit, R. 1998. Thrombin receptor overexpression in physiological and malignant invasion process. *Nature Medicine.* 4: 909-914.

2. Vu, T-K., Hung, H.D.T., Wheaton V.I., & Coughlin, S.R. 1991. Molecular cloning of a functional thrombin receptor reveals a novel proteolytic mechanism of receptor activation. *Cell* 64:1057-1068.

3. Rasmussen UB, Vouret-Craviari V, Jallat S, Schlesinger Y, Pages G, Pavirani A, Lecocq JP, Pouyssegur J, Van Obberghen-Schilling E. 1991. cDNA cloning and expression of a hamster α-thrombin receptor coupled to $Ca^{+2}$ mobilization. *FEBS Lett* 288: 123-128.

4. Gerszten RE, Chen J, Ishii M, Ishii K, Wang L, Nanevicz T, Turck CW, Vu TK, Coughlin SR. 1994. Specificity of the thrombin receptor for agonist peptide is defined by its extracellular surface. *Nature (London)* 368: 648-649.

5. Kahn ML, Zheng YW, Huang W, Bigornia V, Zeng D, Moff S, Farese RV Jr, Tam C, Coughlin SR.1998. A dual thrombin receptor system for platelet activation *Nature.* 394: 690-694.

6. Nakanishi-Matsui M, Zheng YW, Sulciner DJ, Weiss EJ, Ludeman MJ, Coughlin SR 2000. PAR3 is a cofactor for PAR4 activation by thrombin. *Nature.* 404: 609-613.

6. Martin, CB., Mahon, GM., Klinger, MB., Kay, RJ, Symons, M., Der, CJ., and Whitehead IP., 2001. *Oncogene*, 20: 1953-1963.

8. Cohen Even-Ram, S., Maoz, M., Pokroy, E., Reich , R. Katz, B-Z., Gutwein, P., Altevogt, P., and Bar-Shavit, R. 2001. Tumor cell invasion is promoted by activation of protease activated Receptor-1 in cooperation with αvβ5 integrin. *J. Biol. Chem* 276: 10952-10962.

9. Hennighausen, L., and Robinson , G. 1998. Think globally, act locally: the making of a mouse mammary gland. Rev. *Genes & Development* 12: 449-455.

10. Daniel, C.W., and Silberstein, G.B. 1987. Developmental biology of the mammary gland. In The mammary gland (ed. M.C. nevillend C.W. Daniel), pp 3-36 plenum Press new York NY.

11. Korach, K.C., couse, J.F., Curtis, S.W., washburn, T.F., Lindzey, J., Kimbro, K.S., Eddy, E.M., Migliaccio, S., Shedeker, S.M., Lubahn, D.B., Schomberg, D.W., and Smith E.P. 1996. Estrogen receptor gene disruption : molecular characterization and experimental and clinical phenotypes. *Recent. Prog. Horm.* Res. 51: 159-186.

12. Cunha, G.R., Young, P., Hom, Y.K., Cook, P.S., Taylor, J.A. and lubahn, D.B. 1997. Elucidation for a role in for stromal steroid hormone receptors in mammary gland growth and development using tissue recombinants. J. *Mamm. Glan. Biol. Neoplasia* 2: 393-402

13. Lydon, J.P., De Mayo, F.J., Funk, C.R., Mani, S.K., Hughes, A.R., Montgomery, C.A. Jr., Shyamala G., Conneely, O.M., & O'Malley, B.W. 1995. Mice lacking progesterone receptor exhibit pleiotropic reproductive abnormalities.*Genes & Dev.* 9: 2266-2278.

14. Brisken, C., Park, S., vass, T., Lydon, J., O'Malley, B., and Weinberg, R.A. 1998. A paracrine role for the epithelial progesterone receptor in mammary gland development . *Proc..Natl. Acad. Sci. USA* 95: 5076-5081.

15. Brisken, C., Heineman, A., Chavarria, T., Elenbaas, B., tan, J., Dey, S.K., McMahon, J.A., McMahon, A.P. and Weinberg R.A. 2000. Essential function of Wnt-4 in mammary gland development downstream of progesterone signaling.*Genes & Dev.* 14: 650-654.

16. Gavin, B.J., and McMahon, A.P., 1992. Differential regulation of the Wnt gene family during pregnancy and lactation suggests a role in postnatal development of the mammary gland. *Mol. Cell Biol.* 12: 2418-2423.

17. Weber-hall, S.J., Phippard, D.J., Niemeyer, C.C. and Dale, T.C.1994. Developmental and hormonal regulation of Wnt gene expression in the mouse mammary gland. *Differentiation.* 57: 205-214.

18. Stark, K., Vainio, S., Vassileva, C., and McMahon A.P. 1994. Epithelial transformation of metanephric mesenchyme in the developing kidney regulated *Nature.* 372: 579-683.

19. Hennighausen L, Robinson GW, Wagner KU, Liu W. 1997. Prolactin signaling in mammary gland development. *J Biol Chem* ;272(12):7567-9.

20. Liu X, Robinson GW, Wagner KU, Garrett L, Wynshaw-Boris A, Hennighausen L. 1997. Stat5a is mandatory for adult mammary gland development and lactogenesis. *Genes Dev* 11(2): 179-86

21. Teglund S, McKay C, Schuetz E, van Deursen JM, Stravopodis D, Wang D, Brown M, Bodner S, Grosveld G, Ihle JN. 1998. Stat5a and Stat5b proteins have essential and nonessential, or redundant, roles in cytokine responses. Cell 93(5):841-50.

22. Robinson, G., W., Karpf, A.,B., and Kratochwil, k., 1999. Regulation of mammary gland development by tissue interaction. J. Mamm. Gland Biol. Neoplasia 4:9-19.

23. Fata, J., E., Kong, Y-Y., Li, J., sasaki, T., irie-Sasaki, J., Moorehead, R., A., Elliot, R., Scully, S., Voura, E.,B., lacey, D.,L., Boyle, W., J.,Khokha, R., and Penninger, J.M. 2000. The osteoclast differentiation factor osteoprotegerin-ligand is essential for mammary gland development. 103: 41-50.

24. Chu, D.H., Morita, C.T. Weiss, A. 1998. The Syk –family protein tyrosine kinase in T-cell activation and development . Immunol. Rev. 165: 167-180.

25. Coopman, P.J. P., Do, M.T.H., Barth, M., Bowden , E., hayes, A.J., Basyuk, E., Blancato, J. K, vezza, P.R., McLeskey, S.W., Mangeat, P.H. and Mueller, S.C. 2000. The Syk tyrosine kinase suppresses malignant growth of human breast cancer cells. *Nature.* 406: 742-747.

26. Yuan, Y., Mendez, R., Sahin, A. and Dai, J.L. 2001. Hypermethylation leads to silencing of the Syk gene in human breast cancer. *Cancer Research.* 61: 5558-5561.

27. Minobe, K., et al. 1998. Allelic loss on chromosome 9q is associated with lymph node metastasis of primary breast cancer. *Japan. J. Cancer Res.* 89: 916-922.

28. Martin, CB., Mahon, GM., Klinger, MB., Kay, RJ, Symons, M., Der, CJ., and Whitehead IP., 2001. The thrombin receptor, PAR-1, causes transformation by activation of Rho-mediated signaling pathways. *Oncogene*, 20: 1953-1963.

29. Weaver, V., et al., 1997. Reversion of the malignant phenotype of human breast cells in three-dimensional culture and *in vivo* by integrin blocking antibodies. *J Cell Biol* 137, 231- 245.

30. Muthuswamy SK, Li D, Lelievre S, Bissell MJ, Brugge JS, 2001. ErbB2, but not ErbB1, reinitiates proliferation and induces luminal re population in epithelial acini. *Nat Cell Biol* 3:785-92.

31. Ilic D, Furuta Y, Kanazawa S, Takeda N, Sobue K, Nakatsuji N, Nomura S, Fujimoto J, Okada M, Yamamoto T. 1995. Reduced cell motility and enhanced focal adhesion contact formation in cells from FAK-deficient mice. *Nature* 12: 377(6549):539-44.

32. Gilmore AP, Romer LH.1996. Inhibition of focal adhesion kinase (FAK) signaling in focal adhesions decreased cell motility and proliferation. *Mol Biol Cell* 7(8):1209-24.

33. Richardson A, Shannon JD, Adams RB, Schaller MD, Parsons J. 1997. Identification of integrin-stimulated sites of serine phosphorylation in FRNK, the separately expressed C-terminal domain of focal adhesion kinase: a potential role for protein kinase A. *Biochem J* 15;324 ( Pt 1):141-9.

34. Minden A, and Karin, M. 1997. Regulation and function of the JNK subgroup of MAP kinases. *Biochim Biophys. Acta* 1333, F85-104.

35. Coso OA, Chiariello M, Yu JC, Teramoto H, Crespo P, Xu N, Miki T, Gutkind JS. 1995. The small GTP-binding proteins Rac1 and Cdc42 regulate the activity of the JNK/SAPK signaling pathway. *Cell* 30;81(7):1137-46.

36. Minden A, Lin A, Claret FX, Abo A, Karin M. 1995. Selective activation of the JNK signaling cascade and c-Jun transcriptional activity by the small GTPases Rac and Cdc42Hs. Cell 1995 30;81(7):1147-57.

37. Dolfi F, Garcia-Guzman M, Ojaniemi M, Nakamura H, Matsuda M, Vuori K.1998. The adaptor protein Crk connects multiple cellular stimuli to the JNK signaling pathway. *Proc Natl Acad Sci U S A* 22;95(26):15394-9.

38. Tanaka S, Ouchi T, Hanafusa H. 1997. Downstream of Crk adaptor signaling pathway: activation of Jun kinase by v-Crk through the guanine nucleotide exchange protein C3G. *Proc Natl Acad Sci U S A* 18;94(6):2356-61.

39. Chu DH, Morita CT, Weiss A. 1998. The Syk family of protein tyrosine kinases in T-cell activation and development. *Immunol Rev* 165:167-80.

40. Woodside DG, Obergfell A, Leng L, Wilsbacher JL, Miranti CK, Brugge JS, Shattil SJ, Ginsberg MH. 2001. Activation of Syk protein tyrosine kinase through interaction with integrin beta cytoplasmic domains. *Curr Biol* 13;11(22):1799-804.

41. Carmeliet, P. and Jain R.K. 2000. Angiogenesis in cancer and other diseaes .*Nature*. 407:249-257.

42. Folkman, J. 1971. Tumor angiogenic therapoeitic implications. *N. Engl. J.Med.* 285: 1182-1186.

43. Hanahan, D., and Folkman, J. 1996. Pattern and emerging mechanisms of angiogenic switch during tumorigenesis. *Cell.* 86: 353-364.

44. Neufeld, G., Cohen, T. Gengrinovitch , S., and Poltrak, Z. 1999. Vascular endothelial growth factor (VEGF) and its receptors. Rev. FASEB J. 13: 9-22.

45. Keshet, E., and Ben-Sasson, S.,1999. Anticancer drug targets. Approaching angiogenesis. *J.Clin. invest.* 104: 1497-1500.

46. Griffin, C.T. et al, 2001. A role for thrombin receptor signaling in endothelial cells during embryonic development. *Science.* 293:1666-1669.

47. Carmeliet, P. 2001. Clotting factors build blood vessels. *Science.* 293: 1602-1604.

48. Bugge TH, Xiao Q, Kombrinck KW, Flick MJ, Holmback K, Danton MJ, Colbert MC, Witte DP, Fujikawa K, Davie EW, Degen J.1996. Fatal embryonic bleeding events in mice lacking tissue factor, the cell-associated initiator of blood coagulation. *Proc. Natl. acad. Sci. USA.* 93: 6258-2564.

49. Toomey JR, Kratzer KE, Lasky NM, Stanton JJ, Broze GJ Jr. 1996. Targeted disruption of the murine tissue factor gene results in embryonic lethality. *Blood.* 88: 1583-1587.

50. Cui J, O'Shea KS, Purkayastha A, Saunders TL, Ginsburg D. 1996. Fatal haemorrhage and incomplete block to embryogenesis in mice lacking coagulation factor V. *Nature.* 384: 66-68.

51. Sun WY, Witte DP, Degen JL, Colbert MC, Burkart MC, Holmback K, Xiao Q, Bugge TH, Degen SJ 1998. Prothrombin deficiency results in embryonic and neonatal lethality in mice. *Proc. Natl. Acad. Sci.* USA. 95: 7597-7602.

52. Miao, H-Q., Lee, P., Lin, H., Soker, S., and Klagsbrun, M. (2000) Neuropilin-1 expression by tumor cells promotes tumor angiogenesis and progression. *FASEB J* **14,** 2532-2539.

53. Katzav, S. 1993. Single point mutation in the SH2 domain impair the transforming potential of *vav* and fail to activate proto-*vav*. *Oncogene* 8, 1757-1763.

**Legends to Figures:**

**Fig. 1: PAR family : 4 gene members**

**Fig. 2: Scheme of solid tumor development**

**Fig. 3: *In situ* hybridization of PAR1 mRNA in normal and cancerous breast tissues specimens.** Riboprobes probes prepared and labeled by T7 RNA polymrerase (for antisense orientation) or T3 RNA polymerase (for sense orientation - control), using DIG-UTP for labeling mix.Top. IDC staining by PAR1 antisense and sense control (A,B; respectively). Middle. DCIS staining by PAR1 antisense and sense control (C,D; respectively). Bottom. Hyperplasia staining by PAR1 antisense and sense control (E,F; respectively).

**Fig. 4: PAR1 expression in human breast carcinoma cell lines.** Total RNA isolated from human breast carcinoma cell-lines were analyzed by Northern blotting. These are: MDA-435 (lane A), MDA-231 (lane B) and MCF-7, as well as Ha-ras-transfected breast carcinoma cell lines, MCF10AT3B (lane D), MCF10AT (lane E) and MCF10A (lane F). The blots were probed with $^{32}$P-labeled 250 base pair DNA, corresponding to PAR1 (upper part), or with $^{32}$P-labeled β-actin DNA (lower part).
**II.** Western blot analysis of ThR. Western blot analysis of cell lysates (50 μg/lane) of MCF-7 (lane A), MDA-231(lane B) and MDA-435 cells. Specific protein band was detected following incubation with anti ThR antibodies and visualized by the ECL immunoblotting detection system according to the manufacturer's instructions.
**III.** Inhibiton of MDA-435 Matrigel invasion by PAR1 antisense. MDA-435 cells were transiently transfected with pCDNAIII expression plasmid containing the antisense PAR1 including part of the promoter region (i.e. 462 nucleotides). The level of invasion was compared to untreated MDA-435 (lane A) and MCF-7 (lane B) cells. Control transfections of MDA-435 cells were performed in the presence of vector alone - or DOTAP liposomes alone (Gibco -BRL) (lane D). Nearly confluent (60%) cells were treated with various concentrations of the plasmid: transfection with antisense PAR1 - 5 μg/plate (lane E), transfection with antisense PAR1 - 20 μg/plate (lane F). The invasion assay was performed as described under Materials and Methods, 72 h following transfection.
**IV.** Western blot analysis of PAR1 antisense transfectants. MDA-435 cell lysates (50 μg/lane) of PAR1 antisense transfectants (A) were applied on SDS-PAGE and the level of receptor protein was compared to cells transfected with vector alone (B) or untreated cells.

**Fig. 5: *In situ* hybridization of PAR3 in breast carcinoma biopsy specimens.** RNA probes were transcribed and labeled by T7 RNA polymrerase (for antisense orientation) or T3 RNA polymerase (for sense orientation - control), using DIG-UTP for labeling mix. Top panel. IDC (invasive ductal carcinoma) biopsy sample of antisens and sense orientation of PAR1 (*left & right*, respectively). DCIS (ductal carcinoma in situ) antisense and sense (as above, middle panel) and hyperplasia and normal breast tissue (*left & right*, respectively- bottom panel).

**Fig. 6 Transfection by PAR1 DNA confers invasive properties on non-metatastic melanoma cells.** The expression of PAR1 and cellular invasive properties were measured in SB-2 non-metatastic human melanoma cells, in A375 SM highly metatastic human melanoma cells, in stable PAR1 transfectants clone 13 and clone mL, and in SB-2 cells transfected by mock transfectants. Stable PAR1 clones were screened for PAR1 expression (*a*) using anti-PAR1 thrombin receptor mAbs on a Western blot of 50μg of lysates total protein. (*b*) The invasive capabilities of the selected clones were determined by the Matrigel invasion assay. Cell lines marked "activ." were activated by 1 unit/ml thrombin for 1 h before being used in the invasion assay. The data presented here are the averages of data from at least three replicate experiments.

**Fig. 7. Effect of modulation of PAR1 expression on invasiveness.**
*a*, A375SM cells, transiently transfected with PAR1-antisense-containing vector at the indicated concentrations, were tested for their ability to invade through Matrigel-coated filters. The data are representative of at least three replicate experiments.
*b*, Human PAR1 cDNA was used to transiently transfect mouse B16F10 melanoma cells. Two hundred thousand cells were injected into the lateral tail vein of C57BL mice. Mice were killed 14 days later, and the lungs were dissected, fixed, and stained by picric acid solution . A, B16F10 cells; B, vector-transfected B16F10 cells; C, B16F10 cells transfected with 0.5 mg/ml PAR1 plasmid; D, 1 μg/ml PAR1 plasmid; and E) 2 μg/ml PAR1 plasmid.
*c*, Level of PAR1 in B16F10 cells following transient transfection with PAR1 cDNA. RNA was isolated from the cells. RT-PCR was performed, using PAR1 and GAPDH (control) primers. *d*, PAR1-transfected or nontransfected control cells were injected into the tail vein of C57BL mice, and lung metastases were counted after 2 weeks. The numbers indicate mean number of metastases per mouse.

**Fig. 8. Altering PAR1 expression affected cell adhesion and actin fiber re-organization.** Stable PAR1 transfected clones and PAR1 antisense selected clones were analyzed for their adhesive properties to fibronectin (*a, c*) or to Th1 RGD peptide (*b*) coated substrates. Cell adhesion was measured by Methylene blue staining of formaldehyde-fixated cells. The eluted stain was detected by spectrophotometry using a $\lambda$=620 nm filter. The cells tested (*a, b*) were the same as those described in Fig. 6. In addition, we show that in highly metastatic human melanoma A375SM cells stably transfected with PAR1 antisense cDNA (AS clone 4 and AS clone 3) reduced adhesion was observed (*c*) as compared to A375SM or vector. These clones exhibited low PAR1 levels as shown by Northern blot analysis (*d*) of RNA samples from A375SM (A), A375SM cells transfected with vector only (B), AS clone 3 (C) and AS clone 4 (D). The data presented here are the averages of data from at least three replicate experiments. L32 is a ribosomal RNA that we have used as a housekeeping control gene for these experiments. (*e*) SB-2 cells and PAR1 transfectant clone13 were subjected to actin staining by FITC-phalloidin after PAR1 activation by TRAP. Note that the PAR1 transfectants exhibited a more rapid change in actin fiber re-organization and cellular morphology than did the naïve SB-2 cells.

**Fig. 9 Activation of PAR1 induces phosphorylation of FAK and paxillin and their recruitment to FACs.** (*a*) The tyrosine phosphorylated levels of immunoprecipitated FAK (upper section) and paxillin (lower section) were measured by anti-phosphotyrosine mAb (4G10, UBI) in SB-2 naïve cells, in A375SM metastatic cells, and in the stable PAR1 transfectant clone 13. Note that FAK was observed to co-precipitate with paxillin (lower section). (*b*) Immuno-fluorescent staining of phosphotyrosine in PAR1 transfected clone 13 was performed by specific incubations with mAbs (4G10) at 0, 15, and 60 min. Detection was made by Cy3-labeled goat anti-mouse IgG, using confocal microscopy. Following activation by 100μM TRAP, thefocal adhesion contacts (FACs) were observed to be enriched with phosphorylated proteins with a peak at60 min. (*c*) Immuno-fluorescent staining with anti-vinculin, anti-FAK, and anti-paxillin in the stable PAR1 transfectant clone 13 activated with 100μM TRAP for 1 h or not (NA). When the cells were stained with anti-FAK and anti-paxillin, distinct FAC staining was observed only in the activated cells. When the cells were stained with anti-Vinculin, FACs were detectable at a low level in the non-activated (NA); this level was increased following receptor activation by TRAP.

**Fig. 10 PAR1 activation did not alter the levels of integrin expression but did induce αvβ5 recruitment to FACs.** (*a*) Integrin expression levels were measured by flow-cytometry in SB-2 naïve cells and in PAR1 clone13, each activated with thrombin at a concentration of 1 unit/ml. The levels of α5β1 (A, B), αvβ5 (C, D), αvβ3 (E, F) and the integrin αv chain (G, H) were detected by incubating the cells with the appropriate specific mAb, followed by incubation with FITC-labeled anti-mouse IgG. Note that no significant changes were observed in the levels of any of the integrins examined. (*b*) The distribution of integrins was detected by immuno-fluorescent staining (upper panel). Cy-3 red fluorescence was visualized by confocal microscopy. The lower panel shows the same cells as in the upper panel, but visualized by phase-contrast microscopy. Non-activated (NA) PAR1 clone 13, stained

by anti-αvβ5 mAbs revealed a diffused pattern (A). After activation by TRAP, the integrin α5β1 was detected in a random peri-nuclear position (B); the integrin αvβ3 was randomly scattered over the cell membrane (C); the integrin αvβ5 was localized to distinct "spikes" of focal adhesion contacts (D).

**Fig. 11 . Activation of full length PAR1 but not of truncated PAR1 lead to the co-precipitation of αvβ5 with paxillin and FAK and reduced invasiveness in the presence of anti-αvβ5 antibodies.** Co-precipitation of paxillin with αvβ5 (*a*) or with αvβ3 (*b*) was measured in cells lysates of naïve SB-2 cells (C) and of a stable PAR1 tramsfectant clone13 that was either thrombin-activated (A) or not (B). (*c*) Paxillin and FAK were immuno-precipitated from cell lysates of SB-2 cells that had been thrombin activated (A) or not (B) and from a stable PAR1 transfectant clone 13 that was either thrombin-activated (C) or not (D). The blotted membrane was incubated with anti- β5 subunit mAb. (*d*) Non-invasive MCF7 cells, naturally expressing very low levels of PAR1, were transfected with cDNA expression vectors coding either for PAR1 or for truncated-PAR1. In lysates of the PAR1 transfectants, co-precipitation of FAK and paxillin was detected after PAR1 activation by thrombin (B) but not without activation (A). In lysates of truncated-PAR1 transfectants, no co-precipitation of FAK with paxillin with αvβ5 was observed regardless of whether the cells were thrombin activated (D) or not (C). Tyrosine phosphorylated paxillin co-precipitated with αvβ5 (lower panel) in PAR1-transfected cells (A); the level of this precipitation increased following thrombin activation of PAR1 (B); in truncated-PAR1 transfected cells, only minor levels of phosphorylated paxillin were detected with (D) or without (C) thrombin activation. (*e*) FACS analysis of MCF7 cells following transfection by DNA coding for the full length PAR1 (A and C) or for the truncated-PAR1 (B and D) was shown. Their levels were compared to non-transfected cells (first peak, B and A). This is true also when PAR1 or truncated PAR1 expression was measured relative to empty vector transfected cells (first peak, C and D; respectively). (*f*) A375SM cells were activated with 1 unit/ml thrombin (B, C, D) or not (A). The activated cells were then treated with 20 μg/ml of either anti-αvβ5-blocking mAbs (C) or non-specific IgG (D). The treated cells were then subjected to a Matrigel invasion assay. The data presented here are the averages of data from at least three replicate experiments. One hundred percent invasion by the metatastic cells corresponded to 48±3 invading cells as compared to 17±1.5 invading cells by SB-2 non-metastatic cells (data not shown).

**Fig12. MMTV-*hPAR1* transgenic construct.** Full length human *Par1* (1.4kb) was inserted into the multiple cloning site between HindIII and EcoRI. The plasmid was digested with the restriction endonucleases HgaI and EcoRI to generate the DNA fragment for injection.

**Fig 13a. MMTV-*hPAR1* transgenic lines.** Genomic DNA was extracted from tails of the founder mice, ***(a)*** Southern blot and **(b)** PCR were performed. 1: positive control; 2: negative control; 3:transgenic founder; 4: non-transgenic mouse. ***(c)*** Identification of homozygous mice with Southern blot. $S_1$-$S_{12}$: all $F_2$ pups; $P_1$ and $P_2$: positive control; N: negative control.

**Fig 13b. RT-PCR analysis shows the expression of human *PAR1* transgene in different organs of a transgenic mouse.** The experiment is a representative of at least 5 mice tested.
1. Mammary 2. Ovary 3. Brain 4. Colon 5. Heart 6. Kidney 7. Lung 8. Spleen 9. Salivary 10. Liver 11. Positive control.

**Fig. 14. Whole mounts analysis of *hPar1*+/- transgenic mice.** MMTV-LTR driven *hPar1* overexpressed in the mammary gland were analyzed by whole mounts. Mammary glands of 5,8, &10 weeks old virgin normal mice (A,C,E) and *hPar1*+/- mice (B,C &F). Normal pregnant mice of 4, 8 and 12 days (at 13 weeks of age)(G,I &K) as compared to age matched hPar1 (H, J &L).

**Fig.15. *In situ* hybridization analysis of *hPar1*+/- transgenic mammary glands. I.** hPAR1 expression in 10 weeks old virgin (A, B; antisense and sense respectively), pregnant 13 weeks/4day(C, D; antisense and sense respectively), 8days pregnancy (E, F; antisense and sense respectively), 12 days pregnancy (G, H; antisense and sense respectively). Magnification of X20. **II.** Low power magnification

(X5) of hPAR1 in *hPar1*+/- transgenic mice of 8d pregnancy (A, B; antisense and sense respectively). Normal age matched mice (C, D; antisense and sense respectively).

**Fig.16 RT-PCR analysis of Wnts and *hPar*+/- transgenic mice.** Wnt-4 and Wnt-7b expression in normal control mammary glands of virgin (A-C)and pregnant (D-F) as compared to *hPar1*+/- virgin (G-I) and pregnant (J-L). Virgin mice at age of 5, 8 and 10 weeks old. Pregnant mice at 4, 8 and 12 days of pregnancy. Wnts levels were compared to hPAR1 expression in control (A-F) and *hPar1*+/- transgenic mice (G-L). hPAR1 and Wnts expression were compared to a house keeping control gne levels L19.

**Fig.17 Wnt-4 expression in mammary gland of normal and *hPar1*+/- transgenic mice. I.** Immunohistochemistry staining of Wnt-4 at 13 weeks (A), and age matched *hPar1*+/- transgenic mice (B). Pregnant mice mammary glands (C-F)of control 4&8 days (C, E) as compared to *hPar1*+/- transgenic mice (D and F; respectively). **II.** hPAR1 expression in *hPar1*+/- transgenic mice. In situ hybridization analysis of antisense Par1 riboprobe in mammary gland of virgin and pregnant mice. 13 weeks (A), pregnat 4 days (B) and 8 days (C).

**Fig. 18: Expression of RANK and β-casein in *hPar1*$^{+/-}$ transgenic mice.** Total RNA was extracted from the wild type and *hPar1*$^{+/-}$ transgenic mice glands in different development stages; RT-PCR analysis of β-casein and RANK was performed. β-casein level of expression was evaluated at *hPar1*$^{+/-}$ transgenic mice at pregnancy day 8 (n=4) and day 12 (n=6). While induced levels of β-casein is observed at this time period, in *hPar1*$^{+/-}$ transgenic mice as compared to wild type control mice (n=3&5, respectively), no difference is seen there after [pregnancy 18d (n=7&8) and one day of lactation (n=9&10)]. The difference between wild type and *hPar1*$^{+/-}$ transgenic mice is hard to see (n=7&8-pregnant 12d, 9&10-lactin 1d). The expression of β-casein was sharply reduced both in the wild type (n=11) and the *hPar1*$^{+/-}$ transgenic mice (n=12) at 7d lactation. The virgin 13 weeks old mice (1-wild type & 2 for *hPar1*$^{+/-}$ transgenic mice) also no expression of β-casein was detected. RANK expression, in the *hPar1*$^{+/-}$ transgenic mice is observed after pregnancy at day 8 and increased till one day after lactation (n=4, 6, 8 & 10). The wild type mice also have the same pattern (n=3, 5, 7, & 9) but the expression is lower than the *hPar1*$^{+/-}$ transgenic mice are at a simillar stage.

**Fig. 19: PCNA immunostaining in mammay gland of normal and *hPAR1*$^{+/-}$ transgenic a mcie.** High expression of PCNA is seen in 5-weeks-old of *hPAR1*$^{+/-}$ transgenic mice as compared to the normal mice (A and B, respectively. While the mammary gland proliferation in normal mice were reduced in 10 and 13 weeks (C and D, respectively), the *hPAR1*$^{+/-}$ transgenic mice show high expression of PCNA at a similar stage (D and F, respectively).

**Fig. 20: Syk pattern of expression in normal mammary gland development. I.** Whole mounts analysis of mammary glands of virgin 5W, 8W , 10W and 13W . Syk expression and localization in the pregnant wild type mice at day 4, 8 and 14 days of pregnancy (negative control of 14 days pregnant mice).

**Figure 21:** Morph**ogenesis of MCF10A acini formed in 3D matrigel cultures**. MCF10A cells form growth arrested polarized acinar structures in Matrigel. Morphology of acinar structures formed by MCF10A cells plated in Matrigel for 12 days. Phase – image of acini structure at high magnification is shown. Note the cell-cell contacts and the "hollow-like" inner circle of the acini. Acini were labeled with DAPI, showing the labeled nuclei within the acini. Cell-cell contact within the spheroid is shown by immunofluorescence staining of E-cadherin and β-catenin.

**Figure 22: a. Nearly normal acini formation in 3D cultures, versus highly invasive cell intrusion.** Highly organized cell structure acini of MCF10A cells in 3D Matrigel culture. MCF10A cells, infected with the active V12Ras oncogene show highly disorganized intrusion phenotype in 3D Matrigel culture. Likewise, 3TB cells exhibiting high PAR1 levels and of highly metastatic properties show an invasive phenotype in 3D cultures. These cells (3TB cells) when transfected with the dominant negative form of FAK, FRNK; displayed now highly organized architecture in 3D Matrigel cultures.

**b. Inhibited phosphorylation of FAK following PAR1 activation, in the presence of FRNK.** Among the inhibitory properties of FRNK is the reduced FAK phosphorylation , observed at a concentration where FRNK is well expressed in the cells.

**c. Expression levels of FRNK following transfection in 3TB cells.** Dose dependent transfection of the pCDNA3 plasmid of FRNK, showing FRNK expression levels following Ha-tag antibodies.

**Figure 23: a. Morphogenesis of nearly normal breast epithelial cells containing Syk and malignant cells lacking Syk.**
**b. Syk expression in breast non metastatic and *Par*1 overexpressing cells.** MCF-7 cells transfected with *Par*1 (A) as compared to empty vector transfected MCF7 (B) or parental MCF7 cells (C). Syk expression in V12 constitutively activated Ras (D), nearly normal fibrocystic mammary 10a cells (E) as compared with *in-vivo* activated Ras, highly invasive cells-3TB(F).

**Figure 24: Morphogenesis of Syk-3TB versus 3TB cells in 3D Matrigel cultures.** Phase contrast images of Syk-3TB and 3TB cells in 3D cultures. While 3TB cells exhibit an invasive phenotype regardless of PAR1 activation, Syk-3TB cells show invasive phenotype prior to PAR1 activation. A rounded circular form of cells are observed when PAR1 is activated in Syk-3TB cells, in a dose dependent manner.

**Figure 25: PAR1 activation induces Syk phosphorylation in Syk-3Tb cells.** Kinetics of PAR1 activation shows induced Syk phosphorylation following 15' activation upon IP with Syk and WB with 4G10 anti-p-Tyr antibodies. The level of specific phosphorylation was compared to Syk levels.

**Figure 26: a. Activation of PAR1 in Syk-3TB cells inhibits the otherwise induced JNK phosphorylation following PAR1 activation.** PAR1 activation induces JNK phosphorylation within 15 –30 min activation which declines immediately thereafter. Activation of PAR1 however, in Syk-3TB cells, conveyed an inhibitory effect on JNK phosphorylation showing a marked reduction in the phosphorylation levels. The phosphorylated levels are compared with a house keeping gene β-actin.

**b. cCbl phosphorylation is obtained in Syk-3TB cells following PAR1 activation but not in 3TB activated cells.** Cbl, an immediate substrate of Syk is activated in Syk-3TB cells following PAR1 activation. This however, is not the case in 3TB cells lacking Syk, showing very little or no Cbl phosphorylation. Levels of phosphorylation are compared with Cbl protein levels.

**Figure 27: a. Co-IP of Syk and PAR1 in various epithelial cells.** Immuno complexes prepared by anti PAR1 and were blotted with anti Syk antibodies. In cells containing Syk co-association of PAR1 and Syk is observed. **b.** GST-C-tail is cleaved – off the GST beads and used for specific competition during the Co-IP assay. Inhibition in the levels of Syk is observed in the presence of C-tail PAR1 but not when a non-relevant peptide is used. **c.** Cell lysates prepared and applied onto GST-c-tail. Specific binding of Syk is observed in Syk-3TB cells but not on a control GST beads or when cells lacking Syk were used.

**Scheme: PAR1-c-tail cloned into pGEX2T vector.** PAR1 –C-tail GST fusion protein separated on SDS-gel indicating the correct size of the C-tail of PAR1.

**Figure 28: *Par1* induces angiogenesis *in vivo*.** Matrigel plugs containing Cl13 (SB-2 cells stably transfected with *Par1)* or non-transfected SB-2 cells were injected *s.c.* into the peritoneal cavity of BALB/c mice in a bilateral fashion. Mice were divided into four groups dependent on the nature of the injected cells: Group A (n=9) untreated SB-2 cells; Group B (n=8) SB-2 cells treated with TRAP (100μM, 8 hours); Group C (n=11) untreated Cl13 cells; and Group D (n=12) Cl13 cells treated with TRAP (100μM, 8 hours). **I. Matrigel plugs under phase microscopy**. 10 days after *in vivo* implantation, Matrigel plugs were removed and examined. Matrigel containing SB-2 cells remained pale (A). The appearance of the Matrigel plugs containing SB-2 cells pretreated with TRAP was not significantly different (B). Matrigel plugs containing Cl13 cells exhibited a reddish color (C), which was more pronounced in Cl13 cells pretreated with TRAP (D). Magnification 5X. **II. Histolgical**

**evaluation of Matrigel plugs.** Serial sections were prepared from Matrigel plugs, and processed with Mallory's stain. A. Untreated SB-2 cells B. SB-2 cells pretreated with TRAP C. Untreated Cl13 cells D. Cl13 cells pretreated with TRAP. Magnification X 20.
**III. Quantification of capillary vessels in Matrigel plugs.** Six separate fields of each Matrigel plug stained with H&E and Mallory's' Stain were examined under phase microscopy and capillary vessels were counted. Data shown are representative of at least 3 independent Matrigel plug sets of experiments.

**Figure 29. Inducible *Par1* expression in rat prostatic carcinoma increases tumor mass and angiogenesis. I.** Differential expression of *Par1* in the Dunning rat prostate carcinoma cell variants was observed by RT-PCR using primers specific for PAR1. Primers for L19 were used as a loading control. **II.** Inducible *Par1* expression in a rat prostatic carcinoma cell line - AT2.1. AT2.1 cells were transfected with a plasmid containing the human *Par1* coding sequence under the control of a tet-inducible promoter. Two stably transfected clones, AT2.1/Tet-On/*hPar1* clones 4 and 1, were tested for the inducibility of human *Par1* expression by the tetracycline analog, Dox as evaluated by Northern blot analysis. **III.** AT2.1/Tet-On/*hPar1* clone 4 cells and control transfected (vector only) cells were injected into rats *s.c.* Animals were maintained for 2 weeks with regular drinking water or drinking water supplemented with Dox. After 2 weeks, the tumors were excised and examined. Tumors shown were from animals injected with: A. control transfected cells; B. AT2.1/Tet-On/*hPar1*, clone 4; C. AT2.1/Tet-On/*hPar1* clone 4, fed with Dox for 2 weeks. **VI.** Tumor weight. Data shown are the mean at least 3 independent sets of experiments.

**Figure 30: Expression of VEGF isoforms by stable *Par1*-transfected clones. I. Northern blot analysis of VEGF expression**. Total RNA was prepared from SB-2 cells (A), SB-2 cells transfected with an empty expression vector (B), and two clones stably expressing PAR1: Cl13 (C) and MixL(D). The Northern blot was hybridized with a probe specific for $VEGF_{165}$. The bottom panel shows hybridization to the housekeeping gene L32, as a control for RNA loading. **II. Kinetics of VEGF165 mRNA induction following activation of PAR1.** Cl13 or SB-2 cells were treated with Thrombin (1u/ml) or TRAP (100μM) for the indicated times and RNA levels were analyzed by Northern blot. **III. Dose response of VEGF165 mRNA induction by TRAP.** Cl13 cells were treated with the indicated doses of TRAP for 8 hours. RNA was analyzed by Northern blot. **IV. RT-PCR for the detection of VEGF splice forms in *Par1* transfected cells.** RT-PCR was performed using primers directed to exons 1 and 8 to detect all splice forms. Four different splice forms are detected in Cl13 cells: $VEGF_{121}$, $VEGF_{145}$, $VEGF_{165}$, and $VEGF_{189}$. None, or very little, is seen in non- transfected (SB-2) cells, cells transfected with empty vector (SB-2 Vector) and non-metastatic cells (MCF7). The pattern of expression of *Par1* splice forms in TRAP- or thrombin-activated Cl13 cells is similar to that in highly metastatic cells (MDA435).

**Figure 31: PAR1 activity induces functional VEGF. I. Conditioned medium from Cl13 cells increases the complexity of cell tube formation**. Cultures of endothelial cells in a three-dimensional collagen type I matrix were grown with conditioned media from: A) Non metastatic MCF7 cells transfected with an empty vector; B) Non metastatic MCF7 cells /empty vector cells treated with thrombin; C) control, non metastatic MCF7 cells; D) *Par1* transfected MCF7 cells; E) *Par1* transfected MCF7 cells treated with thrombin; or F) highly metastatic MDA435 cells. **II.**

**Conditioned media from *Par1* transfected cells induce the proliferation of BAEC**. BAEC cells were cultured in the presence of conditioned medium from the indicated cells. Cultures were refed with fresh conditioned medium every two days. At each indicated time point, cells were removed from plates with trypsin/EDTA and counted. The data exhibit a typical experiment representing triplicates. **III. Anti-VEGF antibodies inhibit the effects of activated *PAR1* cell conditioned medium on BAEC proliferation.** BAECs were cultured in the presence of conditioned medium from activated Cl13 cells (TRAP, 8 hours) Anti-VEGF antibodies were added to cultures at varying concentrations as indicated and were present for the entire period of the assay. The effects of conditioned medium from control SB-2 cells and the highly metastatic MDA435 line are shown for comparison.

**Figure 32: Induction of VEGF by PAR1 is mediated by PKC, PI3K and Src.**
**I. Dose response of VEGF mRNA induction by PMA**. Various concentrations of PMA were added to cultures of Cl13 cells and VEGF mRNA levels were determined by Northern blot. RNA from non-transfected, non-metastatic cells was included as a control (lane A). **II. Calphostin C inhibits PAR1-induced increases in VEGF mRNA.** Calphostin C was added to Cl13 cultures at the indicated concentrations 30 minutes prior to addition of TRAP. Cells were harvested after 8 hours of TRAP/ calphostin treatment and VEGF mRNA levels were determined by Northen blot. **III. Wortmannin , a PI3K inhibitor, blocks PAR1-induced increases in VEGF mRNA .** Inhbition by Wortmannin is observed at 1μM (F) and up to 10 μM (G) but not at 0.1 μM (E). **IV. PP-2, an inhibitor of Src, blocks PAR1-induced increases inVEGF mRNA.** Inhbition of VEGF is observed at 10 μM (B), 1 μM (C) as compared to *Par1* transfected cells (A) and parental non transfected cells (G).

**Figure 33: Expression of VEGF mRNA splice forms in *ras*-, *src* -and *vav*-transformed NIH3T3 cells. I. Northern blot analysis of transformed NIH 3T3.** NIH 3T3 cells were transfected with activated *ras* or *src* oncogenes, wild type (w.t.) *vav* proto-oncogene, oncogenic *vav* or an SH2 mutant of *vav*. Total RNA was isolated and 15μg were analyzed by Northern blotting using a probe for $VEGF_{165}$. **II. Quantitation of changes in VEGF mRNA levels in transformed cells.** Photoimage was used to quantitate VEGF165 mRNA levels from Northern blots. VEGF165 mRNA levels were normalized to β-actin mRNA levels to control for loading differences. Data shown are representative of 3 independent experiments. **III. RT-PCR analysis of VEGF splice forms.** A representative RT-PCR experiment shows elevated levels of $VEGF_{121}$, $VEGF_{145}$, $VEGF_{165}$ and $VEGF_{189}$ splice forms in *src*-transformed NIH3T3 cells. *Par1* transfected/activated cells (Cl13/TRAP/8h) and non-transfected SB-2 cells are included as positive and negative controls.

# Fig. 1

## PAR-Protease Activated Receptor family

**PAR-1: Thrombin receptor I**
**hPAR-1 Internal Ligand:**
**AA 37-61 TLDPR SFLLRNP NDK YEPF**

**PAR-2: An orphan receptor**
**hPAR-2 Internal Ligand:**
**AA 32-56 SSKGR SLIGKV DGTSHVTGKG**

**PAR-3: Thrombin receptor**
**hPAR-3 Internal Ligand:**
**AA 34-57 TLPIK TFRGAPP N SFEEFPFSALE**

**PAR-4: Thrombin receptor**
**hPAR-4 Internal Ligand:**
**AA 28-52 LPAPR GYPGQV CANDSDT**

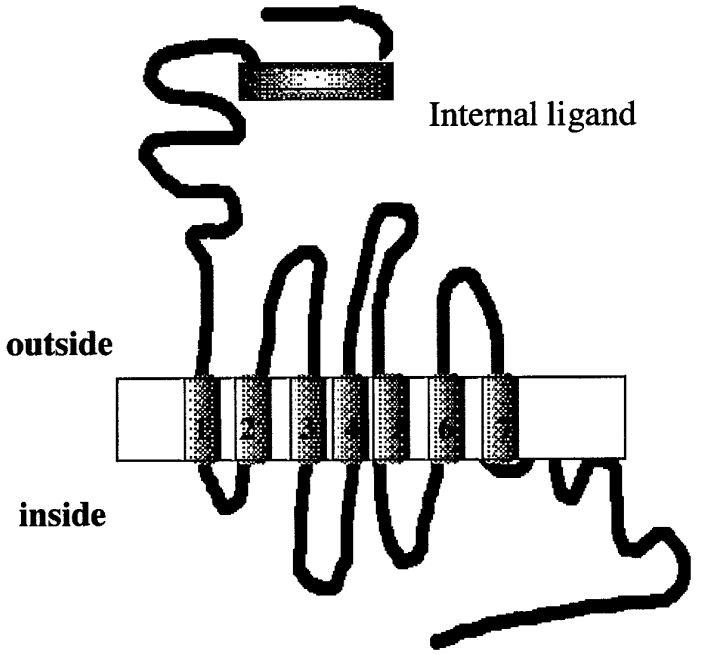


# Fig. 2

## Solid Tumor Development

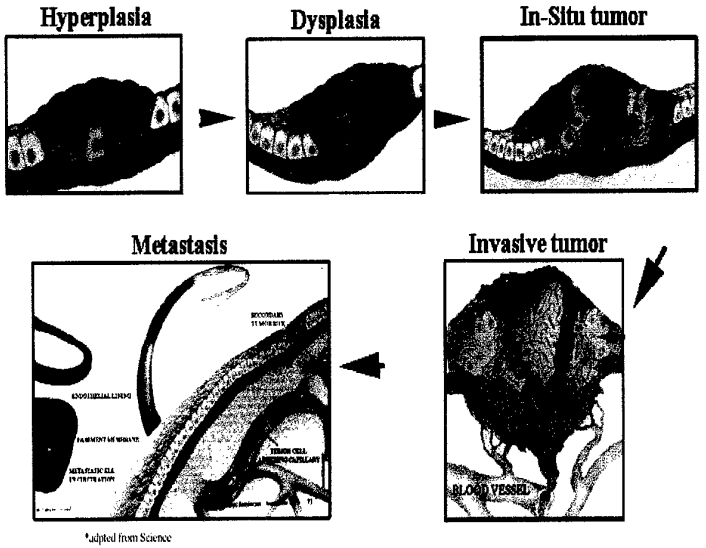

# Fig. 3

## *In situ* hybridization analysis of PAR1 in breast tissue biopsy specimens

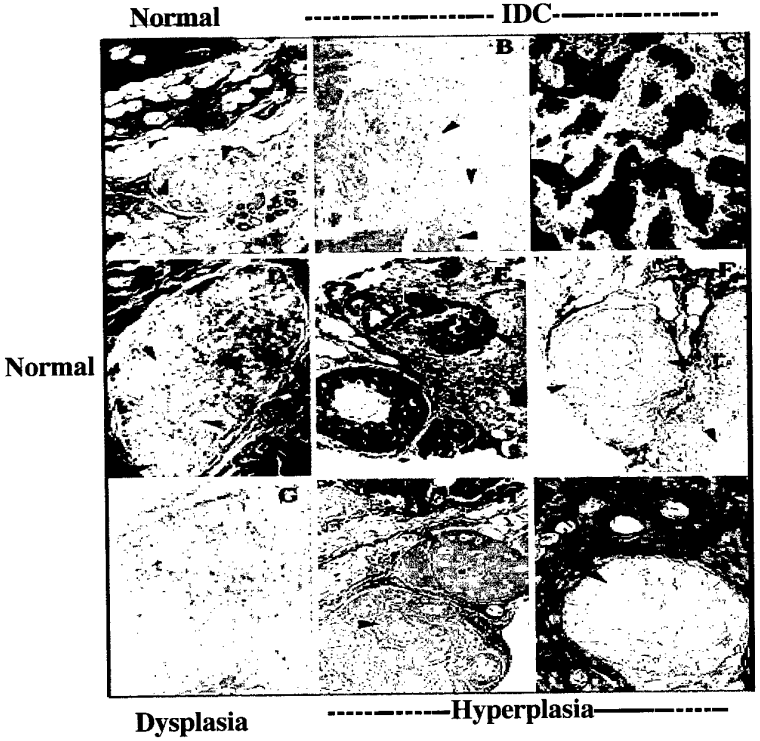


**Fig. 3:** ***In situ*** **hybridization of PAR1 mRNA in normal and cancerous breast tissues specimens.** Riboprobes probes prepared and labeled by T7 RNA polymrerase (for antisense orientation) or T3 RNA polymerase (for sense orientation - control), using DIG-UTP for labeling mix.Top. IDC staining by PAR1 antisense and sense control (A,B; respectively). Middle. DCIS staining by PAR1 antisense and sense control (C,D; respectively). Bottom. Hyperplasia staining by PAR1 antisense and sense control (E,F; respectively).

# Fig. 4

## *Differential expression of PAR1 in Various Metastatic Cell Lines*

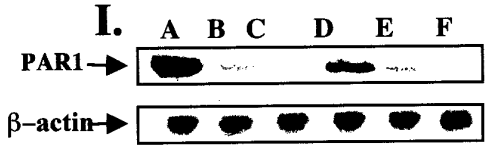


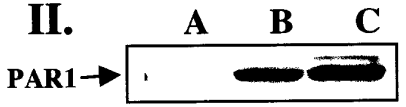


## *PAR1 Antisense inhibits highly metastatic cell invasion*

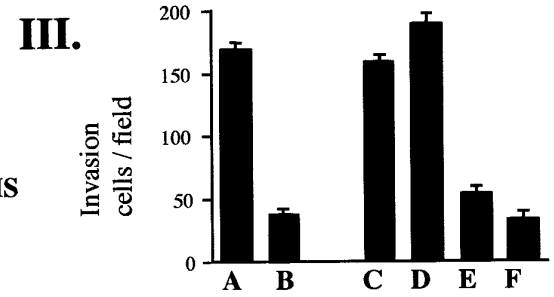


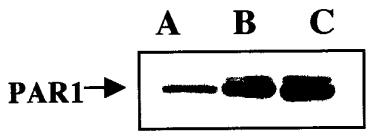


**Fig. 4: PAR1 expression in human breast carcinoma cell lines.** Total RNA isolated from human breast carcinoma cell-lines were analyzed by Northern blotting. These are: MDA-435 (lane A), MDA-231 (lane B) and MCF-7, as well as Ha-ras-transfected breast carcinoma cell lines, MCF10AT3B (lane D), MCF10AT (lane E) and MCF10A (lane F). The blots were probed with $^{32}$P-labeled 250 base pair DNA, corresponding to PAR1 (upper part), or with $^{32}$P-labeled β-actin DNA (lower part).

**II.** Western blot analysis of ThR. Western blot analysis of cell lysates (50 μg/lane) of MCF-7 (lane A), MDA-231(lane B) and MDA-435 cells. Specific protein band was detected following incubation with anti ThR antibodies and visualized by the ECL immunoblotting detection system according to the manufacturer's instructions.

**III.** Inhibiton of MDA-435 Matrigel invasion by PAR1 antisense. MDA-435 cells were transiently transfected with pCDNAIII expression plasmid containing the antisense PAR1 including part of the promoter region (i.e. 462 nucleotides). The level of invasion was compared to untreated MDA-435 (lane A) and MCF-7 (lane B) cells. Control transfections of MDA-435 cells were performed in the presence of vector alone - or DOTAP liposomes alone (Gibco -BRL) (lane D). Nearly confluent (60%) cells were treated with various concentrations of the plasmid: transfection with antisense PAR1 - 5 μg/plate (lane E), transfection with antisense PAR1 - 20 μg/plate (lane F). The invasion assay was performed as described under Materials and Methods, 72 h following transfection.

**IV.** Western blot analysis of PAR1 antisense transfectants. MDA-435 cell lysates (50 μg/lane) of PAR1 antisense transfectants (A) were applied on SDS-PAGE and the level of receptor protein was compared to cells transfected with vector alone (B) or untreated cells.

**Fig. 5**

# PAR3 Expression in Normal and Cancerous Breast

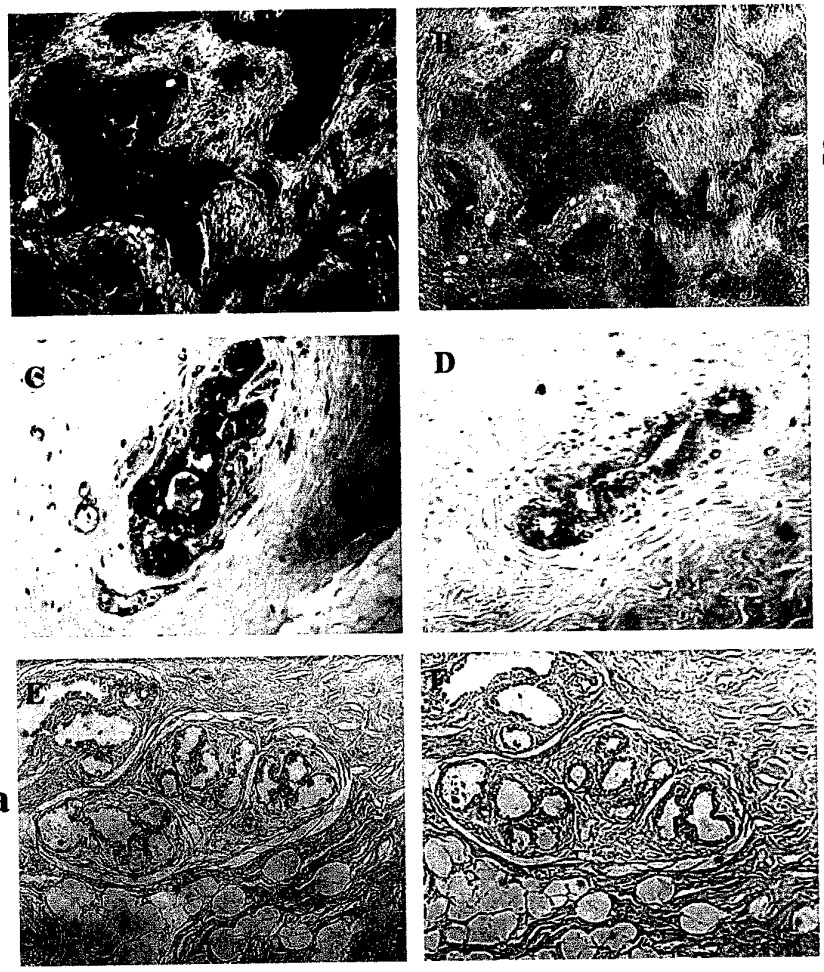


**Fig. 5: *In situ* hybridization of PAR3 in breast carcinoma biopsy specimens.** RNA probes were transcribed and labeled by T7 RNA polymrerase (for antisense orientation) or T3 RNA polymerase (for sense orientation - control), using DIG-UTP for labeling mix. Top panel. IDC (invasive ductal carcinoma) biopsy sample of antisens and sense orientation of PAR1 (*left & right*, respectively). DCIS (ductal carcinoma in situ) antisense and sense (as above, middle panel) and hyperplasia and normal breast tissue (*left & right*, respectively- bottom panel).

# Fig. 6

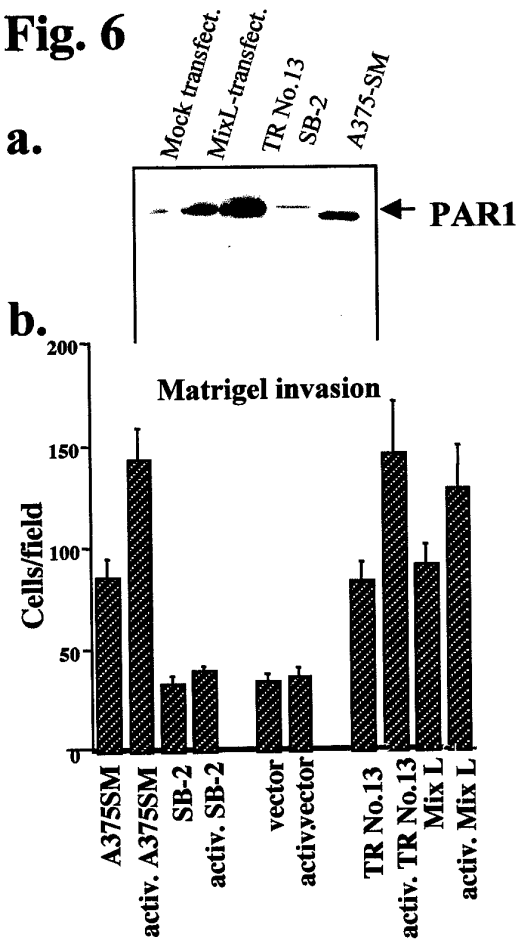


**Fig. 6 Transfection by PAR1 DNA confers invasive properties on non-metatastic melanoma cells.** The expression of PAR1 and cellular invasive properties were measured in SB-2 non-metatastic human melanoma cells, in A375 SM highly metatastic human melanoma cells, in stable PAR1 transfectants clone 13 and clone mL, and in SB-2 cells transfected by mock transfectants. Stable PAR1 clones were screened for PAR1 expression (*a*) using anti-PAR1 thrombin receptor mAbs on a Western blot of 50μg of lysates total protein. (*b*) The invasive capabilities of the selected clones were determined by the Matrigel invasion assay. Cell lines marked "activ." were activated by 1 unit/ml thrombin for 1 h before being used in the invasion assay. The data presented here are the averages of data from at least three replicate experiments.

# Fig. 7 PAR1 activation promotes integrin signaling and invasion

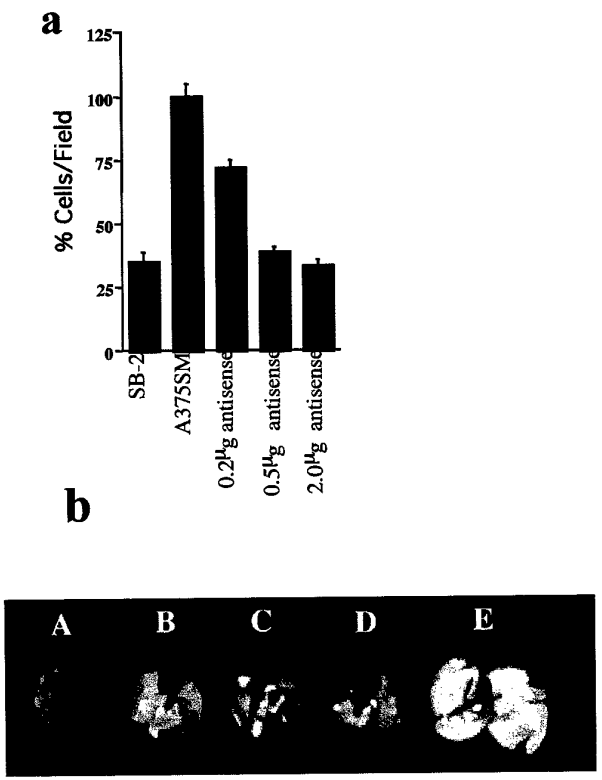


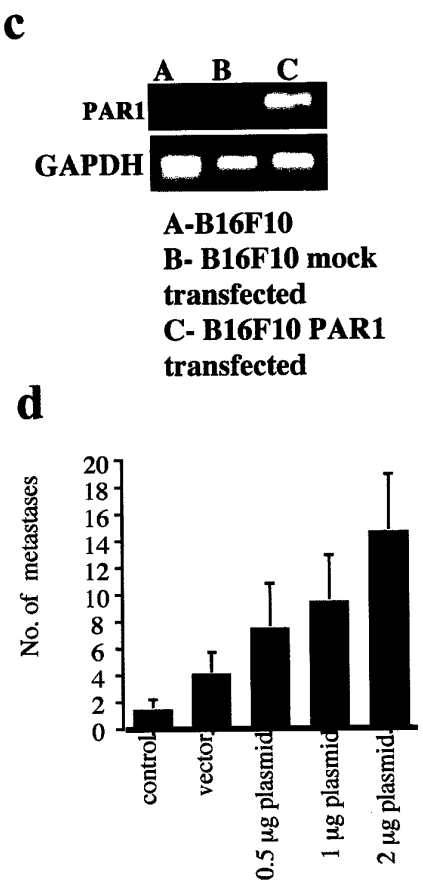


**Fig. 7. Effect of modulation of PAR1 expression on invasiveness.**
*a*, A375SM cells, transiently transfected with PAR1-antisense-containing vector at the indicated concentrations, were tested for their ability to invade through Matrigel-coated filters. The data are representative of at least three replicate experiments.
*b*, Human PAR1 cDNA was used to transiently transfect mouse B16F10 melanoma cells. Two hundred thousand cells were injected into the lateral tail vein of C57BL mice. Mice were killed 14 days later, and the lungs were dissected, fixed, and stained by picric acid solution . A, B16F10 cells; B, vector-transfected B16F10 cells; C, B16F10 cells transfected with 0.5 _g/ml PAR1 plasmid; D, 1 μg/ml PAR1 plasmid; and E) 2 μg/ml PAR1 plasmid.
*c*, Level of PAR1 in B16F10 cells following transient transfection with PAR1 cDNA. RNA was isolated from the cells. RT-PCR was performed, using PAR_ and GAPDH (control) primers. *d*, PAR1-transfected or nontransfected control cells were injected into the tail vein of C57BL mice, and lung metastases were counted after 2 weeks. The numbers indicate mean number of metastases per mouse.

# Fig. 8

## PAR1 activation promotes integrin signaling and invasion

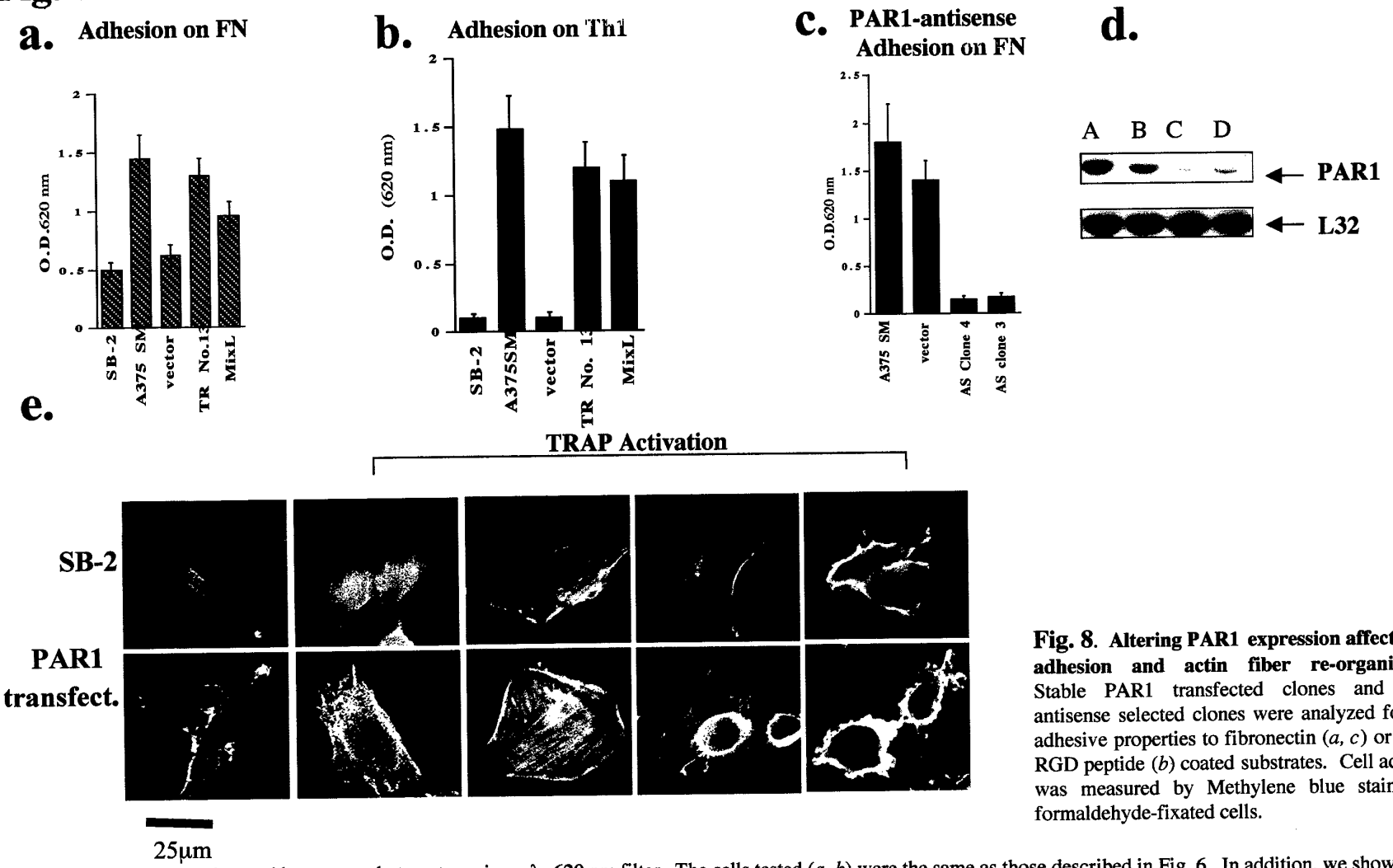


**Fig. 8. Altering PAR1 expression affected cell adhesion and actin fiber re-organization.** Stable PAR1 transfected clones and PAR1 antisense selected clones were analyzed for their adhesive properties to fibronectin (*a, c*) or to Th1 RGD peptide (*b*) coated substrates. Cell adhesion was measured by Methylene blue staining of formaldehyde-fixated cells.

The eluted stain was detected by spectrophotometry using a λ=620 nm filter. The cells tested (*a, b*) were the same as those described in Fig. 6. In addition, we show that in highly metastatic human melanoma A375SM cells stably transfected with PAR1 antisense cDNA (AS clone 4 and AS clone 3) reduced adhesion was observed (*c*) as compared to A375SM or vector. These clones exhibited low PAR1 levels as shown by Northern blot analysis (*d*) of RNA samples from A375SM (A), A375SM cells transfected with vector only (B), AS clone 3 (C) and AS clone 4 (D). The data presented here are the averages of data from at least three replicate experiments. L32 is a ribosomal RNA that we have used as a housekeeping control gene for these experiments. (*e*) SB-2 cells and PAR1 transfectant clone13 were subjected to actin staining by FITC-phalloidin after PAR1 activation by TRAP. Note that the PAR1 transfectants exhibited a more rapid change in actin fiber re-organization and cellular morphology than did the naïve SB-2 cells.

# Fig. 9 PAR1 activation promotes integrin signaling and invasion

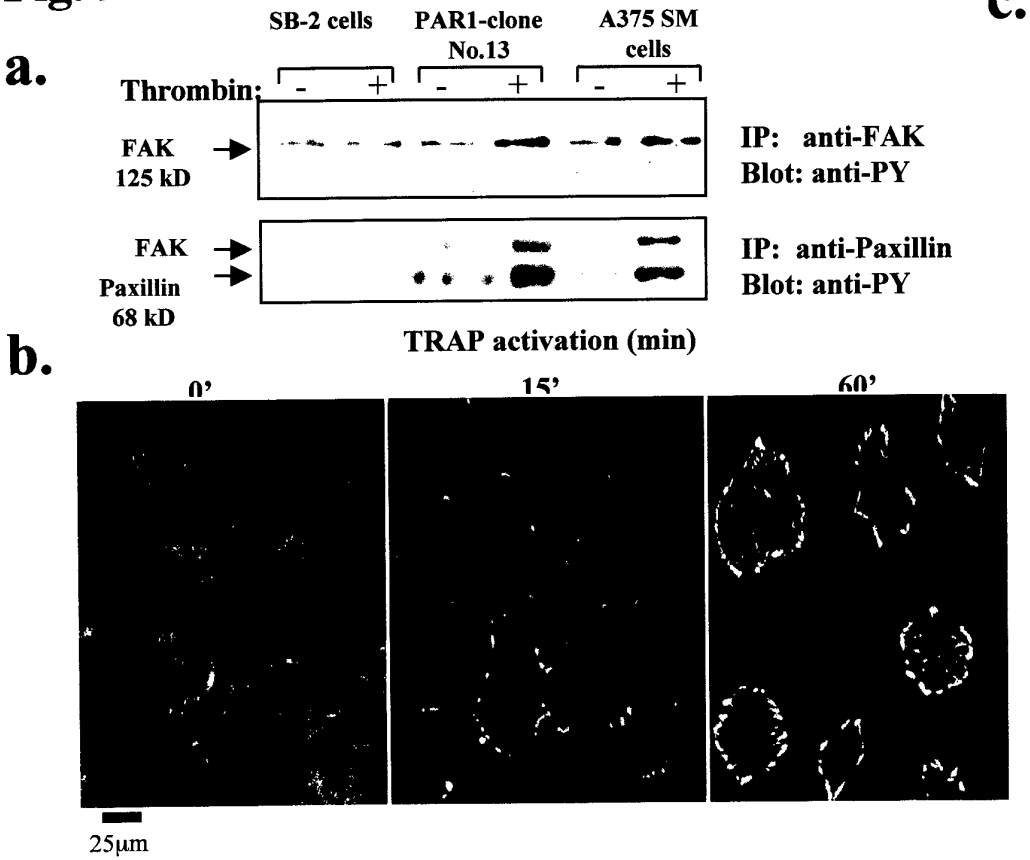


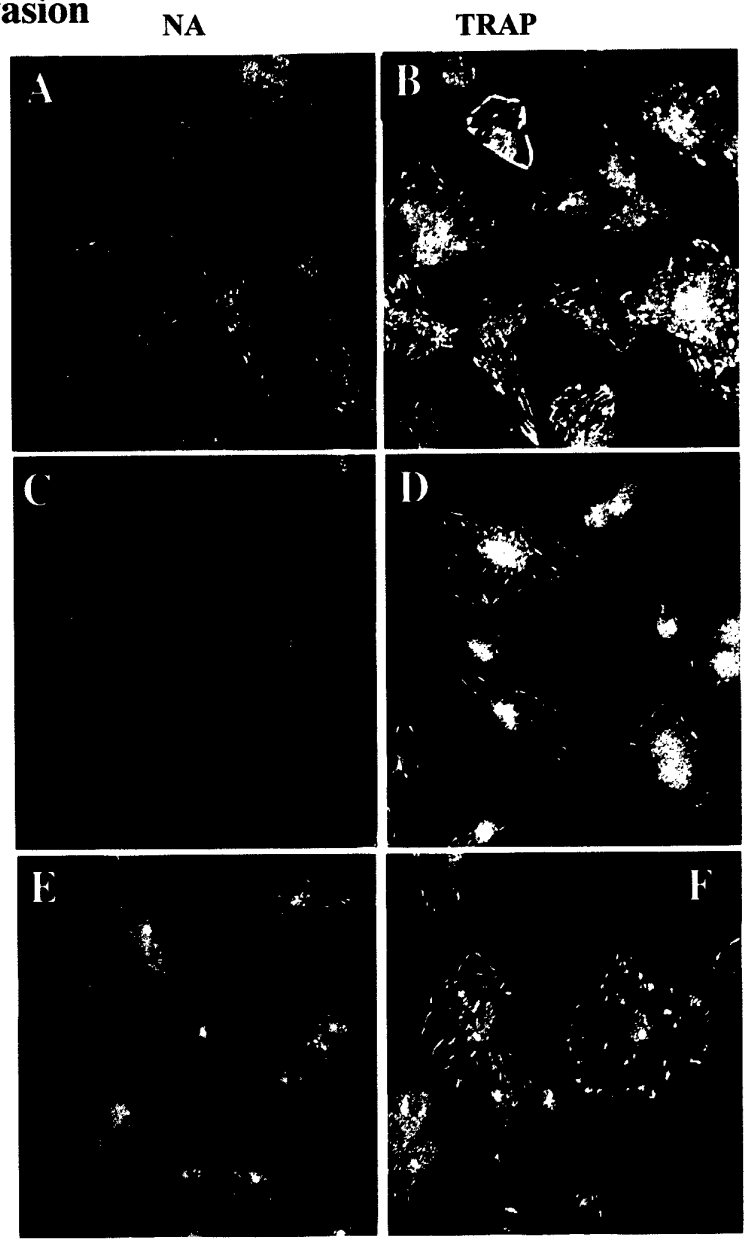


**Fig. 9 Activation of PAR1 induces phosphorylation of FAK and paxillin and their recruitment to FACs.** (*a*) The tyrosine phosphorylated levels of immunoprecipitated FAK (upper section) and paxillin (lower section) were measured by anti-phosphotyrosine mAb (4G10, UBI) in SB-2 naïve cells, in A375SM metastatic cells, and in the stable PAR1 transfectant clone 13. Note that FAK was observed to co-precipitate with paxillin (lower section). (*b*) Immuno-fluorescent staining of phosphotyrosine in PAR1 transfected clone 13 was performed by specific incubations with mAbs (4G10) at 0, 15, and 60 min. Detection was made by Cy3-labeled goat anti-mouse IgG, using confocal microscopy. Following activation by 100μM TRAP, thefocal adhesion contacts (FACs) were observed to be enriched with phosphorylated proteins with a peak at60 min. (*c*) Immuno-fluorescent staining with anti-vinculin, anti-FAK, and anti-paxillin in the stable PAR1 transfectant clone 13 activated with 100μM TRAP for 1 h or not (NA). When the cells were stained with anti-FAK and anti-paxillin, distinct FAC staining was observed only in the activated cells. When the cells were stained with anti-Vinculin, FACs were detectable at a low level in the non-activated (NA); this level was increased following receptor activation by TRAP.

# Fig. 10

## PAR1 activation promotes integrin signaling and invasion

a.

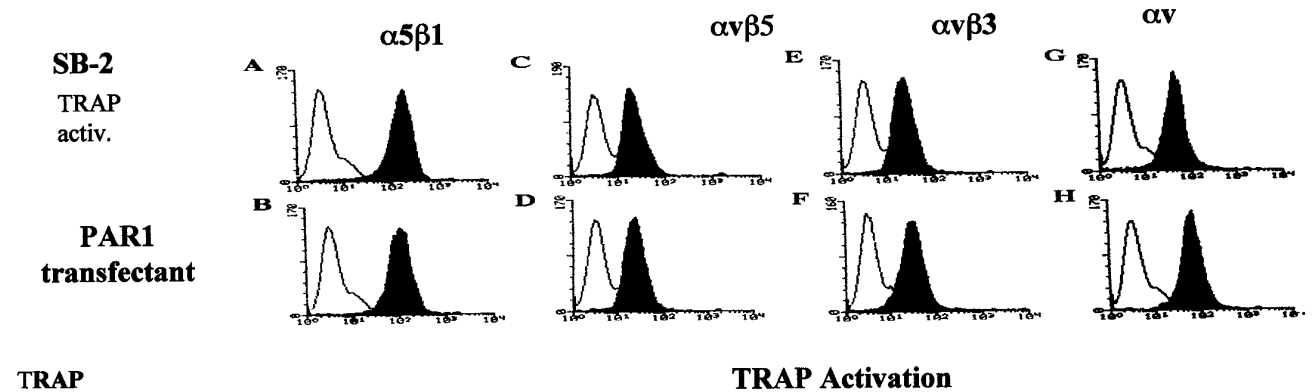


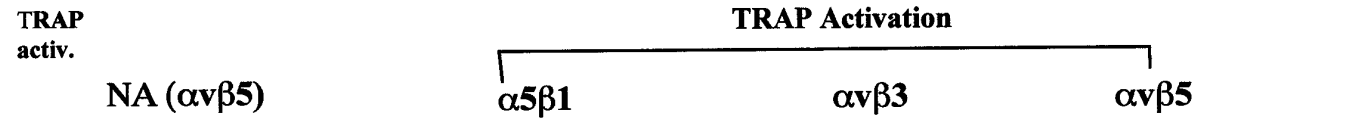


b.

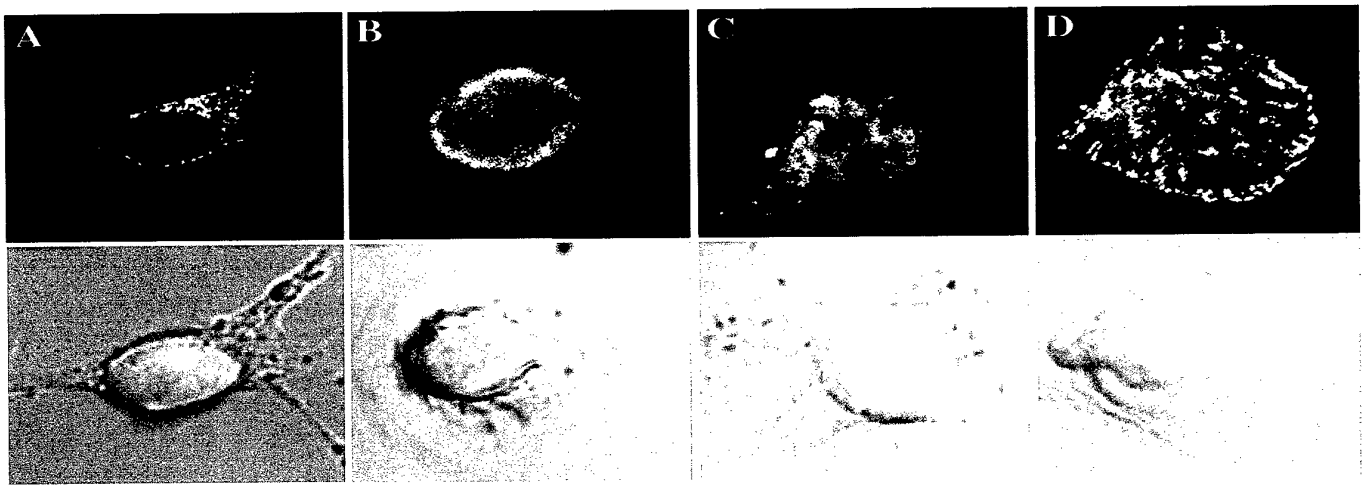


**Fig. 10 PAR1 activation did not alter the levels of integrin expression but did induce αvβ5 recruitment to FACs.** (*a*) Integrin expression levels were measured by flow-cytometry in SB-2 naïve cells and in PAR1 clone13, each activated with thrombin at a concentration of 1 unit/ml. The levels of α5β1 (A, B), αvβ5 (C, D), αvβ3 (E, F) and the integrin αv chain (G, H) were detected by incubating the cells with the appropriate specific mAb, followed by incubation with FITC-labeled anti-mouse IgG. Note that no significant changes were observed in the levels of any of the integrins examined. (*b*) The distribution of integrins was detected by immuno-fluorescent staining (upper panel). Cy-3 red fluorescence was visualized by confocal microscopy. The lower panel shows the same cells as in the upper panel, but visualized by phase-contrast microscopy. Non-activated (NA) PAR1 clone 13, stained by anti-αvβ5 mAbs revealed a diffused pattern (A). After activation by TRAP, the integrin α5β1 was detected in a random peri-nuclear position (B); the integrin αvβ3 was randomly scattered over the cell membrane (C); the integrin αvβ5 was localized to distinct "spikes" of focal adhesion contacts (D).

# Fig. 11

## PAR1 activation promotes integrin signaling and invasion

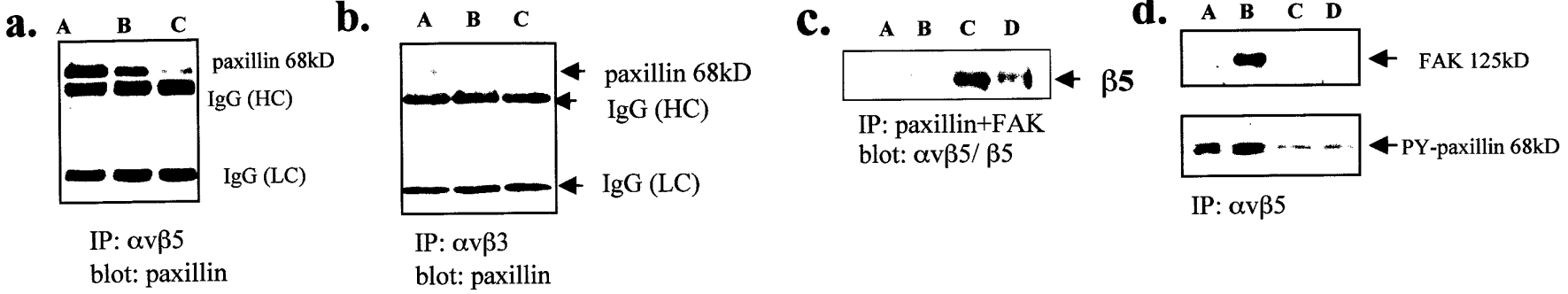


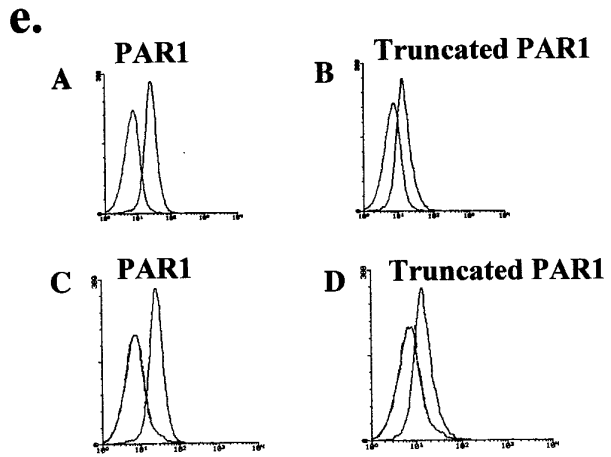


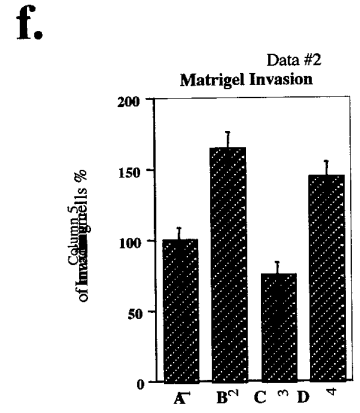


**Fig. 11 . Activation of full length PAR1 but not of truncated PAR1 lead to the co-precipitation of αvβ5 with paxillin and FAK and reduced invasiveness in the presence of anti-αvβ5 antibodies.** Co-precipitation of paxillin with αvβ5 (*a*) or with αvβ3 (*b*) was measured in cells lysates of naïve SB-2 cells (C) and of a stable PAR1 tramsfectant clone13 that was either thrombin-activated (A) or not (B). (*c*) Paxillin and FAK were immuno-precipitated from cell lysates of SB-2 cells that had been thrombin activated (A) or not (B) and from a stable PAR1 transfectant clone 13 that was either thrombin-activated (C) or not (D). The blotted membrane was incubated with anti- β5 subunit mAb. (*d*) Non-invasive MCF7 cells, naturally expressing very low levels of PAR1, were transfected with cDNA expression vectors coding either for PAR1 or for truncated-PAR1. In lysates of the PAR1 transfectants, co-precipitation of FAK and paxillin was detected after PAR1 activation by thrombin (B) but not without activation (A). In lysates of truncated-PAR1 transfectants, no co-precipitation of FAK with paxillin with αvβ5 was observed regardless of whether the cells were thrombin activated (D) or not (C). Tyrosine phosphorylated paxillin co-precipitated with αvβ5 (lower panel) in PAR1-transfected cells (A); the level of this precipitation increased following thrombin activation of PAR1 (B); in truncated-PAR1 transfected cells, only minor levels of phosphorylated paxillin were detected with (D) or without (C) thrombin activation. (*e*) FACS analysis of MCF7 cells following transfection by DNA coding for the full length PAR1 (A and C) or for the truncated-PAR1 (B and D) was shown. Their levels were compared to non-transfected cells (first peak, B and A). This is true also when PAR1 or truncated PAR1 expression was measured relative to empty vector transfected cells (first peak, C and D; respectively). (*f*) A375SM cells were activated with 1 unit/ml thrombin (B, C, D) or not (A). The activated cells were then treated with 20 μg/ml of either anti-αvβ5-blocking mAbs (C) or non-specific IgG (D). The treated cells were then subjected to a Matrigel invasion assay. The data presented here are the averages of data from at least three replicate experiments. One hundred percent invasion by the metatastic cells corresponded to 48±3 invading cells as compared to 17±1.5 invading cells by SB-2 non-metastatic cells (data not shown).

**Scheme: Molecular Mechanism of PAR1 Cross-Talk with Integrins**

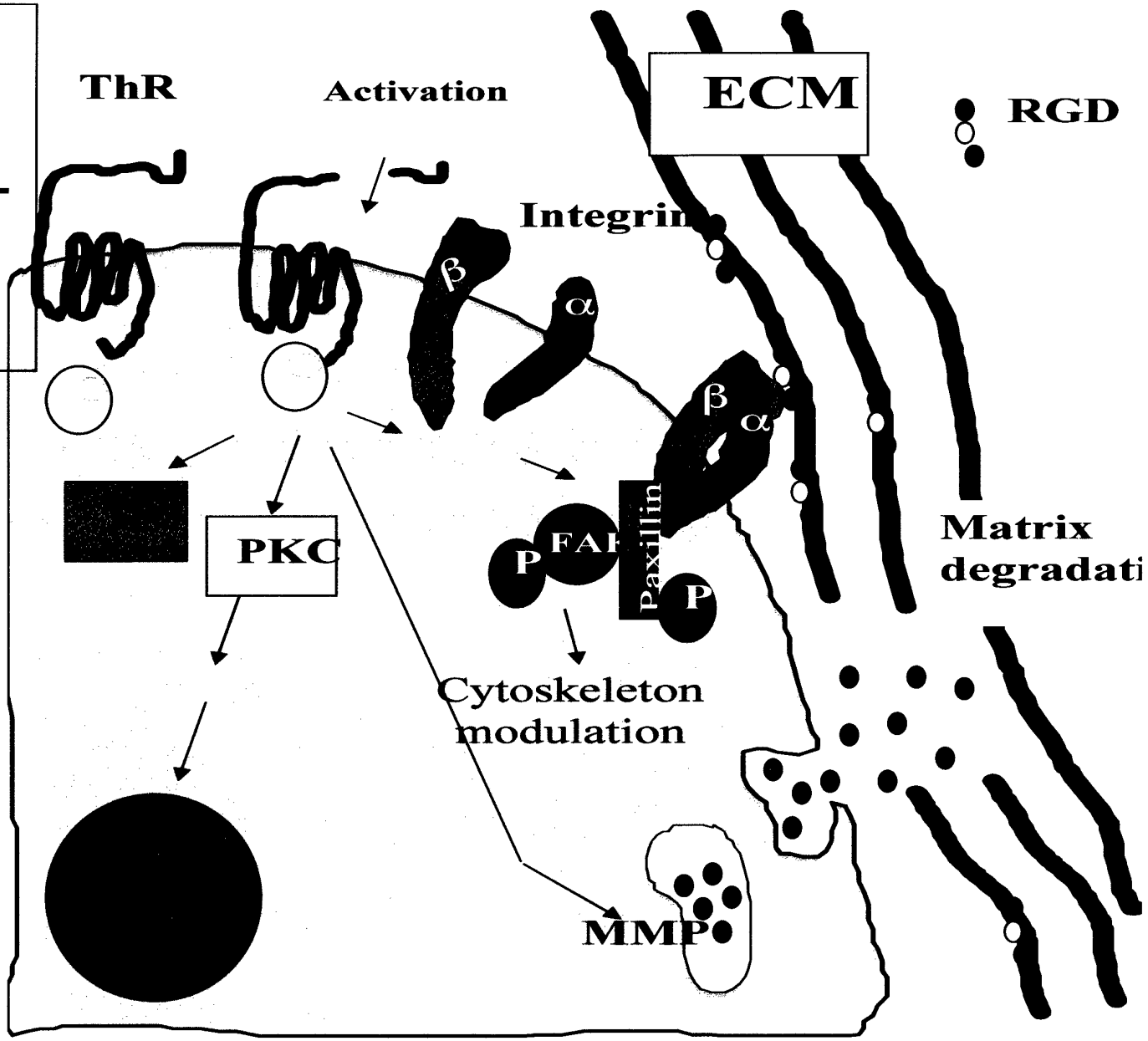

# Fig. 12

**MMTV-*hPAR1* transgenic construct**

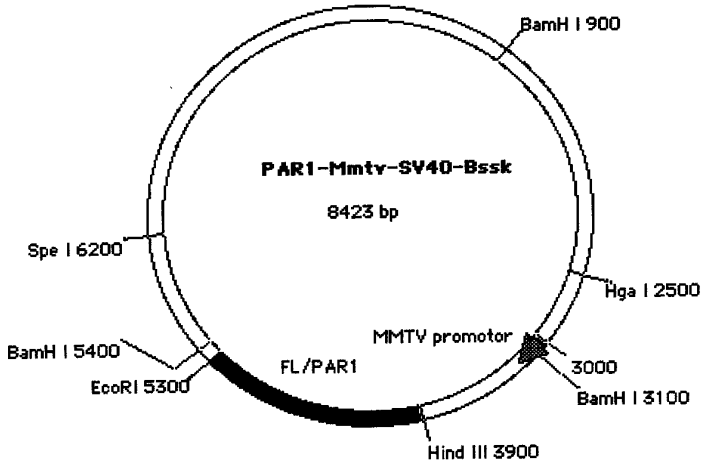


**Fig12. MMTV-*hPAR1* transgenic construct.** Full length human *Par1* (1.4kb) was inserted into the multiple cloning site between HindIII and EcoRI. The plasmid was digested with the restriction endonucleases HgaI and EcoRI to generate the DNA fragment for injection.

**Fig 13II. RT-PCR analysis shows the expression of human *PAR1* transgene in different organs of a transgenic mouse.** The experiment is a representative of at least 5 mice tested.

1. Mammary 2. Ovary 3. Brain 4. Colon
5. Heart 6. Kidney 7. Lung 8. Spleen
9. Salivary 10. Liver 11. Positive control

# Fig. 13

**I. a. Genomic DNA/Mice tail Southern Blot**

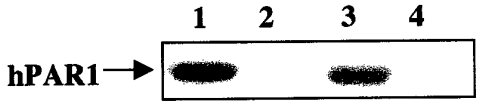


**b. Genomic DNA/Mice tail PCR**


**Southern Blot of genomic DNA: Identification of homozygous mice**

**c.**

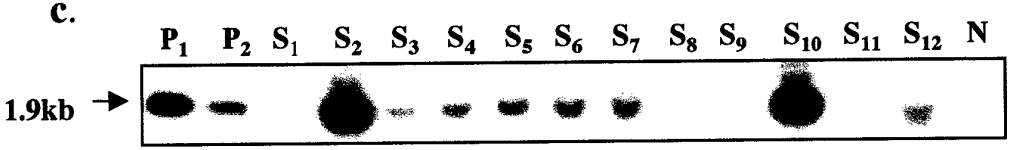


**Fig 13I. MMTV-*hPAR1* transgenic lines**

Genomic DNA was extracted from tails of the founder mice, ***(a)*** Southern blot and **(b)** PCR were performed. 1: positive control; 2: negative control; 3:transgenic founder; 4: non-transgenic mouse. ***(c)*** Identification of homozygous mice with Southern blot. $S_1$-$S_{12}$: all $F_2$ pups; $P_1$ and $P_2$: positive control; N: negative control.

**II. Expression of hPAR1 in different organs of a representative transgenic mouseRT-PCR analysis**

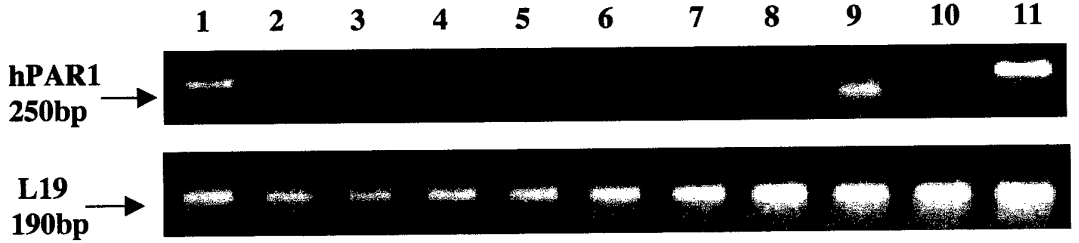

Fig. 14

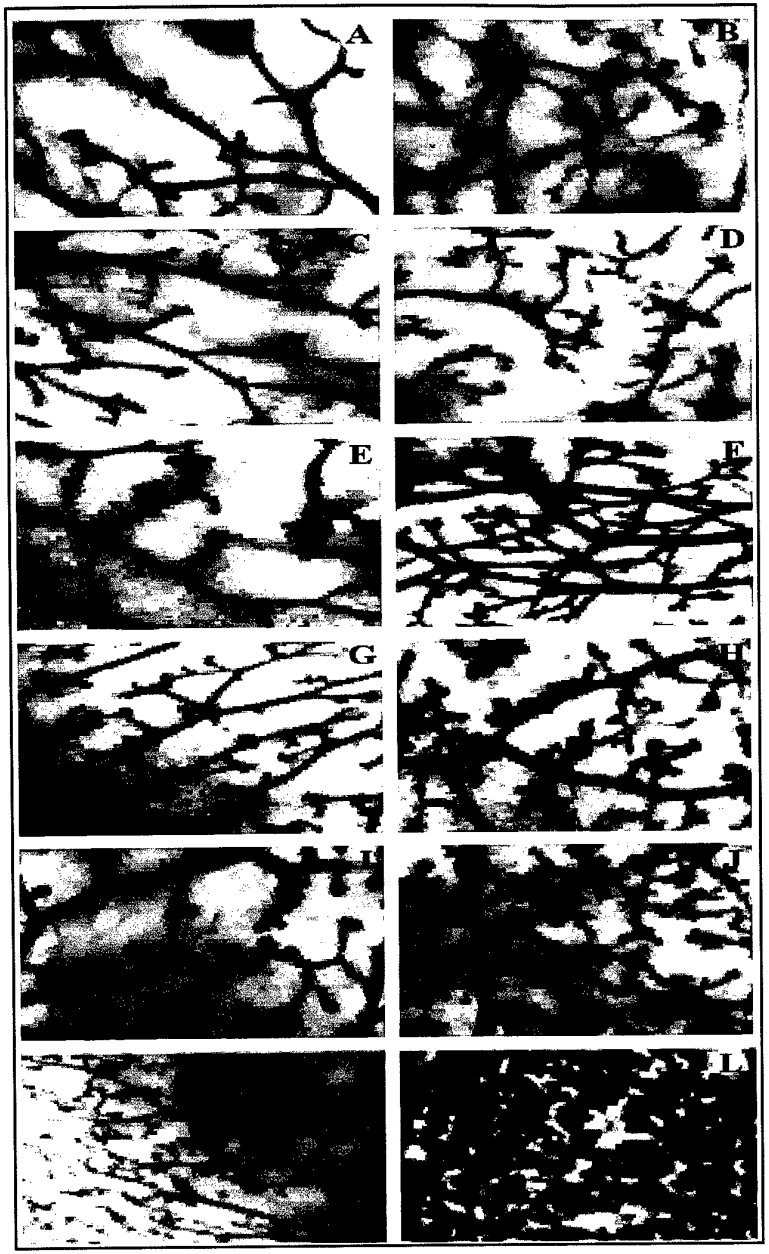


## Whole mount histology of *hPar1*$^{+/-}$ Mammary gland

**Fig. 14. Whole mounts analysis of *hPar1*$^{+/-}$ transgenic mice.** MMTV-LTR driven *hPar1* overexpressed in the mammary gland were analyzed by whole mounts. Mammary glands of 5,8, &10 weeks old virgin normal mice (A,C,E) and *hPar1*$^{+/-}$ mice (B,C &F). Normal pregnant mice of 4, 8 and 12 days (at 13 weeks of age)(G,I &K) as compared to age matched hPar1 (H, J &L).

# Fig. 15 *In situ* hybridization analysis of *hPar1*$^{+/-}$ transgenic mammary glands

I.

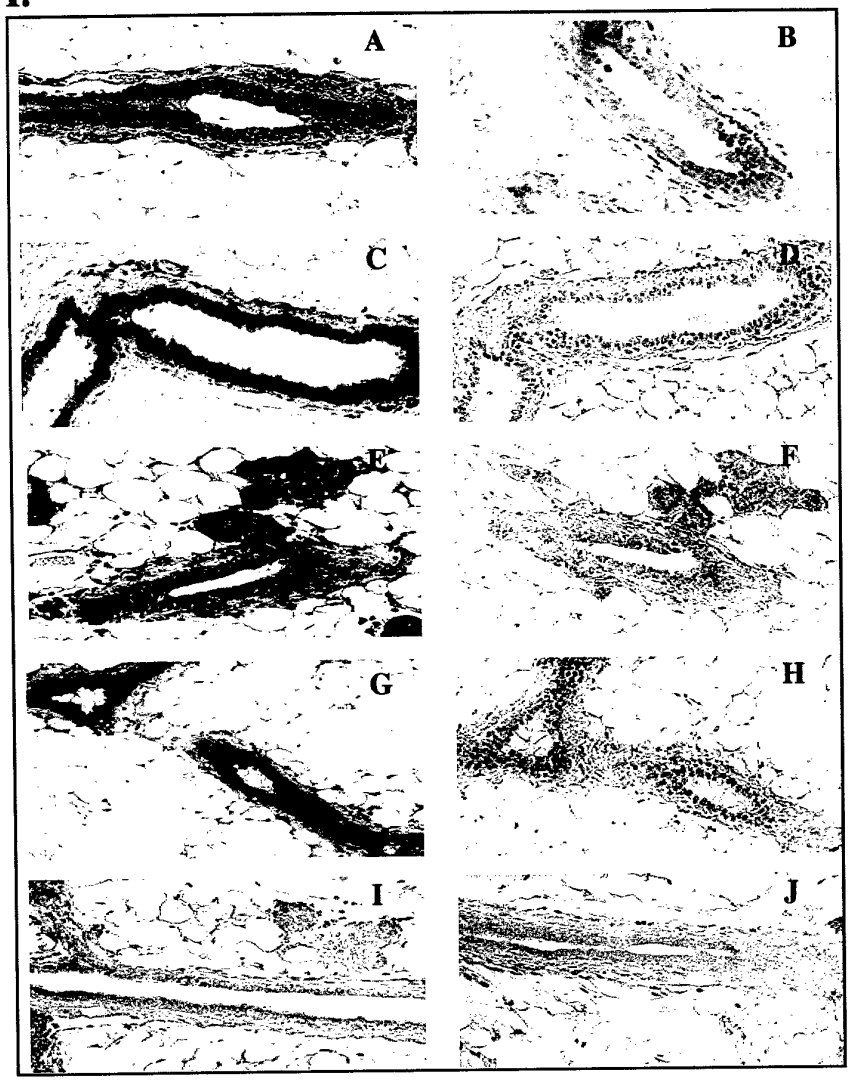


II.

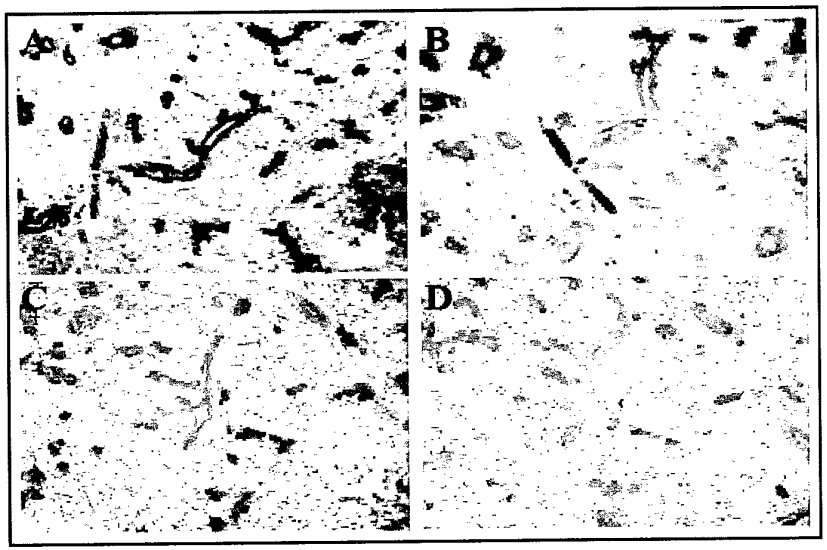


**Fig.15.** ***In situ*** **hybridization analysis of** ***hPar1***$^{+/-}$ **transgenic mammary glands. I.** hPAR1 expression in 10 weeks old virgin (A, B; antisense and sense respectively), pregnant 13 weeks/4day(C, D; antisense and sense respectively), 8days pregnancy (E, F; antisense and sense respectively), 12 days pregnancy (G, H; antisense and sense respectively). Magnification of X20. **II.** Low power magnification (X5) of hPAR1 in *hPar1*$^{+/-}$ transgenic mice of 8d pregnancy (A, B; antisense and sense respectively). Normal age matched mice (C, D; antisense and sense respectively).

# Fig.17

**Wnt-4 expression in mammary gland of *w.t.* and *hPar1*$^{+/-}$ transgenic mice**

**I.**

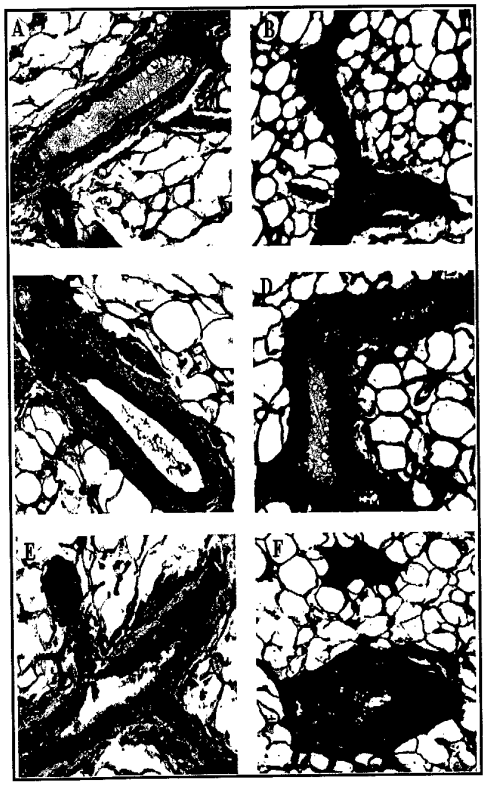


| | |
|---|---|
| A. *WT* 13w | B. *hPar1*$^{+/-}$ 13w |
| C. *WT* P4d | D. *hPar1*$^{+/-}$ P4d |
| E. *WT* P8d | F. *hPar1*$^{+/-}$ P8d |

**II.**

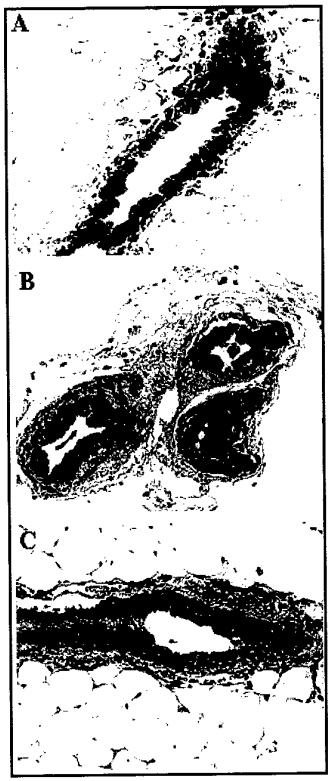


A. *hPar1*$^{+/-}$ 13w

B. *hPar1*$^{+/-}$ P4d

C. *hPar1*$^{+/-}$ P8d

# Fig.16

**RT-PCR analysis of Wnts in *hPar*$^{+/-}$ transgenic mice**

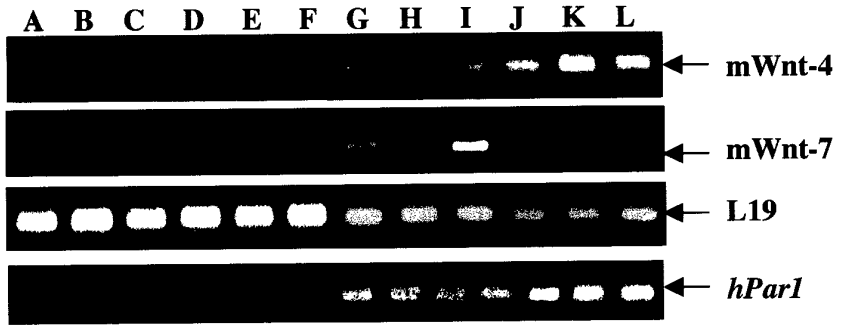


| | | | |
|---|---|---|---|
| A. *WT* 5w | D. *WT* P4d | G. *hPar1*$^{+/-}$ 5w | J. *hPar1*$^{+/-}$ P4d |
| B. *WT* 8w | E. *WT* P8d | H. *hPar1*$^{+/-}$ 8w | K. *hPar1*$^{+/-}$ P8d |
| C. *WT* 10w | F. *WT* P12d | I. *hPar1*$^{+/-}$ 10w | L. *hPar1*$^{+/-}$ P12d |

**Wnt-4 expression in**

***hPar1*$^{+/-}$ transgenic and *w.t.* mice**

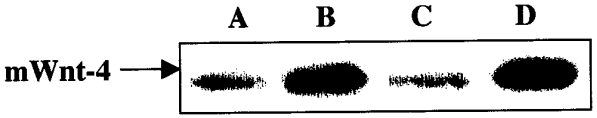


| | |
|---|---|
| A.. *WT* P8d | C. *WT* P12d |
| B. *hPar1*$^{+/-}$ P8d | D. *hPar1*$^{+/-}$ P12d |

Fig. 18

# RANKL, RANK and β-casein, expression in *hPar1*$^{+/-}$ transgenic mice

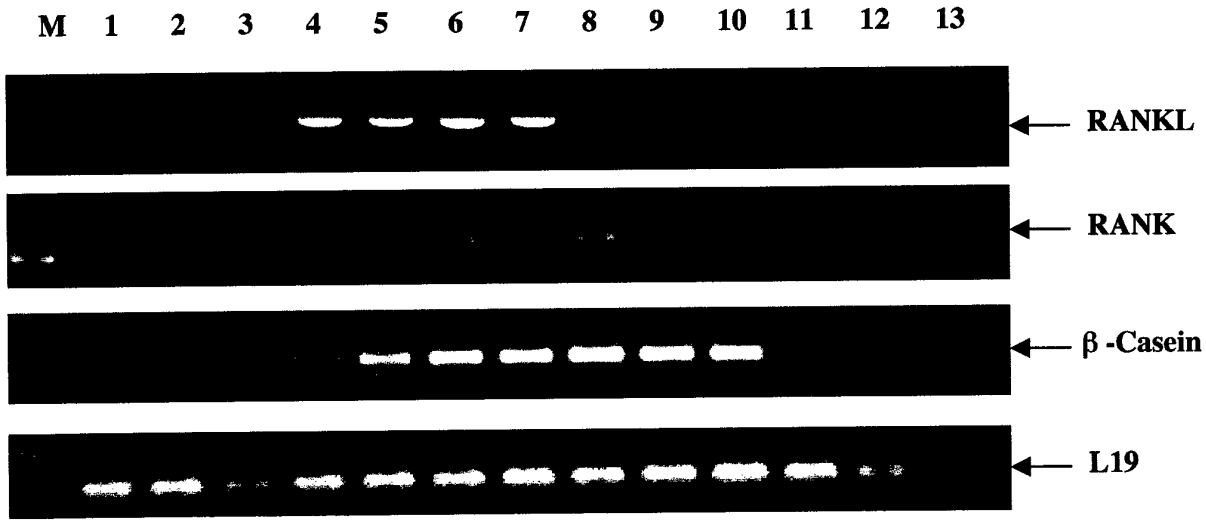


| | | | |
|---|---|---|---|
| 1. CB6/F1 13W | 5. CB6/F1 P12d | 9. CB6/F1 L1d | 13. Negativ control |
| 2. *hPar1*$^{+/-}$ 13W | 6. *hPar1*$^{+/-}$ P12d | 10. *hPar1*$^{+/-}$ L1d | |
| 3. CB6/F1 P8d | 7. CB6/F1 P18d | 11. CB6/F1 AL7d | |
| 4. *hPar1*$^{+/-}$ P8d | 8. *hPar1*$^{+/-}$ P18d | 12. *hPar1*$^{+/-}$ AL7d | |

**Fig. 19** **PCNA immunostaining in mammay gland of normal and *hPar1*$^{+/-}$ transgenic and mcie**

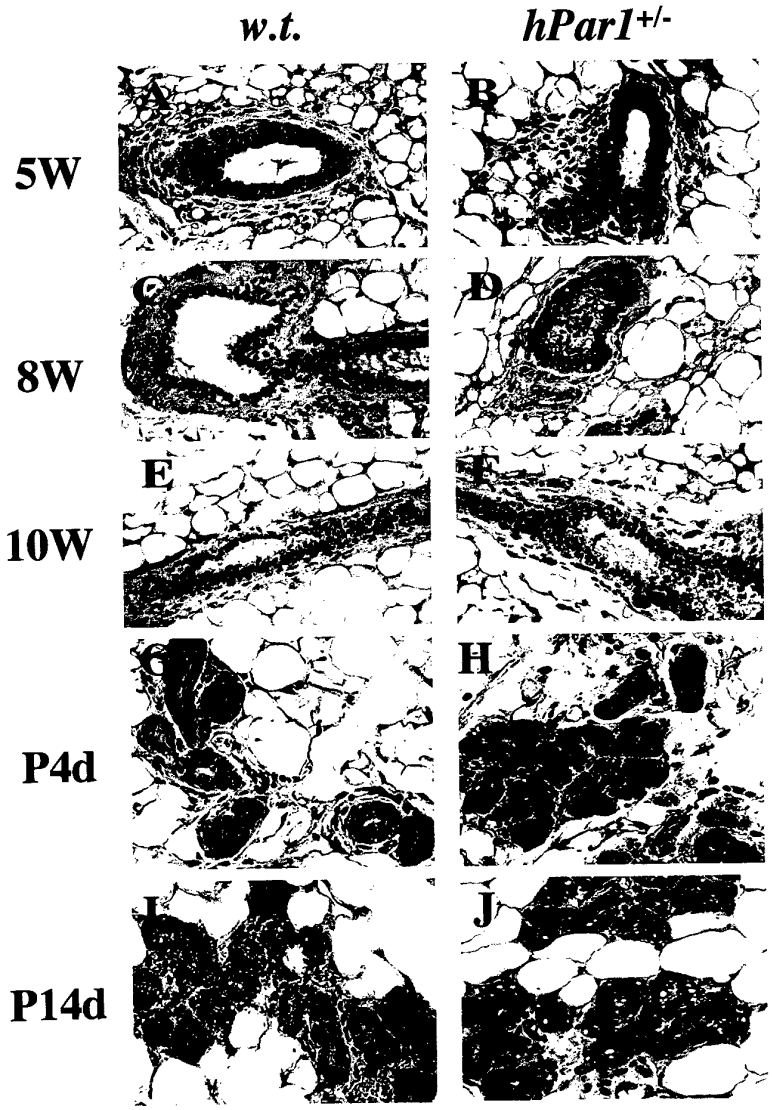


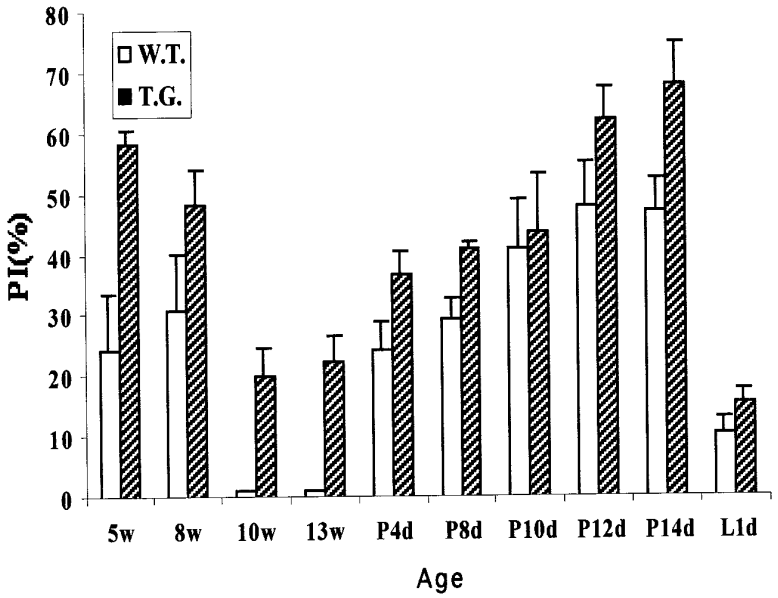


The proliferation index (**PI**) was defined as the number of PCNA-positive nuclei of mammary gland epithelial cells/total nuclei(500).

**Fig. 20**

## Syk expression in the mammary gland of *w.t.* mice

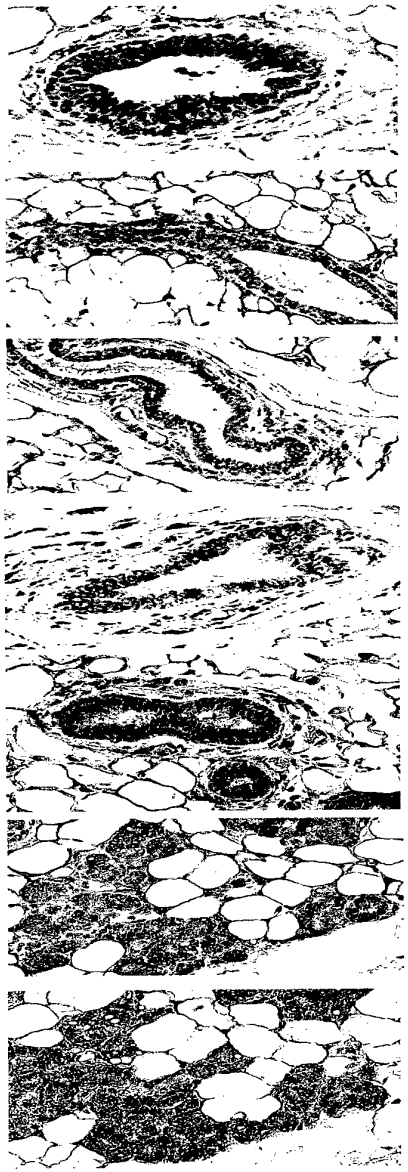


Immunostaining of Syk in mammary gland. Syk expression is observed in 5W of virgin mice and during pregnancy.

Fig. 21

# Morphogenesis of MCF10A in 3D Matrigel Cultures

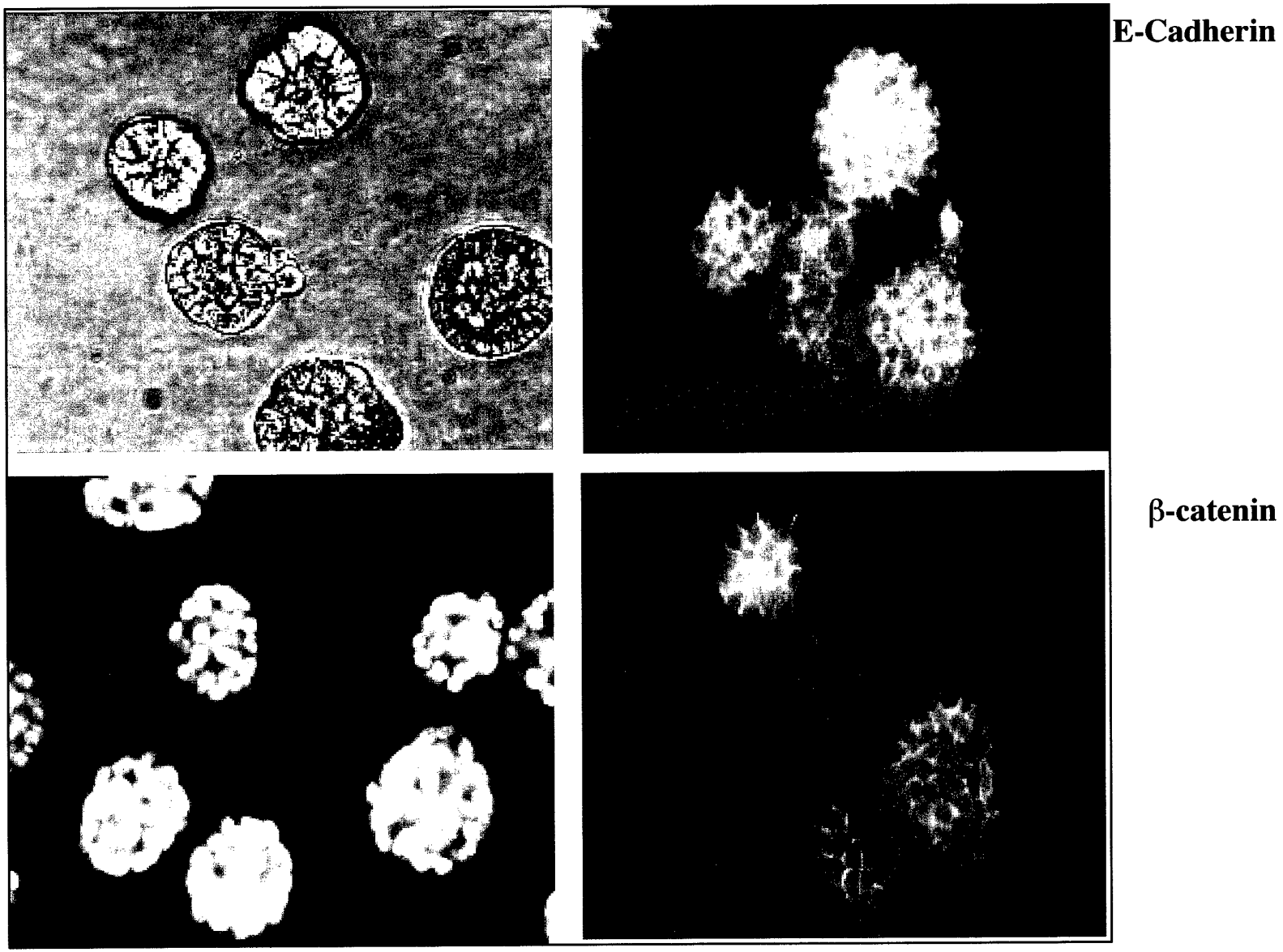

Fig. 22

a. Morphogenesis assay in 3D Matrigel cultures

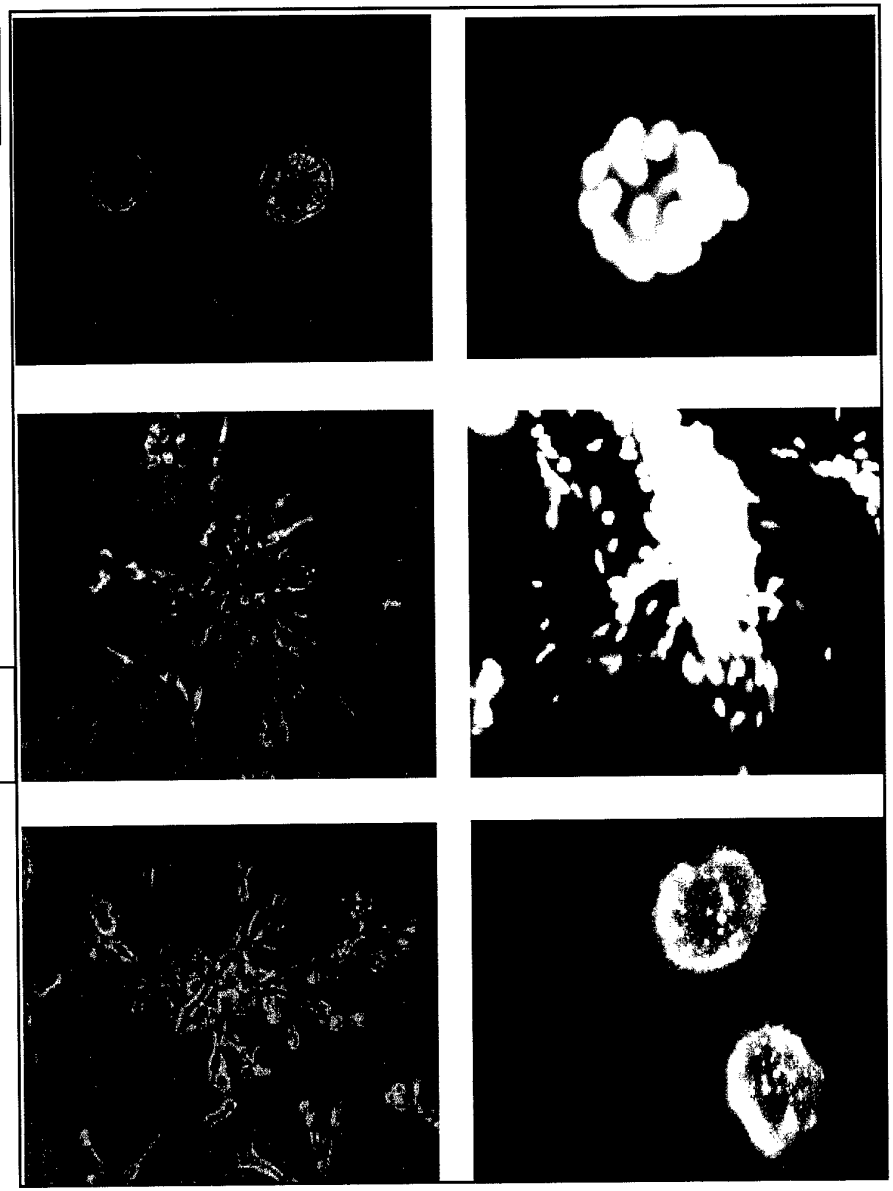


b.

Dominant negative FRNK: Inhibited phosphorylation & Level of expression

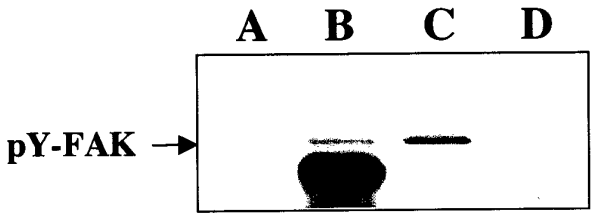


c. Expression levels

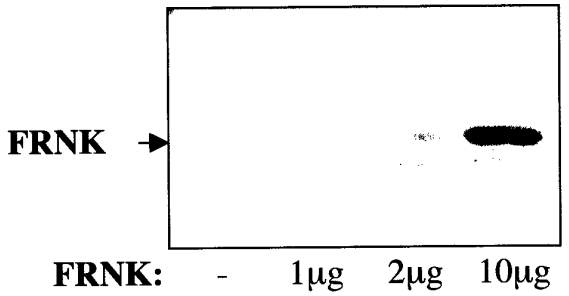


FRNK transfected 3TB Morphogenesis assay

Fig. 23

a.

**Morphogenesis of normal and invasive breast cells**

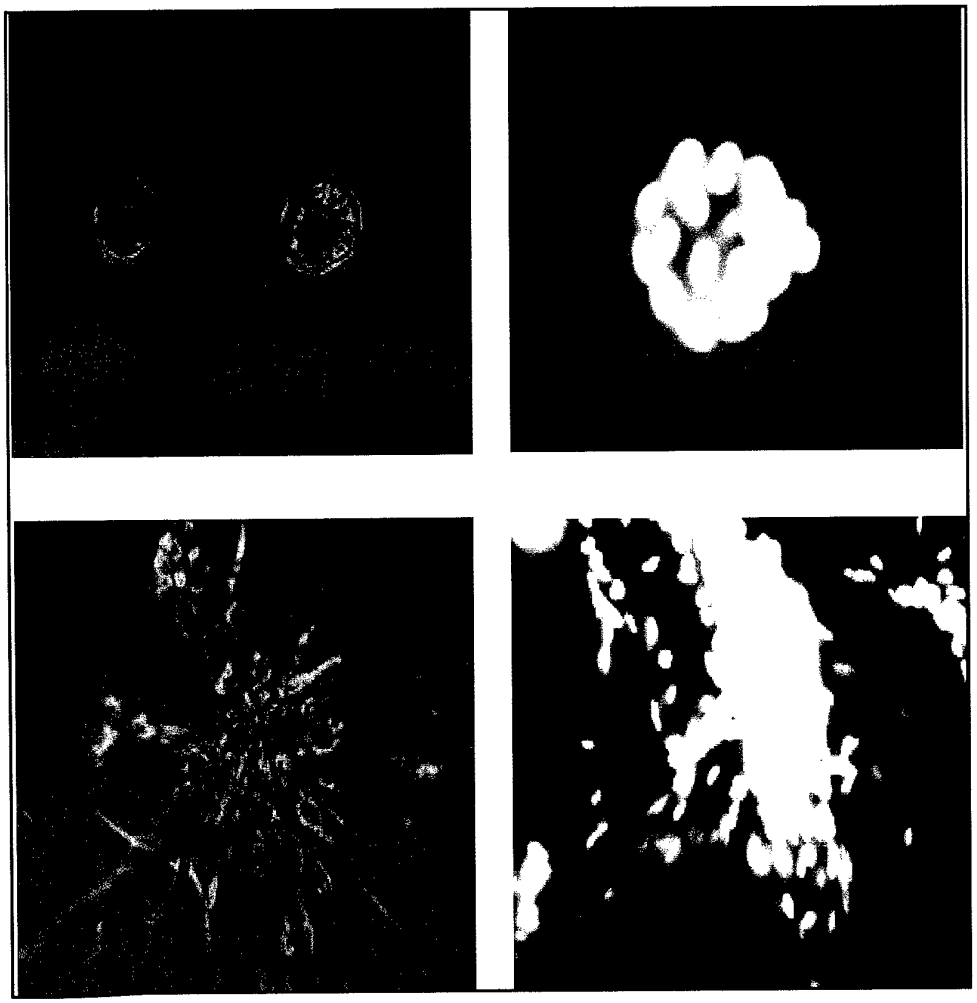

b.

**Syk expression levels in Normal and malignant breast Epithelial cells**

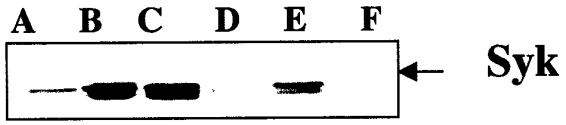


A. PAR1 transfected MCF-7 cells
B. MCF7/ empty vector transfected cells
C. Non metstatic breast MCF7 cells
D. 10A V12 Ras transfected highly metastaic cells
E. Parental 10A cells/non metastatic
F. 3TB Ras transfected 10A cells /metastatic

**Morphogenesis of Syk-3TB following PAR1 activation**

**Fig. 24**

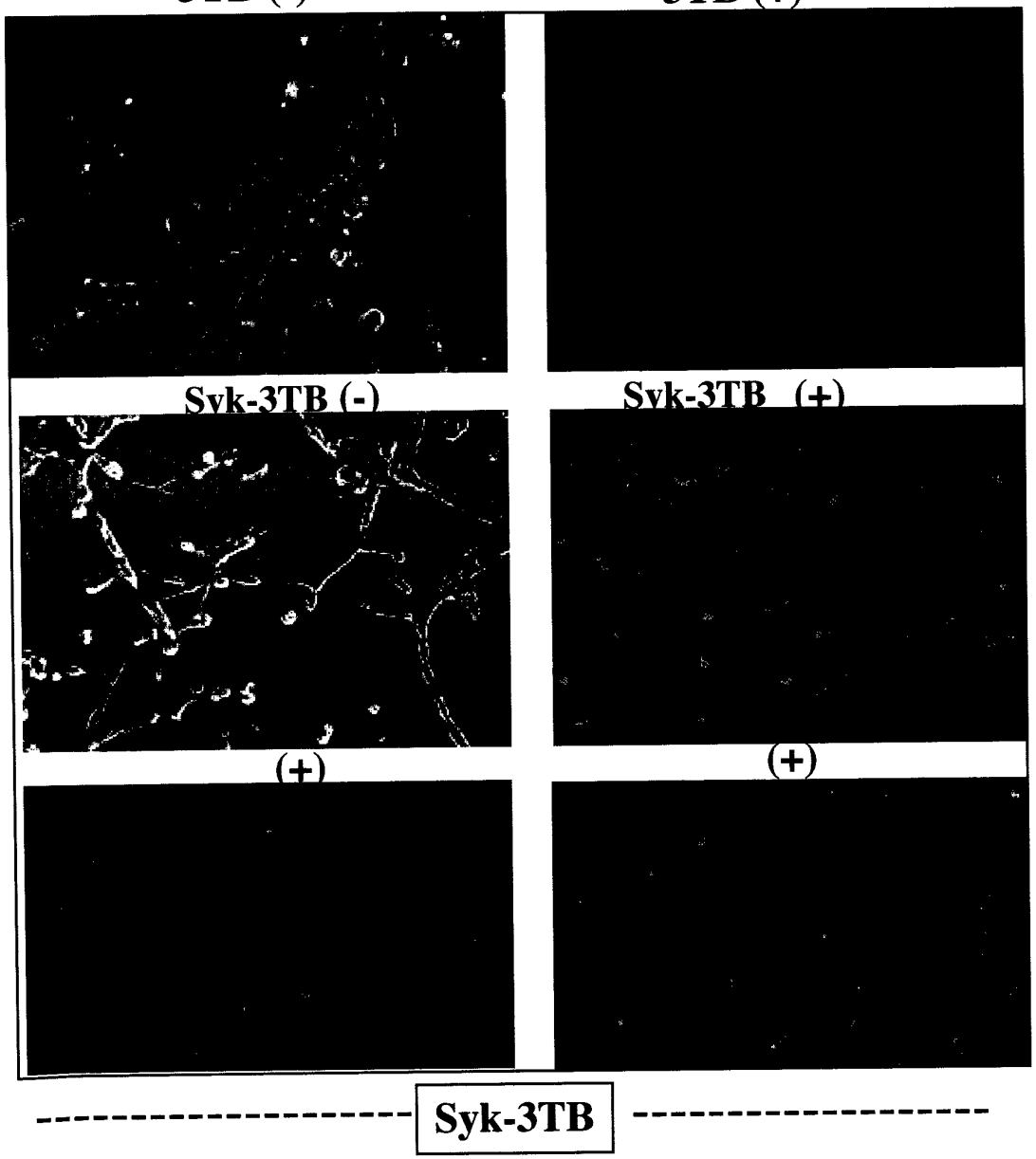


**Fig. 25**

**Activation of PAR1 induces phosphorylation of Syk**

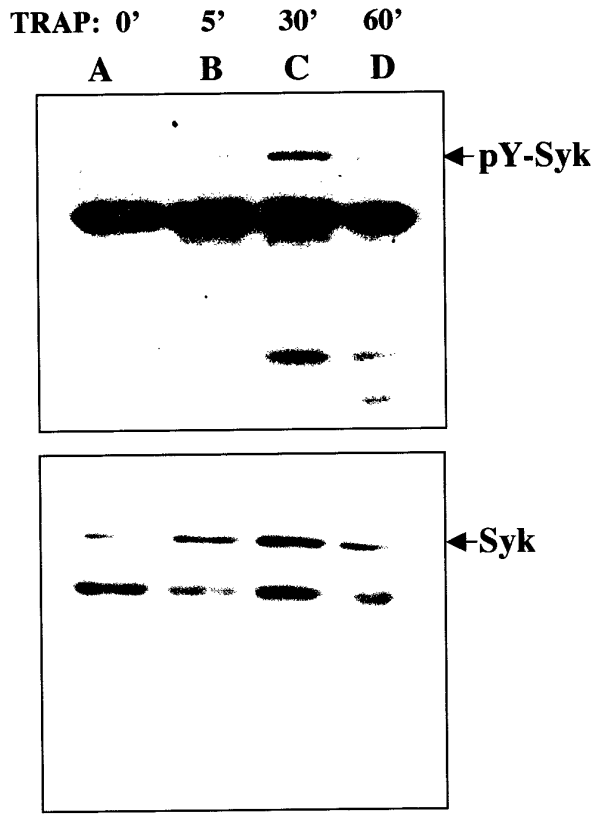

# Fig. 26

## Activation of PAR1 inhibits JNK phosphorylation and induces pCbl

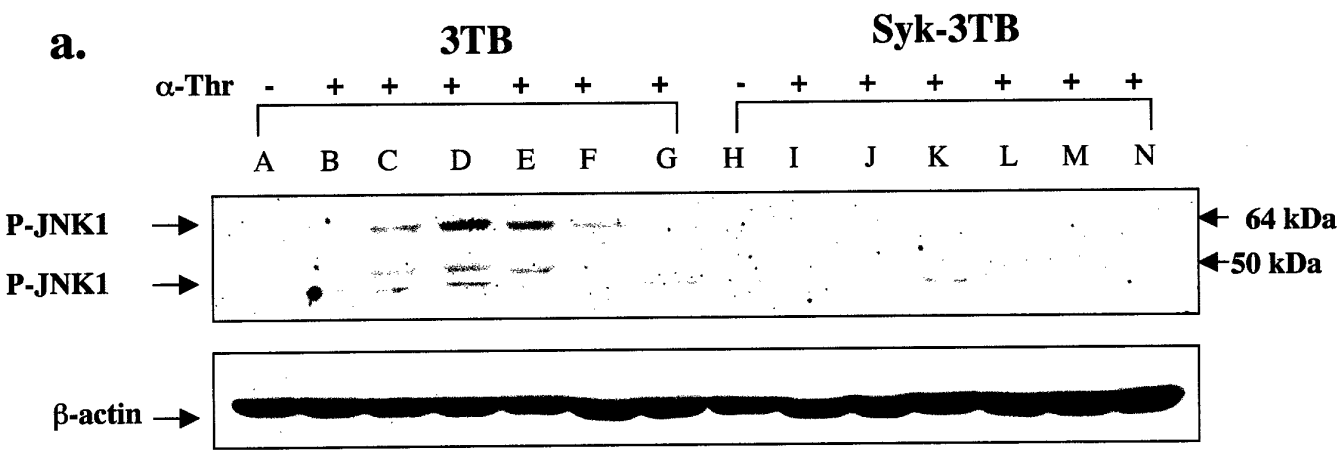


| Syk-3TB | 3TB |
|---|---|
| H- No activ. | A- No activ. |
| I- 5 min | B- 5 min |
| J- 10 min | C- 10 min |
| K- 15 min | D- 15 min |
| L- 20 min | E- 20 min |
| M- 30 min | F- 30 min |
| N- 1hr | G- 1hr |

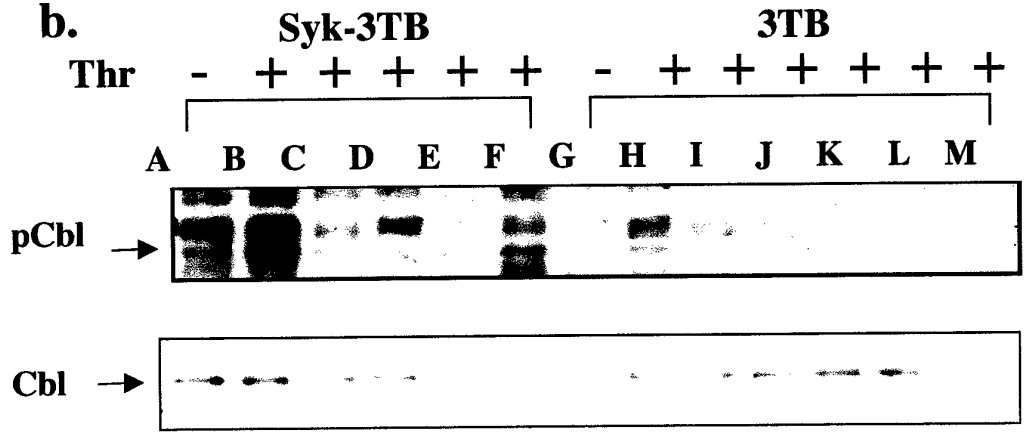


| | |
|---|---|
| A. 3TB SyK | G. 3TB |
| B. 3TB SyK Thr 5min | H. 3TB Thr 5min |
| C. 3TB SyK Thr 10min | I. 3TB Thr 10min |
| D. 3TB SyK Thr 20min | J. 3TB Thr 15min |
| E. 3TB SyK Thr 30min | K. 3TB Thr 20min |
| F. 3TB SyK Thr 1hr | L. 3TB Thr 30min |
| | M. 3TB Thr 1hr |

Scheme I

# GST-PAR1 -C-tail plasmid

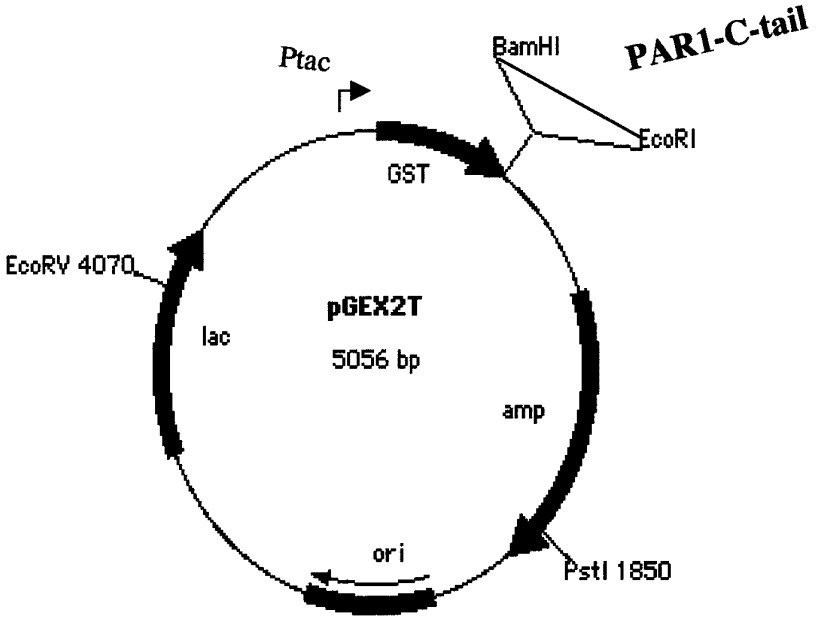


**Amino-Acid sequence for PAR1 C- tail:**

**$NH_2$ - S S E C Q R Y V Y S I L C C K E S S D P S S Y N S S G Q L M A S K M O T C S S N L N N S I Y K K L L T Z - COOH**

**GST-C tail of PAR1**

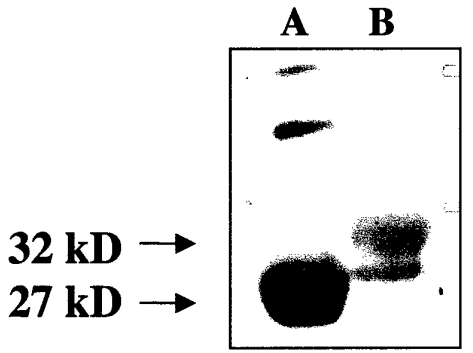


A- GST protein

B- GST-PAR1 C tail fusion protein

# Fig. 27

## Co-IP of PAR1 and Syk in different epithelial cells

**a.**

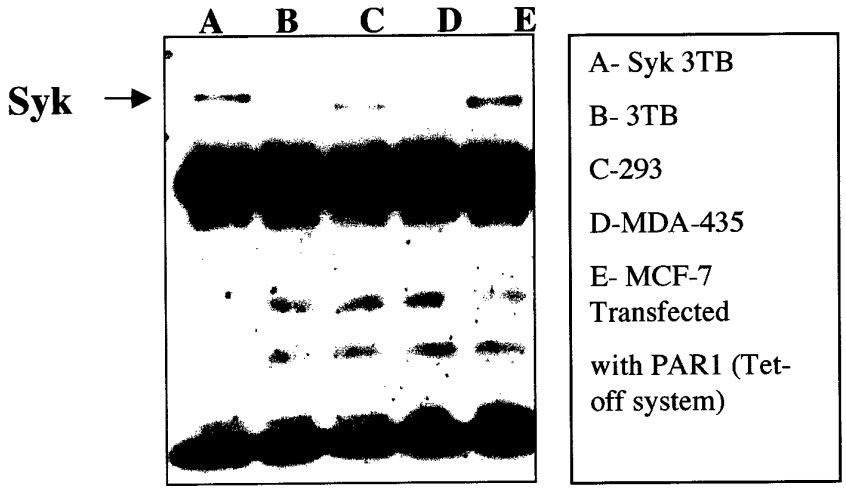


**b.** **PAR1 C-tail competes for PAR1-Syk complex**

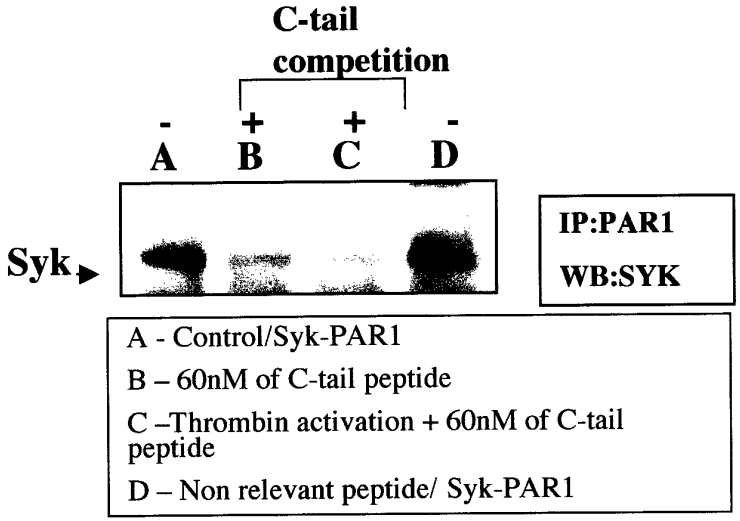


**c.** **Syk is bound to PAR1 GST-C-tail**

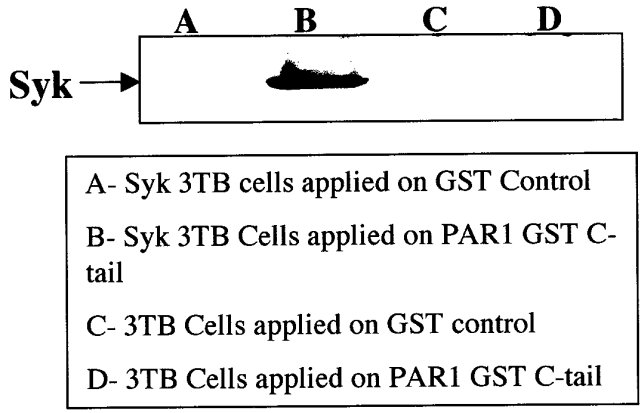


**GST-C tail of PAR1**

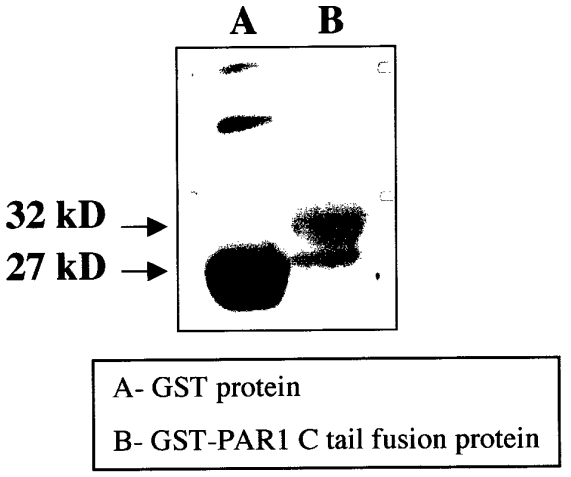

**Fig.28 I.**

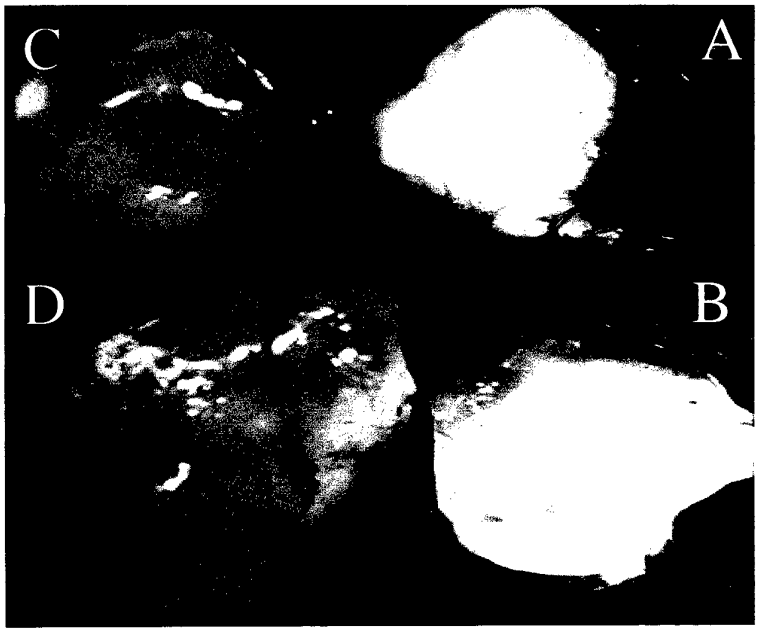


**II.**

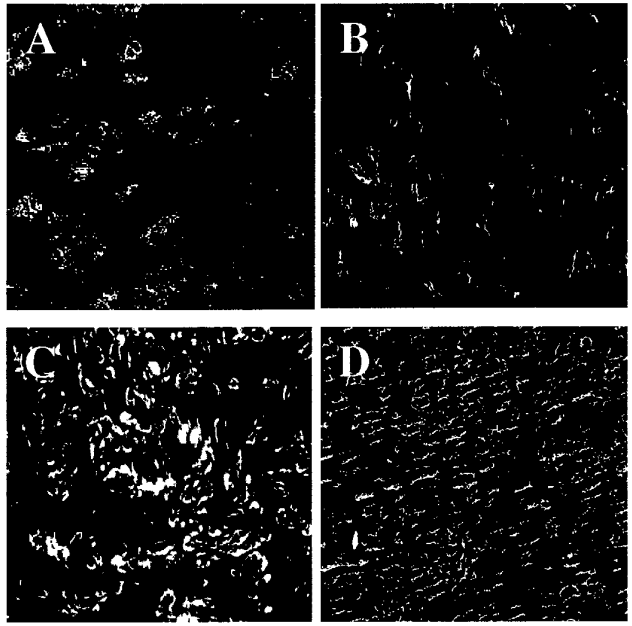


**III.**

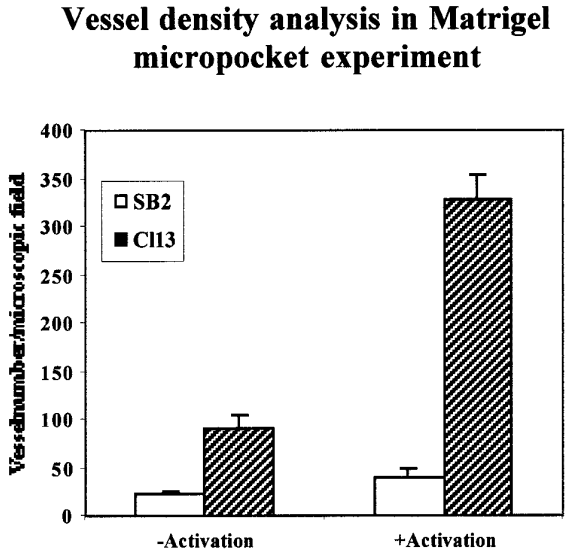


**Figure 28.** ***Par1*** **induced angiogenesis** ***in vivo-Matrigel plug assay.*** BABL/c mice were implanted (s.c.) dorsa with either *Par1* stable transfected cells; Cl13 or non-transfected cells; SB-2 into the peritoneal cavity in a bilateral fashion. Mice were divided into four groups. Group 1 (n=9) of SB-2 cells. Group 2 (n=8) were injected with TRAP (100μM) activated SB-2 cells. Group 3 (n=11) Cl13 cells and Group 4 (n=12) were injected with TRAP (100μM) activated Cl13 cells. **I. Matrigel plugs under phase microscopy.** Matrigel containing non-transfected, noninvasive cells remained practically pale with very low levels of blood vessels. Activation of PAR1 either with TRAP (100μM) (B), or without activation (A) Matrigel embedded cells. Matrigel plugs of *Par1* transfected cells Cl13 exhibited reddish color indicative of the blood vessels recruited (C), and PAR1 activation with TRAP exhibited a further induction of blood vessel recruitment (D). Mock transfected SB-2 cells either activated or not remained pale similar to the non transfected SB-2 cells (data not shown). Magnification 5X. **II. Histolgical evaluation of the various Matrigel embedded groups.** Serial sections were prepared from Matrigel plugs, 10 days after *in vivo* implantation and processed with Mallory's stain. SB-2 with (A) and without activation (B), Cl13 with (D) and without activation (C). Magnification 200X. **III. Quantification of the capillary vessels.** Six separated fields of Matrigel section after H&E and Mallory's' Staining were carefully counted using phase microscopy. Data shown are the mean ± SD of six fields.

# Fig. 29

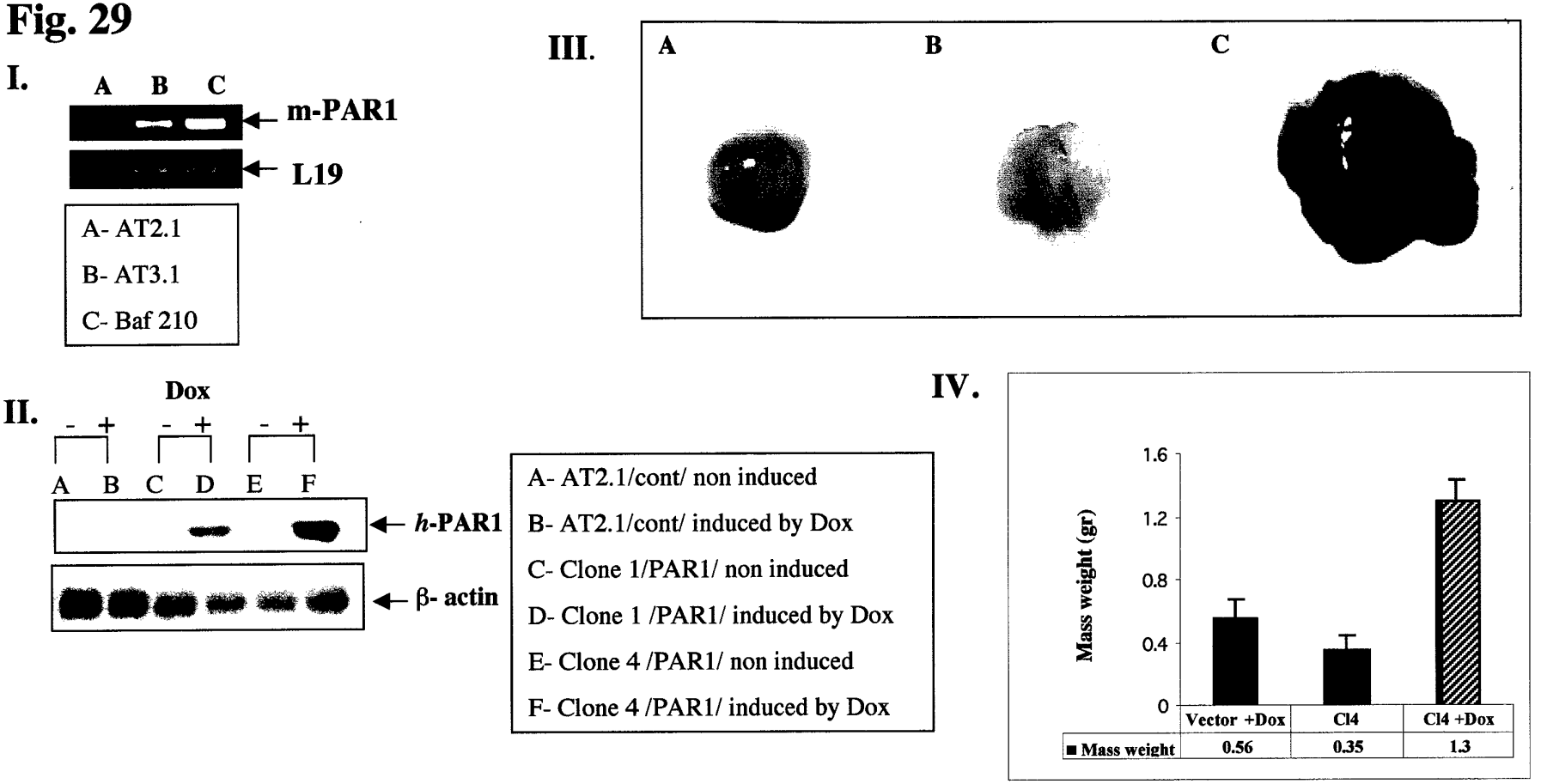


**Figure 29: Inducible PAR1 expression in rat prostatic carcinoma increases tumor mass and angiogenesis. I.** Differential expression of *Par1* in the Dunning rat prostate carcinoma cell variants was observed by RT-PCR. **II.** Inducible Par1 expression in a rat prostaic carcinoma cell line. *hPar1* expression were strongly induced by a tetracyclin analog Dox in of the two AT2.1/Tet-On/*hPar1* clones 4 and 10 by Northern blot analysis. **III.** AT2.1/Tet-On/*h*Par1 cells and mock transfected cells were injected into rats s.c., fed Dox in their drinking water, after 4 weeks the tumor mass sizes were compared. **VI.** Evaluation of the tumor mass.

# Fig. 30

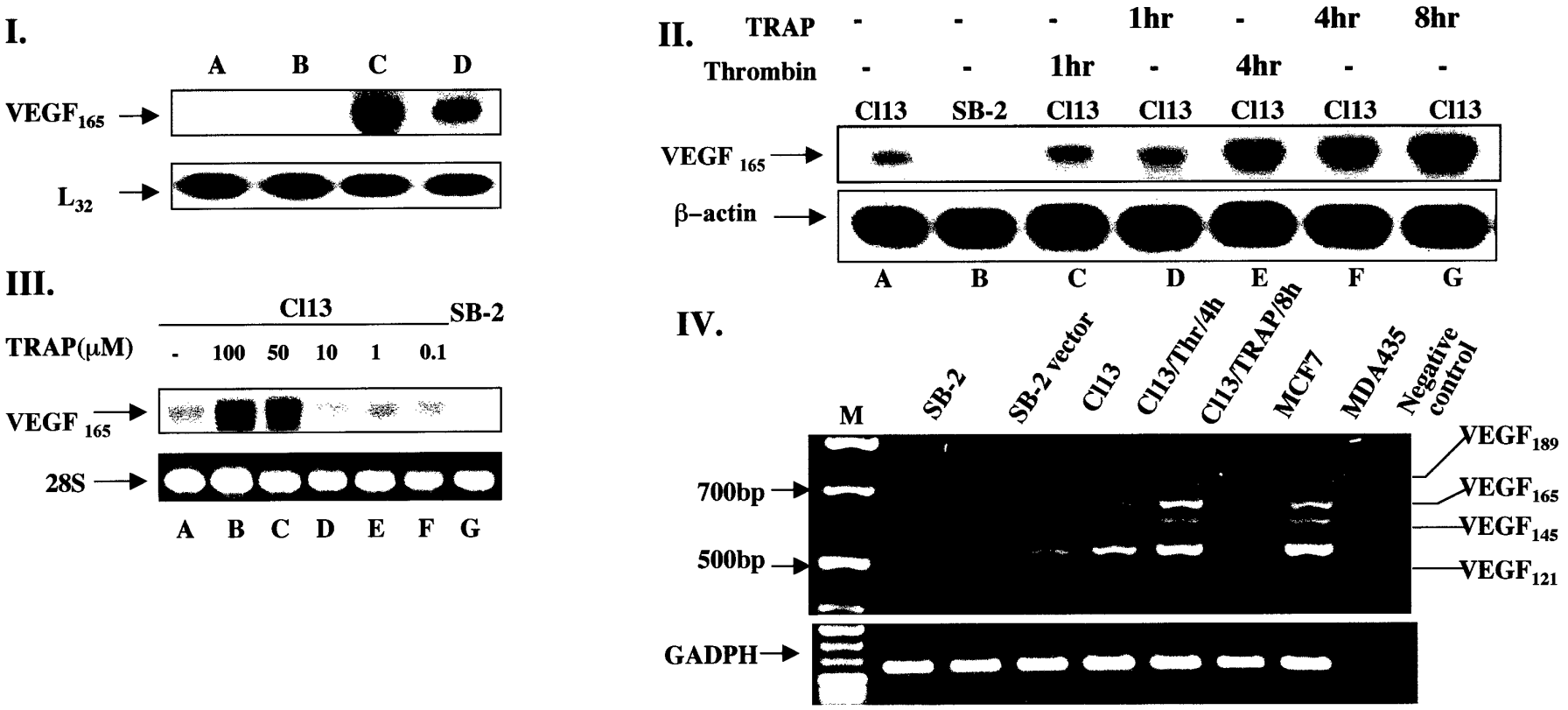


**Figure 30. Expression of VEGF isoforms by *Par1* transfected cells. I. Northern blot analysis of *Par1* stable clones.** The clones(Cl13 & MixL), expressing $VEGF_{165}$ (C, D) as compared to empty an vector (B) and parental non metastatic SB-2 cells (A). The bottom panel exhibits RNA loading, by hybridization to a house keeping gene L32. **II. Kinetics of $VEGF_{165}$ expression in the presence and activation of PAR1.** Activation of *Par1* transfected cells induces markedly $VEGF_{165}$ levels (either by Thrombin 1u/ml or TRAP 100μM). Maximal induction observed following 8 hr of TRAP activation (G). **III. Dose response of TRAP activation.** Maximal induction of $VEGF_{165}$ is observed at 100μM of TRAP activation (B) as compared to non-activated cell (A), and parental non-transfected SB-2 cells (G). **IV. RT-PCR of *Par1* transfected cells.** Four different splice forms are detected: $VEGF_{121}$, $VEGF_{145}$, $VEGF_{165}$, and $VEGF_{189}$. None, or very little is seen in either non- transfected (SB-2) cells, empty vector (SB-2 Vector) or non-metastatic cells (MCF7). The pattern of *Par1* activated cells is similar to highly metastatic cells (MDA435).

# Fig. 31

I.

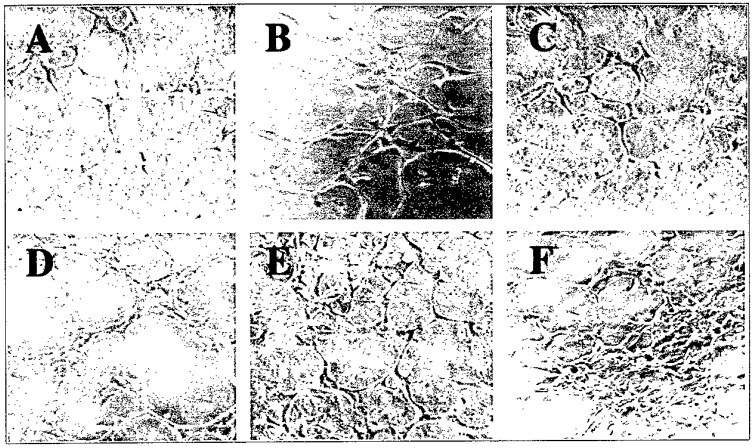


II.

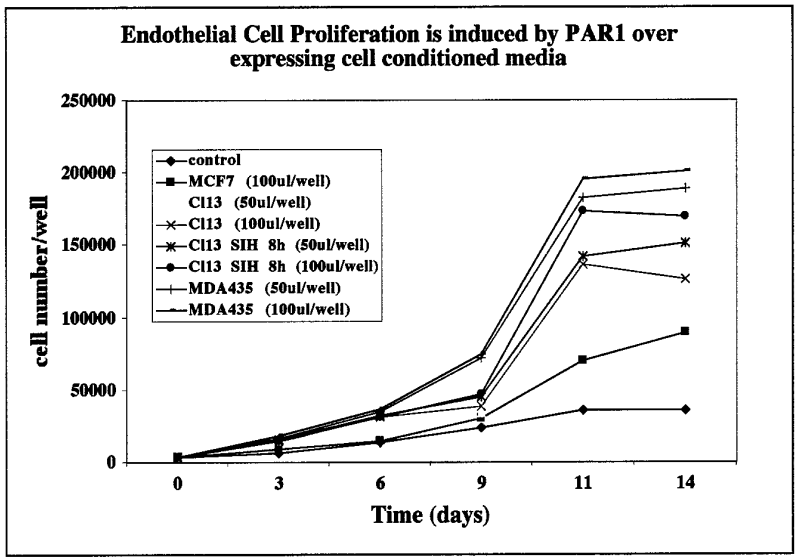


**Figure 31. Functional properties of PAR1 induced VEGF. I. Tube formation in 3-dimensional cultures and endothelial cell proliferation.** Conditioned medium of *Par1* transfected cells applied on a three dimensional collagen type I, culture is effective in endothelial cell tube formation, as compared to control (C), highly metastatic cell conditioned media (F), *Par1* transfected cells (D, E) and empty vector transfeted cells (A, B). **II. Condition media of *Par1* transfected cells induce the proliferation of BAEC.** Plates were fed repeatedly every 2 days with conditioned medium of various treated cells. **III. Anti-VEGF antibodies neutralize the proliferation activity of activated PAR1 cell conditioned medium.** Antibodies (R&D) were applied to the proliferation assay at different concentrations (1:100-1:5000), for the entire period of the assay.

III.

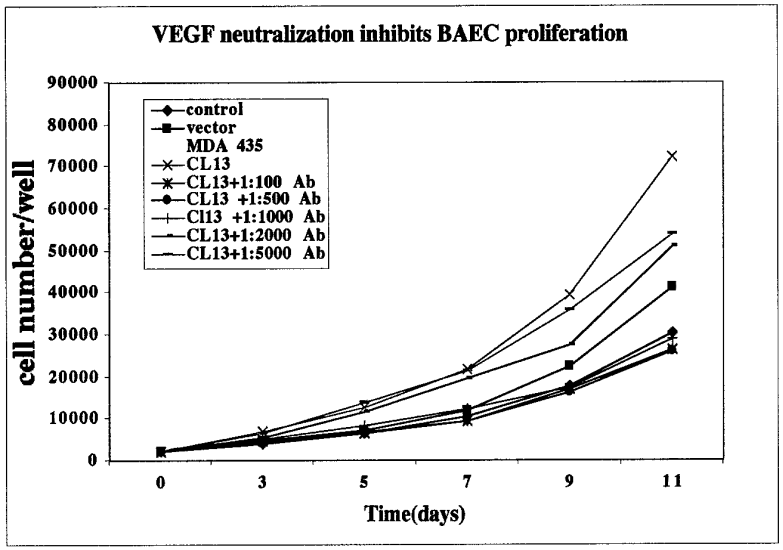

Fig. 32

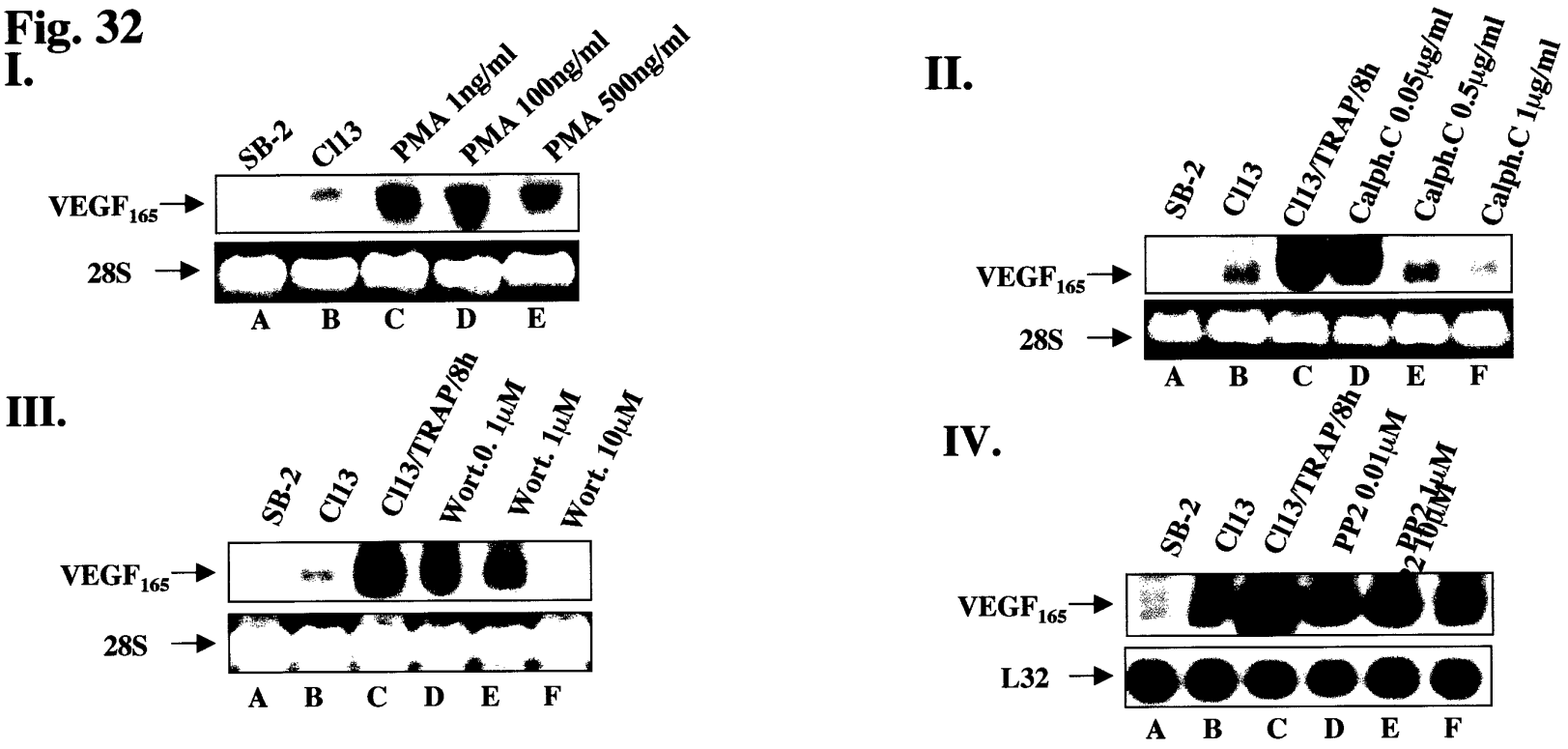


**Figure 32. PAR1 induced VEGF is mediated via PKC, PI3K and Src. I. Induction of VEGF by PMA.** Dose response of PMA induced VEGF. PMA 500ng/ml induces maximally VEGF as compared to non-transfected, non-metastatic cells (SB-2). **II. Calphostin C inhibits PAR1 activated VEGF induction.** Maximal inhibition is obtained at 0.5µg/ml and 1µg/ml (R&G) as compared with Cl13 TRAP activated cells and *Par1* transfected cells (Cl13). Lower level (50ng/ml) of Calphostin C did not inhibit VEGF (R&E) as compared to parental non-transfected cell (SB-2). **III. Inhibition of PAR1 induced VEGF by Wortmannin a PI3K inhibitor.** Inhibition by Wortmannin observed at 0.1µM, 1µM and up to 10 µM. **IV. Inhibition of PAR1 induced VEGF by a Src inhibitor-PP2.** Inhibition of VEGF is observed at 10µM, 1µM as compared to *Par1* transfected cell (Cl13) and parental non transfected cells (SB-2).

# Fig. 33

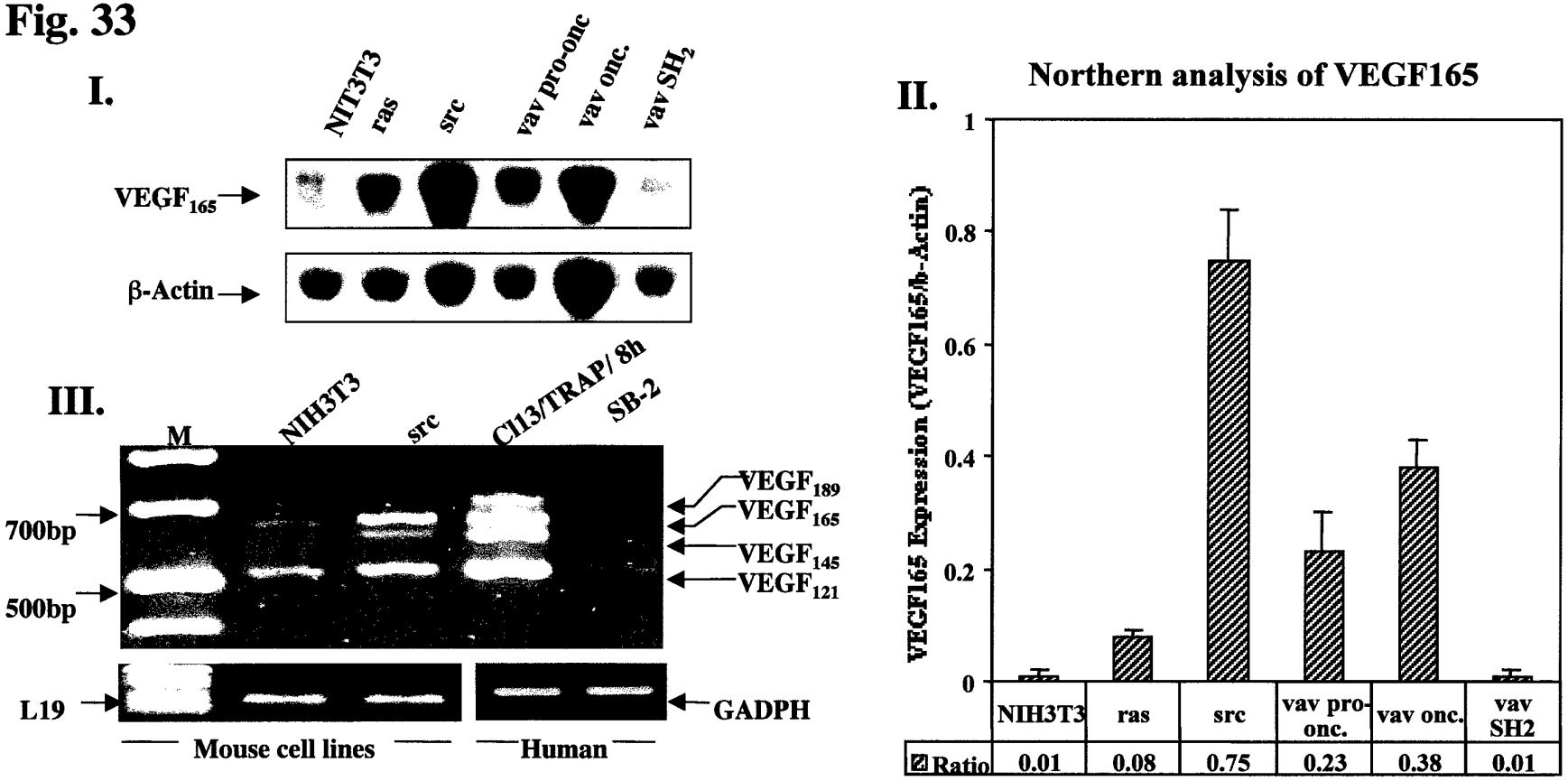


**Figure 33. Expression of VEGF splice forms mRNA in *ras, src* and *vav* transformed NIH3T3 cells. I. NIH3T3 cells transformed either by *ras* or *src* oncongene, wild type (w.t.) *vav* proto-oncogene, an oncogenic *vav* and a SH2 mutant of *vav*.** Total RNA was isolated and 15μg were analyzed by Northern blotting using $VEGF_{165}$, $VEGF_{145}$ and $VEGF_{189}$ probes. **II. Evaluation of the specific fold induction.** Photoimage was used to evaluate the expression of the VEGFs using β-Actin as a house keeping control gene. **III. RT-PCR analysis.** A representative RT-PCR experiment showing elevated levels of $VEGF_{121}$, $VEGF_{145}$, $VEGF_{165}$ and $VEGF_{189}$ splice forms expression. This is compared to the positive *Par1* transfected/activated cells (Cl13/TRAP/8h) and the negative non-transfected cells (SB-2).

THE JOURNAL OF BIOLOGICAL CHEMISTRY
Vol. 276, No. 14, Issue of April 6, pp. 10952–10962, 2001
Printed in U.S.A.


# Tumor Cell Invasion Is Promoted by Activation of Protease Activated Receptor-1 in Cooperation with the $\alpha_v\beta_5$ Integrin*

Received for publication, August 3, 2000, and in revised form, January 25, 2001
Published, JBC Papers in Press, January 26, 2001, DOI 10.1074/jbc.M007027200

**Sharona Cohen Even-Ram‡, Miriam Maoz‡, Elisheva Pokroy‡, Reuven Reich§, Ben-Zion Katz¶, Paul Gutwein‖, Peter Altevogt‖, and Rachel Bar-Shavit‡****

*From the Departments of ‡Oncology and §Pharmacology at the Hadassah-Hebrew University Hospital, Jerusalem 91120, Israel, the Department of ¶Hematology, Medical Center, Tel Aviv 64239, Israel, and the ‖Tumor Immunology Program, German Cancer Research Center, D-69120 Heidelberg, Germany*

**The first prototype of the protease activated receptor (PAR) family, the thrombin receptor PAR1, plays a central role both in the malignant invasion process of breast carcinoma metastasis and in the physiological process of placental implantation. The molecular mechanism underlying PAR1 involvement in tumor invasion and metastasis, however, is poorly defined. Here we show that PAR1 increases the invasive properties of tumor cells primarily by increased adhesion to extracellular matrix components. This preferential adhesion is accompanied by the cytoskeletal reorganization of F-actin toward migration-favoring morphology as detected by phalloidin staining. Activation of PAR1 increased the phosphorylation of focal adhesion kinase and paxillin, and the induced formation of focal contact complexes. PAR1 activation affected integrin cell-surface distribution without altering their level of expression. The specific recruitment of $\alpha_v\beta_5$ to focal contact sites, but not of $\alpha_v\beta_3$ or $\alpha_5\beta_1$, was observed by immunofluorescent microscopy. PAR1 overexpressing cells showed selective reciprocal co-precipitation with $\alpha_v\beta_5$ and paxillin but not with $\alpha_v\beta_3$ that remained evenly distributed under these conditions. This co-immunoprecipitation failed to occur in cells containing the truncated form of PAR1 that lacked the entire cytoplasmic portion of the receptor. Thus, the PAR1 cytoplasmic tail is essential for conveying the cross-talk and recruiting the $\alpha_v\beta_5$ integrin. While PAR1 overexpressing cells were invasive *in vitro*, as reflected by their migration through a Matrigel barrier, invasion was further enhanced by ligand activation of PAR1. Moreover, the application of anti-$\alpha_v\beta_5$ antibodies specifically attenuated this PAR1 induced invasion. We propose that the activation of PAR1 may lead to a novel cooperation with the $\alpha_v\beta_5$ integrin that supports tumor cell invasion.**

The ability of tumor cells to invade beyond controlled hemostatic boundaries and re-emerge from blood vessels to establish new metastatic colonies continuous to present a major obstacle in cancer cure. It is well known that in tumor invasion and metastasis, the pericellular proteolytic systems, consisting of proteases and their specific cell surface receptors, are tightly regulated to modulate cellular functions and degrade selective matrix barriers (1, 2). We have previously demonstrated that the proteolytically activated receptor 1 (PAR1,[1] thrombin receptor) plays a central role in the malignant and physiological invasion processes of both breast carcinoma metastasis and placental implantation (3). At the molecular level, tumor invasion is mediated via the combined interactions of the host cell signaling machinery and the regulation of the stromal extracellular matrix (ECM). Extensive proteolysis in the tumor microenvironment is also responsible for the activation of several enzymatic precursors, like plasminogen, pro-matrix metalloproteinase, and prothrombin (4–6). In addition, the extravascular deposition of fibrin within the tumor microenvironment is well established (7), pointing to the significant role of the coagulation proteins in tumor progression. Indeed, the tissue factor (TF), a protease receptor that plays a central role in hemostasis, has also been implicated in angiogenesis and tumor cell metastasis by means of intracellular events mediated by its cytoplasmic tail and by the perivascular extracellular proteolysis (8–10). These features are shared by other cellular receptors involved in the proteolytic modification of the tumor environment. Among these is the receptor for the serine protease urokinase, which, when bound to its cell surface receptor (uPAR), converts plasminogen to plasmin; plasmin, in turn, is known to effectively degrade various matrix glycoproteins (1, 11). It has been shown also that uPAR serves as an adhesion receptor for vitronectin (12) and that the vitronectin receptor $\alpha_v\beta_3$ not only supports the migration of tumor cells on various matrix-proteins but also binds matrix metalloproteinase-2, thus presenting an immobilized enzyme with improved matrix-collagen degradation properties at the invasive front (13). Additional cell surface protease receptors include the PAR family, which are proteolytically cleaved G-coupled receptors of seven transmembrane-spanning domains. Unlike most cellular growth factor receptors, the PAR family members do not require the traditional ligand-receptor complex formation for ac-

* This work was supported in part by grants from the Ministry of Health, the Ministry of Science and the Arts, the Joint German and Israeli Research Program, the Middle East Cancer Constridium, the Israel Cancer Association, and the Israel Science Foundation of Science and Humanities (to R. B.-S.). The costs of publication of this article were defrayed in part by the payment of page charges. This article must therefore be hereby marked "*advertisement*" in accordance with 18 U.S.C. Section 1734 solely to indicate this fact.

** To whom all correspondence should be addressed. Permanent address: Dept. of Oncology, Sharett Inst., Hadassah University Hospital, P.O. Box 12000, Jerusalem 91120, Israel. Tel.: 972-2-677-7563; Fax: 972-2-642-2794; E-mail: barshav@md2.huji.ac.il. Current address (during the academic year 2000–2001): Dept. of Cell Biology, Harvard Medical School, 240 Longwood Ave., Boston, MA 02115. Tel.: 617-432-3971/3972; Fax: 617-432-3969; E-mail: rachel_barshavit@hms.harvard.edu.

[1] The abbreviations used are: PAR, protease activated receptor; FAC, focal adhesion complex; FAK, focal adhesion kinase; ECM, extracellular matrix; TRAP, thrombin receptor-activating peptide; AS, antisense; FACS, fluorescence-activated cell sorting; DMEM, Dulbecco's modified Eagle's medium; FCS, fetal calf serum; FITC, fluorescein isothiocyanate; mAb, monoclonal antibodies; BSA, bovine serum albumin; PBS, phosphate-buffered saline; TF, tissue factor; uPA, urokinase; uPAR, urokinase receptor.

tivation. Instead, they are activated by a specific cleavage within their extracellular N-terminal portion to unmask a new amino acid terminus, which serves then as an internal ligand for activation (14–18). Until now, four members of the PAR family have been identified and of these, three (PAR1, PAR3, and PAR4) have been established collectively as "thrombin receptors," possibly serving as a redundant receptor system for the coagulation protease cellular response (14).

Since solid tumors are in close contact with ECM components, malignant cell invasion into the surrounding tissues is facilitated by mutual interactions that convey essential signaling cues to the cells (19, 20). These cell-ECM interactions are mediated by integrins, a family of adhesion receptors that mediate the attachment of the cell to both structural and matrix-immobilized proteins to promote cell survival, proliferation, and migration (21, 22). It is widely recognized that integrins perform a significant function in cellular invasion and metastasis (23–26). Non-ligated integrins are generally distributed diffusely over the cell surface with no apparent linkage to the actin cytoskeleton. However, ECM-bound integrins frequently cluster into specialized structures termed focal adhesion complexes (FACs), thus providing a convergence site for multiple signaling components (26, 27) and also physically linking the receptors to the actin filaments (28–30). The known signaling events that follow receptor clustering include tyrosine phosphorylation of proteins like focal adhesion kinase (FAK) and paxillin (31), as well as the recruitment of other FAC components like vinculin, talin, tensin, and p130 Cas (32–36). A growing number of studies indicate that signals driven by integrins act in concert with signals initiated by the G-protein-coupled receptors and with receptors for tyrosine kinase to promote the pathological tumor cell invasion process, on the one hand, and physiological activities like angiogenesis and wound healing (37, 38) on the other. The combined signals involved with the activation of focal adhesion proteins indicate that the cooperation between the signaling pathway takes place most likely within these FAC structures.

In the present work, we have studied the molecular mechanism of PAR1 involvement in tumor cell invasion. We show here that PAR1 modulates the invasive phenotype of melanoma cell lines, inducing the otherwise non-invasive cells to migrate effectively through Matrigel barriers. This process is accompanied by the increased adherence of the cells to various matrix components, actin stress fiber formation, and adhesion-triggered signaling, with no alteration of the cell surface integrin levels. We demonstrate now, for the first time, that PAR1 mediates these functions via selective cross-talk with the $\alpha_v\beta_5$ integrin to confer FAC formation, distinct signaling events, and cytoskeletal reorganization. Combined, these processes promote tumor cell invasion.

## EXPERIMENTAL PROCEDURES

*Cells*—SB-2 non-invasive human melanoma and A375-SM "super-metastatic" human melanoma cells (kindly provided by J. Fidler and M. Bar-Eli, Department of Cell Biology, University of Texas, M. D. Anderson Cancer Center, Houston, TX) were grown in 10% FCS-DMEM supplemented with 50 units/ml penicillin and streptomycin (Life Technologies, Inc.) and maintained in a humidified incubator with 8% $CO_2$ at 37 °C. The PAR1 stable transfectants, clone 13 and clone Mix L, were grown under the same conditions; for long term maintenance, these were supplemented also with 200 μg/ml G418 antibiotics. MCF-7 cells were maintained as previously described (3).

*Cell Transfection*—Cells were grown to 30–40% confluence and then transfected with 0.5–2 μ g/ml plasmid DNA in Fugene 6 transfection reagent (Roche Molecular Biochemicals) according to the manufacturer's instructions. After 10 days of selection, stable, transfected clones were established in medium containing 400 μg/ml G418. Antibiotic-resistant cell colonies were transferred to separate culture dishes and were grown in 200 μg/ml G418 medium. Forty-eight hours after transfection, transiently transfected cells were collected and tested by immunoprecipitation analyses (see below).

*Preparation of Truncated PAR1*—Using polymerase chain reaction, we constructed a PAR-1 mutant protein truncated in its cytoplasmic tail after the amino acid Leu-369. As a template, we used PAR-1 cDNA in the pCDNA 3 vector. For amplification, we used a T7 sense primer and the reverse primer GGTCTAGAAAACTATAGGGGGTCGATG-CACGAGCT containing a STOP codon and an *Xba*I site. The amplified DNA fragment was subcloned using the polymerase chain reaction-blunt technique (Invitrogen) and confirmed by DNA sequencing. The insert was released from the vector by *Xba*I digestion and cloned into plasmid pCDNA3. To confirm the functional integrity of the DNA constructs, wild type and mutant cDNAs were transiently expressed in 293 cells that were subsequently stained with a PAR-1-specific antibody (WEDE15, Immunotech, Cedex, France).

*Western Blot Analysis*—Cells were solubilized in lysis buffer containing 10 mM Tris-HCl, pH 7.4, 150 mM NaCl, 1 mM EDTA, 1% Triton X-100, and protease inhibitors (5 μg/ml aprotinin, 1 μM phenylmethylsulfonyl fluoride, and 10 μg/ml leupeptin) at 4 °C for 30 min. The cell lysates were subjected to centrifugation at 10,000 × *g* at 4 °C for 20 min. The supernatants were saved and their protein contents were measured; 50 μg of the lysates were loaded onto 10% SDS-polyacrylamide gels. After the proteins were separated, they were transferred to an Immobilon-P membrane (Millipore). Membranes were blocked and probed with 1 μg/ml amounts of the appropriate antibodies as follows: anti-PAR1 thrombin receptor mAb, clone II aR-A (Biodesign Int.); anti-paxillin monoclonal antibody (mAb), clone 349 (Transduction Laboratories, Lexington KY); anti-human focal adhesion kinase, rabbit polyclonal IgG (Upstate Biotechnology Inc., Lake Placid, NY); anti-phosphotyrosine mAb, clone 4G10 (Upstate Biotechnology Inc.); anti-vinculin mAb (Transduction Laboratories). The antibodies were suspended in 1% BSA in 10 mM Tris-HCl, pH 7.5, 100 mM NaCl, and 0.5% Tween 20. After washes with 10 mM Tris-HCl, pH 7.5, 100 mM NaCl, and 0.5% Tween 20, the blots were incubated with secondary antibodies conjugated to horseradish-peroxidase. Immunoreactive bands were detected by the enhanced chemiluminescence (ECL) reagent using Luminol and *p*-cumaric acid (Sigma).

*Immunoprecipitation*—Cells were treated for 30–60 min with thrombin at a concentration of 1 NIH unit/ml of serum-free DMEM medium (0.5% BSA), and then lysed as described above. We used 400 μg of total protein for immunoprecipitation of $\alpha_v\beta_3$, $\alpha_v\beta_5$, paxillin, FAK, or both paxillin and FAK. All the antibodies were used at a concentration of 10 μg/ml. After overnight incubation, Protein A-Sepharose beads (Amersham Pharmacia Biotech) were added to the suspension (50 μl) that was subsequently rotated at 4 °C for 1 h. Elution of the reactive proteins was made by re-suspending the beads in protein 2× sample buffer (63 mM Tris-HCl, pH 6.8, 20% glycerol, 20% SDS, 0.01% bromphenol blue, 5% β-mercaptoethanol, 0.02 M dithiothreitol) and boiling for 5 min. The supernatant was loaded on a 10% SDS-polyacrylamide gel followed by the same procedure as in Western blotting.

*Matrigel Invasion Assay*—We used blind-well chemotaxis chambers with 13-mm diameter filters. Polyvinylpyrrolidone-free polycarbonate filters with 8-μm pores (Costar Scientific Co., Cambridge, MA) were coated with basement membrane Matrigel (25 μg/filter) as described previously (39). Briefly, the Matrigel was diluted to the desired final concentration with cold distilled water, applied to the filters, dried under a hood, and reconstituted with serum-free medium. In the upper compartment of the Boyden chamber, we placed 2–3 × $10^5$ cells suspended in DMEM containing 0.1% bovine serum albumin. As a chemoattractant, into the lower compartment of the Boyden chamber, we put 3T3 fibroblast conditioned medium. Assays were carried out in 5% $CO_2$ at 37 °C. After 2 h of incubation, we observed that more than 90% of the cells were attached to the filter. At this time, the cells on the upper surface of the filter were removed by wiping with a cotton swab. The filters were fixed in DifQuick system (American Scientific Products) and stained with hematoxylin and eosin. Cells from various areas of the lower surface were counted. Each assay was performed in triplicate. For chemotaxis studies (a control of Matrigel invasion), the filters were coated with collagen type IV alone (5 mg/filter) to promote cell adhesion. Cells were added to the upper chamber and conditioned medium to the lower compartment.

*Adhesion Assay*—The medium of cells grown in 10% FCS was replaced by DMEM with 0.5% BSA, and the cells were detached from the plate by treating with 0.05% trypsin in a solution of 0.02% EDTA in 0.01 M sodium phosphate, pH 7.4 (Biological Industries, Beit Ha'emek, Israel). After washing, 0.5 × $10^6$ cells/ml cells were re-suspended in a serum-free DMEM medium (as above) and laid on 13-mm culture dishes pre-coated with either 100 μg/ml fibronectin or Th-1, a thrombin-de-

rived RGD (arginine-glycine-aspartic acid) peptide. After a 45-min incubation period to allow cell adhesion, the excess cells were washed away. The adhered cells were fixed to the plates with 4% formaldehyde in PBS, pH 7.4, for at least 2 h. After fixation, the plates were washed in 1% boric acid solution and the cells were stained with 1% methylene blue reagent (Sigma) in 1% boric acid for 30 min. After extensive washing with tap water, the methylene stain was eluted by the addition of 500 μl of 1 M HCl. The intensity of the color staining was measured by color spectrometry at a wavelength of 620 nm.

*Immunofluorescence*—Cells were plated on glass coverslips in 16-mm culture dishes; after the cells had grown to subconfluence, they were washed with PBS, permeabilized in 0.5% Triton X-100-containing 3.5% paraformaldehyde/PBS solution on ice for 2 min, and finally fixed with 3.5% paraformaldehyde/PBS for 20 min. Reactions with the appropriate antibodies were performed in room temperature for 60 min, after which the cells were washed extensively in PBS. The antibodies included the following: anti-$\alpha_v\beta_3$ mAb clone LM609, anti-$\alpha_v\beta_5$ clone P1F6, and anti-$\alpha_5\beta_1$ clone JBS5, (all from Chemicon Int.). After the 60-min incubation with the primary antibodies, followed by extensive washes in PBS, an additional 60-min incubation was carried out in the dark with secondary antibodies, goat-anti-rabbit or goat-anti-mouse IgG each conjugated with Cy-3 (Jackson Immunoresearch Laboratories) diluted 1:700. Labeling of filamentous actin by 1 μ g/ml FITC-conjugated phalloidin (Sigma) was performed similarly. The labeled cells were visualized and photographed by fluorescent confocal microscopy (MRC-1024 confocal imaging system, Bio-Rad).

*Flow Cytometry Analysis*—The medium of cells grown in 10% FCS-DMEM was replaced by serum-free DMEM containing 0.5% BSA. Thrombin at a concentration of 1 IU/ml was added to the plates that were activated by incubation for 60 min. The plates were washed with PBS, and the cells were detached from the plates by treatment with 0.05% trypsin in a solution of 0.02% EDTA in 0.1 M sodium phosphate at pH 7.4 (Biological Industries). After being washed twice in PBS, the cells were re-suspended in 200 μl of PBS and the appropriate antibodies were added to a concentration of 10 μg/ml. These reactions, performed at room temperature for 60 min, were followed by extensive washing in PBS. A 1-h incubation with a secondary antibody goat-anti-mouse IgG (Jackson Immunoresearch Laboratories) conjugated with FITC and diluted 1:500 was carried out in the dark. The treated cells were washed extensively, re-suspended in 100 μl of PBS, and analyzed by FACS.

## RESULTS

*Altering the Expression of PAR1 Affected Tumor Cell Invasiveness*—In previous work (3), we showed that there is a direct correlation between PAR1 expression and the metastatic potential of primary tumor biopsies and tumor cell lines, as reflected by their *in vitro* potential to invade through a Matrigel barrier.[2] In a physiological invading model system of placenta trophoblast implantation, we have also shown that PAR1 is part of the invasive program of trophoblast, as evaluated by their villi extension and matrix metalloproteinase synthesis.[3] Here, to clarify how high levels of PAR1 may confer invasiveness, we transfected a non-invasive melanoma cell line (SB-2 cells) with PAR1 cDNA and compared the properties of the transfected cells to those of the highly invasive melanoma cell line A375SM. We used PAR1 cDNA under the control of the cytomegalovirus viral promoter in the pCDNA3 expression vector. We selected several stable clones that expressed high levels of PAR1, as evaluated by Western blot analysis (Fig. 1*a*) and Northern blot analysis (data not shown). The selected clones were then tested for their ability to invade through Matrigel-coated filters. Indeed, clones expressing high levels of PAR1 had an increased ability to invade the Matrigel layer, as compared with control clones transfected with empty vectors or SB-2 cells that had not been transfected at all (Fig. 1*b*). In addition, we observed that, whereas highly invasive A375SM cells invaded Matrigel coated membranes more efficiently than did non-metastatic cells (Fig. 1*b*, *SB-2*), activating the A375SM cells with PAR1 increased their ability to invade Matrigel to an even higher level (Fig. 1*b*, *activ. A375SM*). In addition, the invasiveness of PAR1-transfected cells was further increased when they were either activated by thrombin, as shown in two separate PAR1-transfected clones (Fig. 1*b*, *clones 13* and *Mix L*), or when they were treated with the thrombin-receptor-activating peptide (TRAP) that corresponds to PAR1 internal ligand SFFLRN (data not shown).

Circulating tumor cells can invade into a new metatastic site only if they can adhere to the basement membrane. We analyzed the adhesion properties of cells suspended in a serum-free medium and then incubated for 60 min on plates coated with either fibronectin, a major component of the ECM, or with Th-1, an 11-amino acid peptide, corresponding to the thrombin RGD motif (40). Highly invasive A375 SM melanoma cells adhered strongly to both Th-1 and fibronectin; however, under the same conditions, the non-invasive SB-2 cells failed to adhere. We observed a marked increase in the adherence to both of these matrices of PAR1-transfected SB-2 cells (Fig. 2, *a* and *b*). The level of adherence of these PAR1 transfectants was directly correlated both with their level of PAR1 expression and with their ability to invade the Matrigel barrier. To assure that this increase in their adherence was actually caused by the presence of PAR1, we asked if reducing the expression of PAR1 in malignant cells would reduce the adhesion properties of these cells. To do this, we evaluated the effect of transfection by PAR1 antisense DNA on the adhesion properties of the invasive A375SM cells. We used a 462-base pair oligonucleotide fragment corresponding to the 5′ region of PAR1 that included part of the near promoter sequence and the coding region for the internal ligand. We cloned this DNA segment into pCDNA3 mammalian expression vector in an antisense orientation, selecting for stable clones expressing the plasmid bearing the PAR1 antisense DNA as compared with cells transfected by empty vectors or non-transfected control cells. Northern blot analysis (Fig. 2*d*) indicated that, whereas empty vector transfection (Fig. 2*d*, *B*) had no significant effect on PAR1 expression (Fig. 2*d*, *A*), clones AS -3 (Fig. 2*d*, *C*) and AS-4 (Fig. 2*d*, *D*), which were transfected by the PAR1 antisense DNA, did exhibit reduced PAR1 expression. When we analyzed clones AS-3 and AS-4 for their adhesion properties, we found that the cell adherence properties to fibronectin (Fig. 2*c*) and to Th-1 (data not shown) of both of these clones were significantly lower than those of the A375 SM parental cells.

The organization of the cytoskeleton is critically influenced by adhesion interactions. To explore the effect of PAR1 activation on cytoskeletal reorganization, we plated PAR1-transfected cells (clone 13) and control non-transfected cells (SB-2 cells) on glass coverslips and then treated them with TRAP for various periods of time (Fig. 2*e*). After activation by TRAP, the cells were permeabilized, fixed, and stained with FITC-labeled phalloidin to detect filamentous actin (F-actin). Cytoskeletal reorganization was observed as early as 15 min after activation by TRAP (Fig. 2*e*). Thirty to 60 min after PAR1 activation, we observed a transition in the PAR1 transfectants from elongated spindle-like shapes to spreading, jellyfish-like structures. Ninety minutes to 2 h after activation, the cells became rounder and we observed the appearance of a ringlike bundle of actin filaments at the base of the cells (typical of migrating cells). These changes occurred more rapidly and were more dramatic in PAR1-overexpressing cells than they did in the non-transfected control cells. Altogether, these data show that the adhesive properties of tumor cells were affected by changes in PAR1 expression.

*PAR1 Activation Induced Signaling and Led to Establish-*

[2] E. Pokroy, B. Uziely, S. Even-Ram Cohen, M. Maoz, I. Cohen, S. Ochayon, R. Reich, J. Pe'er, O. Drize, M. Lotem, and R. Bar-Shavit, submitted for publication.

[3] S. Even-Ram Cohen, S. Grisaru-Granovsky, M. Maoz, S. Zaidoun, Y.-J. Yin, and R. Bar-Shavit, submitted for publication.

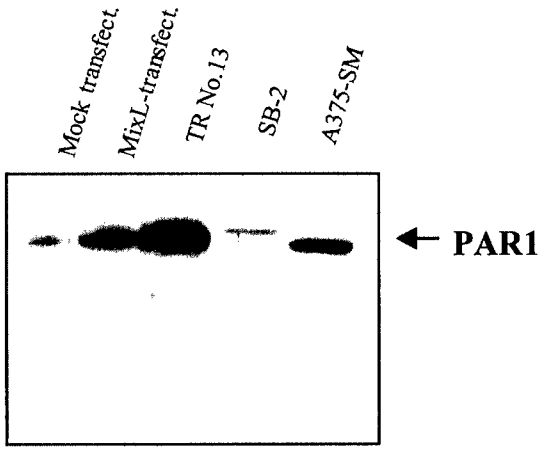


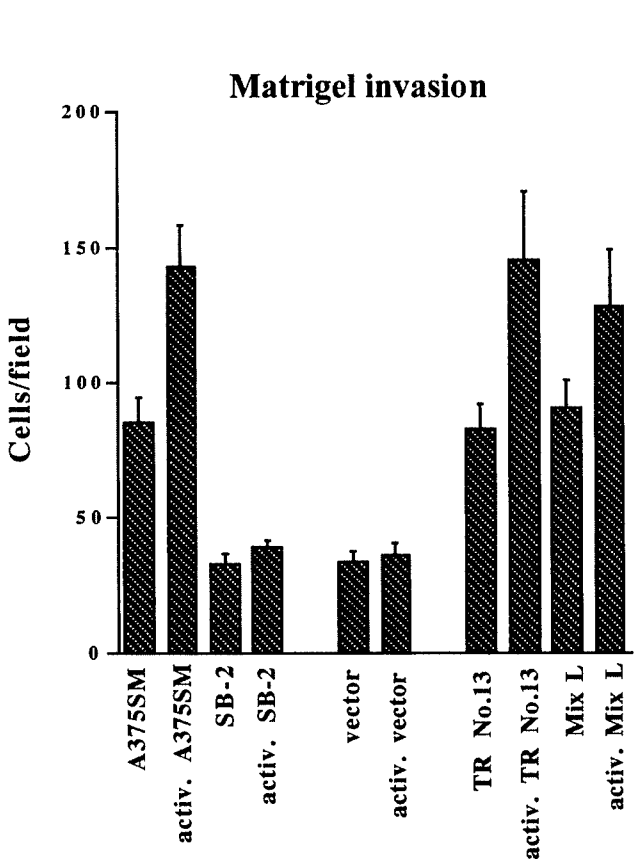


FIG. 1. **Transfection by PAR1 DNA confers invasive properties on non-metatastic melanoma cells.** The expression of PAR1 and cellular invasive properties were measured in SB-2 non-metatastic human melanoma cells, in A375 SM highly metatastic human melanoma cells, in stable PAR1 transfectants clone 13 and clone Mix L, and in mock-transfectant SB-2 cells transfected by empty vectors. Stable PAR1 clones were screened for PAR1 expression (*a*) using anti-PAR1 thrombin receptor mAbs on a Western blot of 50 $\mu$g of lysates total protein. *b*, the invasive capabilities of the selected clones were determined by the Matrigel invasion assay. Cell lines marked "*activ.*" were activated by 1 unit/ml thrombin for 1 h before being used in the invasion assay. The data presented here are the averages of data from at least three replicate experiments.

*ment of Focal Contacts*—Integrin activation typically leads to the assembly of focal adhesion contacts; this takes place by phosphorylation on tyrosine leading to the recruitment of various signaling and structural molecules. FAK and paxillin are the most common signaling components of FAC that are phosphorylated upon integrin activation. To analyze the phosphorylation levels of FAK and paxillin in PAR1-transfected cells, we immunoprecipitated these proteins from cell lysates of either thrombin-activated or non-activated control cells. The immunoprecipitated proteins were blotted onto a nylon membrane and probed with anti-phosphotyrosine mAb to detect their phosphorylation levels. FAK and paxillin proteins from parental, non-invasive SB-2 cells exhibited low levels of phosphorylation (Fig. 3*a*). On the other hand, FAK and paxillin from PAR1 transfectant cells exhibited increased phosphorylation to high levels similar to those observed in the metastatic line A375 SM (Fig. 3*a*). By immunofluorescent analysis using anti-phosphotyrosine mAb followed by a Cy-3 fluorescence-labeled secondary antibody, we detected FAC formation as soon as 15 min following PAR1 activation, reaching a maximum

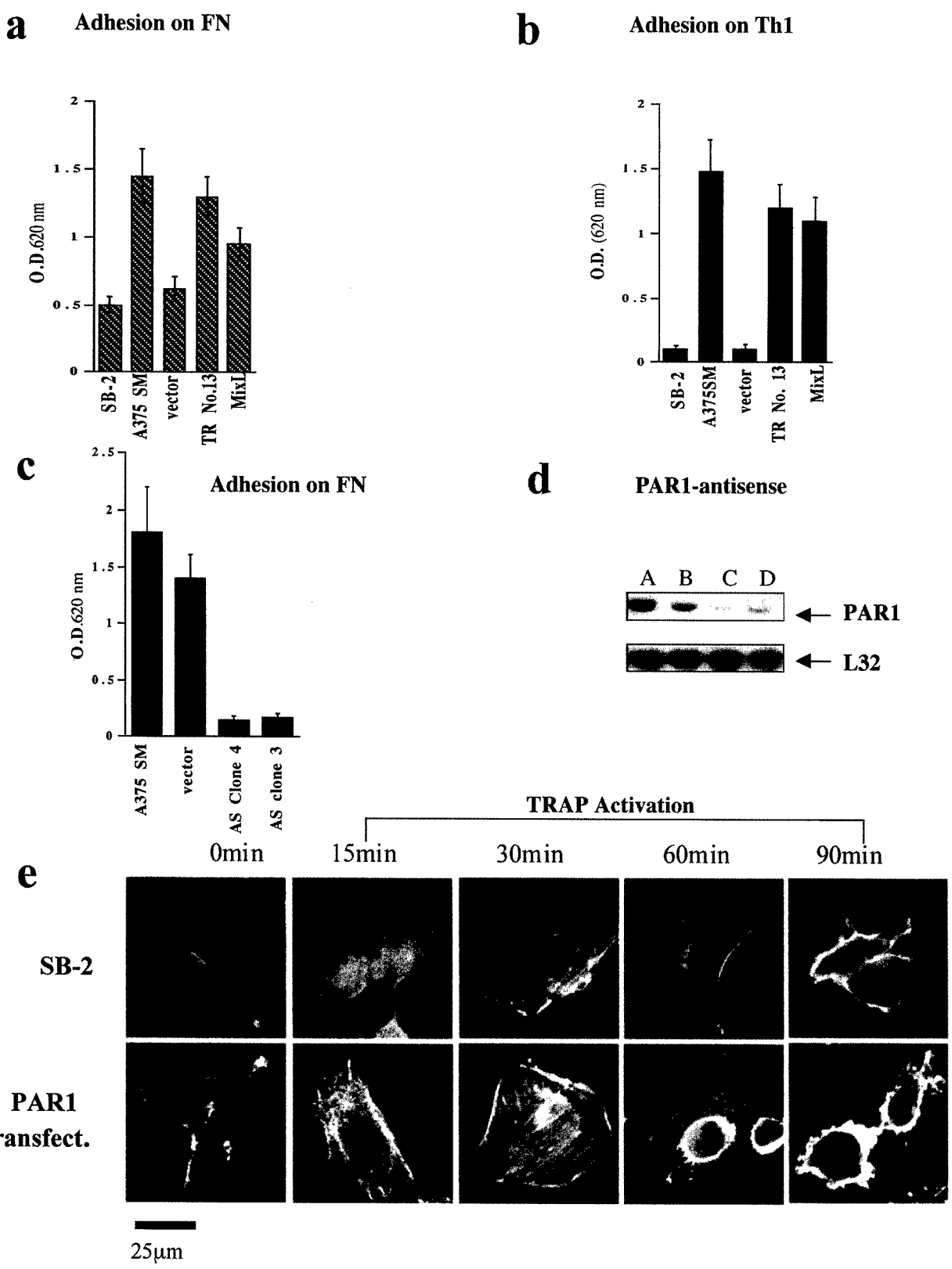


FIG. 2. **Altering PAR1 expression affected cell adhesion and actin fiber re-organization.** Stable PAR1-transfected clones and PAR1 antisense selected clones were analyzed for their adhesive properties to substrates coated with fibronectin (*a* and *c*) or Th-1 RGD peptide (*b*). Cell adhesion was measured by Methylene blue staining of formaldehyde-fixated cells. The eluted stain was detected by spectrophotometry using a $\lambda$ = 620 nm filter. The cells tested (*a* and *b*) were the same as those described in Fig. 1. In addition, we show that in highly metastatic human melanoma A375SM cells stably transfected by PAR1 antisense cDNA (AS clone 4 and AS clone 3), reduced adhesion was observed (*c*) as compared with A375SM cells that were not transfected or that were transfected by an empty vector. These clones exhibited low PAR1 levels as shown by Northern blot analysis (*d*) of RNA samples from A375SM (*A*), A375SM cells transfected with vector only (*B*), AS clone 3 (*C*), and AS clone 4 (D). The data presented here are the averages of data from at least three replicate experiments. L32 is a ribosomal RNA that we have used as a housekeeping control gene for these experiments. *e*, SB-2 cells and PAR1 transfectant clone13 were subjected to actin staining by FITC-phalloidin after PAR1 activation by TRAP. Note that the PAR1 transfectants exhibited a more rapid change in actin fiber re-organization and cellular morphology than did the naive SB-2 cells.

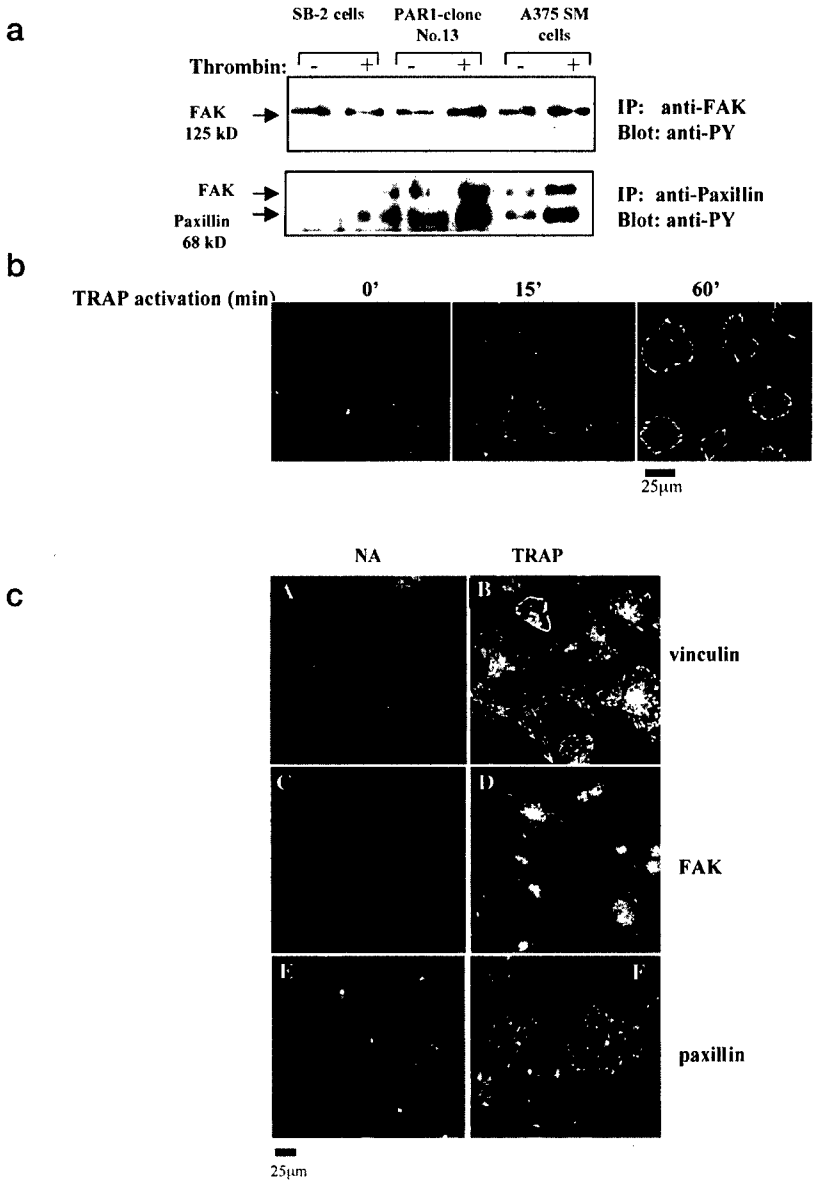


FIG. 3. **Activation of PAR1-induced phosphorylation of FAK and paxillin and their recruitment to FACs.** *a*, the tyrosine-phosphorylated levels of immunoprecipitated FAK (*upper section*) and paxillin (*lower section*) were measured by anti-phosphotyrosine mAb (4G10, UBI) in SB-2 naïve cells, in A375SM metastatic cells, and in the stable PAR1 transfectant clone 13. Note that FAK was observed to co-precipitate with paxillin (*lower section*). *b*, immunofluorescent staining of phosphotyrosine in PAR1-transfected clone 13 was performed by specific incubations with mAbs (4G10) at 0, 15, and 60 min. Detection was made by Cy3-labeled goat anti-mouse IgG, using confocal microscopy. Following activation by 100 μM TRAP, the FACs were observed to be enriched with phosphorylated proteins with a peak at 60 min. *c*, immunofluorescent staining with anti-vinculin, anti-FAK, and anti-paxillin in the stable PAR1 transfectant clone 13 activated with 100 μM TRAP for 1 h or not (*NA*). When the cells were stained with anti-FAK and anti-paxillin, distinct FAC staining was observed only in the activated cells. When the cells were stained with anti-vinculin, FACs were detectable at a low level in the non-activated (*NA*); this level was increased following receptor activation by TRAP.

after 60 min (Fig. 3*b*). Together, these data demonstrate that, following activation, overexpressed PAR1 is capable of initiating high levels of integrin signaling.

We characterized FAC assembly by immunofluorescent staining, using mAb anti-vinculin, anti-paxillin, and FAK polyclonal antibodies. Following activation, we observed some FAC formation in all of the cell types that we examined; however, the complexes in the activated PAR1 transfectants were far more distinct and larger than those that we observed in non-activated cells (Fig. 3*c*), in cells that had been transfected by empty vectors, or in cells that had not been transfected (data not shown). In the activated PAR1 clones, vinculin staining of FACs was intense; however, we also observed clear, although less intense, vinculin staining of FACs in activated non-transfected and mock-transfected cells. This may be explained by the fact that, rather than having a signaling function, vinculin functions mainly as a structural protein, and it has been reported to play a role in the maintenance of the FAC and adherence junctions (41). It has also been reported that both vinculin and talin are phosphorylated even under basal conditions (42).

*The $\alpha_v\beta_5$ Integrin Is Specifically Recruited to FACs in Response to PAR1 Activation without Alteration of the Cell-surface Integrin Level*—Having established that signaling was induced by PAR1 ligand activation, that also led to establishment of focal contacts, we asked whether altering the adhesive phenotype would be accompanied by *de novo* integrin expression. Here we used flow cytometry analysis carried out with a battery of anti-integrin antibodies directed against the $\alpha_v\beta_3$, $\alpha_5\beta_1$, and $\alpha_v\beta_5$ integrins. Following activation, we observed no significant differences between the cell-surface integrin profiles of the PAR1 transfectants and of the parental cells (Fig. 4*a*). Nevertheless, the fact that PAR1 activation did not alter integrin expression does not exclude the possibility of affinity modulation of the integrins in an inside-out manner.

We then asked which of these integrins would respond to PAR1 by participating in the induction of the cytoskeleton signaling events. We examined the cell surface integrins by immunofluorescent visualization before and after PAR1 activation. Although $\alpha_5\beta_1$ and $\alpha_v\beta_3$ (Fig. 4*b*, *B* and *C*) are distributed diffusely over the cell surface both before and after PAR1 activation, after PAR1 activation we found that $\alpha_v\beta_5$ was localized to distinct sites of FACs (Fig. 4*b*, *D*). However, we only detected $\alpha_v\beta_5$ within the focal contacts in the activated PAR1-overexpressing cells (Fig. 4*b*, *E*) but not in the PAR1-transfected cells prior to PAR1 activation cells (Fig. 4*b*, A), nor in the mock transfectants or in the parental non-transfected cells (data not shown). Based on our results, we hypothesized that

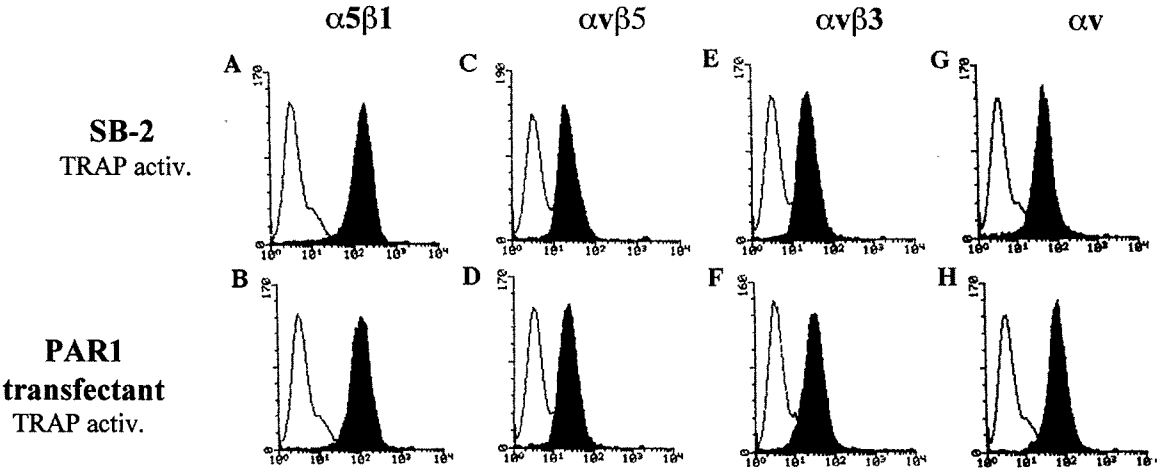


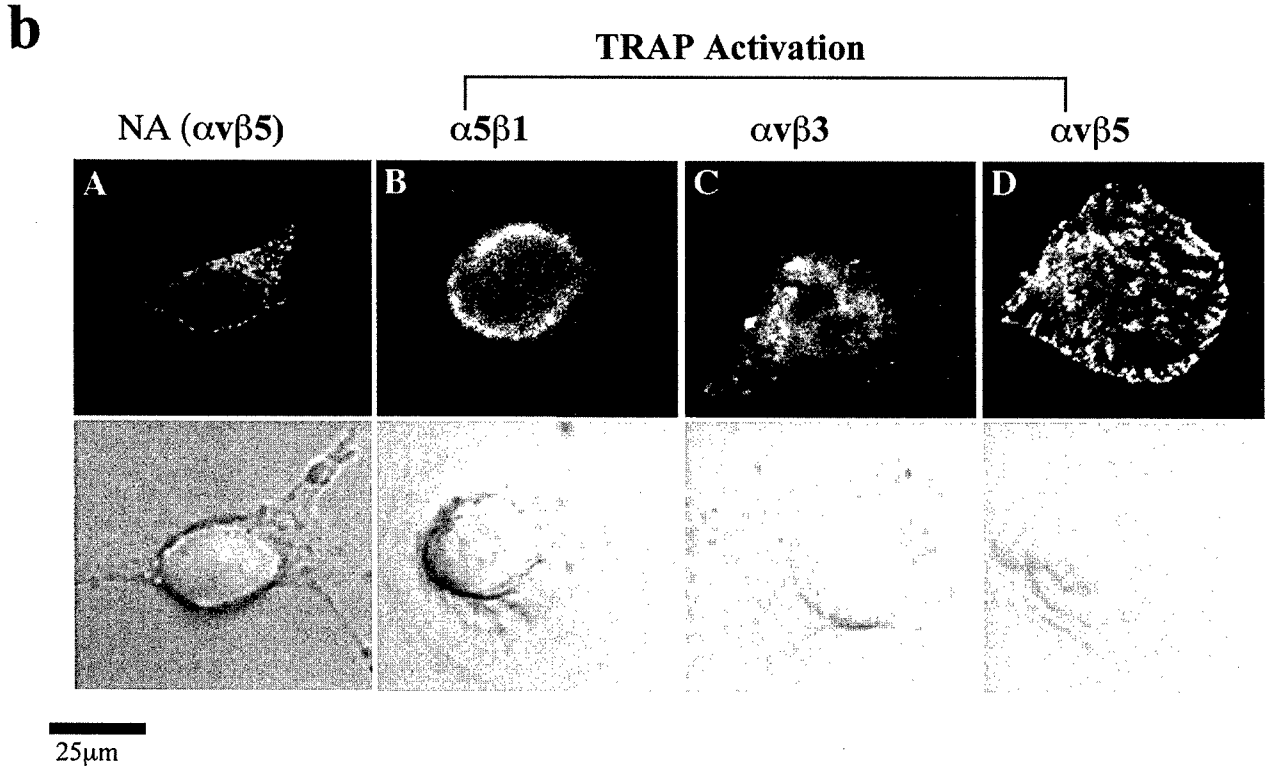


FIG. 4. **PAR1 activation did not alter the levels of integrin expression but did induce $\alpha_v\beta_5$ recruitment to FACs.** *a*, integrin expression levels were measured by flow cytometry in SB-2 naive cells and in PAR1 clone13, each activated with thrombin at a concentration of 1 unit/ml. The levels of $\alpha_5\beta_1$ (*A* and *B*), $\alpha_v\beta_5$ (*C* and *D*), $\alpha_v\beta_3$ (*E* and *F*), and the integrin $\alpha_v$ chain (*G* and *H*) were detected by incubating the cells with the appropriate specific mAb, followed by incubation with FITC-labeled anti-mouse IgG. The *white peaks* correspond to the expression levels of control secondary isotype-specific mouse IgG antibodies. Note that no significant changes were observed in the levels of any of the integrins examined. *b*, the distribution of integrins was detected by immunofluorescent staining (*upper panel*). Cy-3 red fluorescence was visualized by confocal microscopy. The *lower panel* shows the same cells as in the *upper panel*, but visualized by phase-contrast microscopy. Non-activated (*NA*) PAR1 clone 13, stained by anti-$\alpha_v\beta_5$ mAbs revealed a diffused pattern (*A*). After activation by TRAP, the integrin $\alpha_5\beta_1$ was detected in a random perinuclear position (*B*); the integrin $\alpha_v\beta_3$ was randomly scattered over the cell membrane (*C*); the integrin $\alpha_v\beta_5$ was localized to distinct "spikes" of focal adhesion contacts (*D*).

the $\alpha_v\beta_5$ integrin would respond to signals conveyed by the activated PAR1. It seemed that $\alpha_v\beta_5$ was specifically recruited to the focal adhesion contacts, where it played a major role in the reorganization of the cytoskeleton. Our hypothesis was confirmed by the results of the following reciprocal co-precipitation experiments. We analyzed the co-precipitation of paxillin with either $\alpha_v\beta_5$ or with $\alpha_v\beta_3$ in cell lysates of naive SB-2 cells and of the stable PAR1 transfectant clone 13 that was either thrombin-activated or not. The blotted membranes were incubated with the mAb of the anti-$\beta_5$ subunit. As we expected, in the parental cells, we found only basal levels of paxillin precipitation with either of the two integrins (Fig. 5, *a* and *b*). In the PAR1 clone 13, we found that paxillin co-precipitated with $\alpha_v\beta_3$ at a low level, and that level was not increased significantly by thrombin activation of PAR1 (Fig. 5*b*). However, in PAR1 clone 13, we did find a high level of co-precipitation of $\alpha_v\beta_5$ with paxillin, and that level was significantly increased by thrombin activation of PAR1. We also analyzed co-immunoprecipitation of paxillin and FAK from cell lysates of SB-2 cells and from the stable PAR1 transfectant clone 13, both of which were thrombin-activated or not. Again, the blotted membranes were incubated with the mAb of anti-$\beta_5$ subunit. As we expected, there was no co-immunoprecipitation in the parental cells, whether or not they were activated; however, there was a significant level of co-precipitation of $\beta_5$ subunit in the PAR1 clone 13, that was greatly increased upon activation by thrombin (Fig. 5*c*). When, instead of anti-$\alpha_v\beta_5$, we used anti-$\alpha_v\beta_3$ to probe the same blot, we found no evidence of the $\beta_3$ subunit (data not shown). These results indicate that $\alpha_v\beta_5$ and the typical signaling molecules, paxillin and FAK, were tightly associated and thus co-precipitated. We found that this kind of association was likely to occur within focal adhesions rather than in other cellular compartments, as demonstrated by the induced assembly and signaling of FACs. Furthermore, this association appeared to be labile and seemed to occur in response to PAR1 activation, indicating that the $\alpha_v\beta_5$ integrin was present within newly assembled FACs. Our data do not exclude the possibility that $\alpha_v\beta_3$ is present on the cell surface. Our data do suggest, however, that the $\alpha_v\beta_3$ integrin probably does not cooperate with PAR1-specific signaling to induce the cellular responses described here.

To substantiate the cooperative cross-talk and the recruitment of $\alpha_v\beta_5$ following PAR1 activation, we used a truncated form of PAR1, consisting of the extracellular and seven transmembrane domains but lacking the entire cytoplasmic portion of the receptor, and compared its function to the intact receptor. We carried out these experiments in MCF7 cells, which are non-invasive cells that naturally express very low levels of PAR1. These parental cells were transiently transfected with cDNA coding for either the intact PAR1 or truncated PAR1; 48 h after transfection, the transient transfectants were either activated or not and then subjected to immunoprecipitation analysis as described above. In lysates of the MCF7 PAR1 transient transfectants, we detected high levels of co-precipitation of FAK, paxillin, and $\alpha_v\beta_5$ after PAR1 activation by thrombin but not without activation. In lysates of truncated PAR1 transfectants, we observed no co-precipitation of FAK with paxillin, and $\alpha_v\beta_5$ regardless of whether the cells were thrombin activated or not (Fig. 5*d*, *upper panel*). In the PAR1 transfectants, tyrosine phosphorylated paxillin co-precipitated with $\alpha_v\beta_5$ and the level of this precipitation increased following thrombin activation of PAR1; in truncated PAR1-transfected cells, we detected only minor levels of phosphorylated paxillin with or without thrombin activation (Fig. 5*d*, *lower panel*). As seen by the results of the flow cytometry (FACS) analysis (Fig. 5*e*), the failure to immunoprecipitate FAK by anti-$\alpha_v\beta_5$ in PAR1-truncated transfectants did not result from the inability to express properly on the cell surface. Transfectants of either PAR1 (Fig. 5*e*, *A*) or truncated PAR1 (Fig. 5*e*, *B*) showed cell surface expression of the truncated receptor protein as determined by flow cytometry (FACS) analysis (Fig. 5*e*). Using anti-PAR1 WEDE15 mAbs, we found similar levels of expression in both the PAR1 (Fig. 5*e*, *A*, *second peak*) and the truncated PAR1 (Fig. 5*e*, *B*, *second peak*) transfectants, relative to the expression levels in naive cells (Fig. 5*e*, *A* and *B*, *first peaks*). We obtained similar results when we compared the levels of expression of the transfectants (Fig. 5*e*, *C* and *D*, *second peaks*) to those of empty vector-transfected cells (Fig. 5*e*, *C* and *D*, *first peaks*). The results of these experiments strongly support the notion that following activation the PAR1 cytoplasmic tail recruits and activates the $\alpha_v\beta_5$ integrin. That the PAR1 molecule participates in other signaling activities is supported by our finding that, although Shc was phosphorylated in the presence of the full-length activated PAR1, this was not the case in the presence of the activated truncated PAR1 (data not shown). We conclude that, although, like the full-length PAR1, the truncated PAR1 is expressed and assembled on the cell surface, unlike the full-length PAR1, the truncated PAR1 is incapable of carrying out PAR1 signaling. To ascertain that in fact the $\alpha_v\beta_5$ integrin may cooperate with PAR1 during tumor invasion, we asked whether neutralizing the activity of the $\alpha_v\beta_5$ integrin would affect the invasive properties of the highly invasive A375 SM cells. A375 SM cells were activated or not with 1 unit/ml thrombin; the activated cells were then either not treated at all or treated with anti-$\alpha_v\beta_5$-blocking mAbs antibodies (clone P1F6) or with nonspecific IgG. The cells were then subjected to a Matrigel invasion assay. As one can see, PAR1 activation further induced the invasive properties of the cells by 60% while the addition of anti-$\alpha_v\beta_5$ antibodies attenuated this induction; the addition of a non-related IgG led to no significant effect (Fig. *5f*).

## DISCUSSION

In this study, we have shown that changes in the expression of PAR1 in a cell affect its invasive capabilities. These changes come about through the specific recruitment of the $\alpha_v\beta_5$ integrin, through cytoskeletal reorganization, and through distinct signaling at FACs. The fact that PAR1 alters the invasive properties of tumor cells reinforces our initial observations that PAR1 expression correlates with the invasive potential of both the malignant invasion processes of breast carcinoma (3) and the physiological invasion processes of placenta trophoblast implantation (3)[3] emphasizing the central role of PAR1 during invasion. The on-going process of invasion by cells is characterized by extensive proteolytic remodeling, in part by serine proteases, of the tumor microenvironment (1, 2). Serine proteases also serve as ligands for several cell-surface receptors, among which is uPAR, which, through binding uPA, efficiently converts plasminogen to plasmin (11). TF is another protease cell surface receptor that binds factor VII, thereby initiating the coagulation pathway during perivascular hemostasis (43). It is interesting that, in addition to their involvement in hemostasis, these receptors are also implicated as central players in tumor progression and metastasis (8–10). The extracellular proteolytic activation of factor VII by TF is also responsible for the generation of thrombin from circulating plasma prothrombin (44, 45). In fact, thrombin production is probably the direct result of disseminated overactivation of the coagulation system, a widely described pathology among cancer patients (46). The abundant localization of either soluble or immobilized thrombin in the vicinity of the tumor milieu enables the excessive activation of PAR1 and the subsequent cellular response during invasion. In fact, although the repertoire of signaling

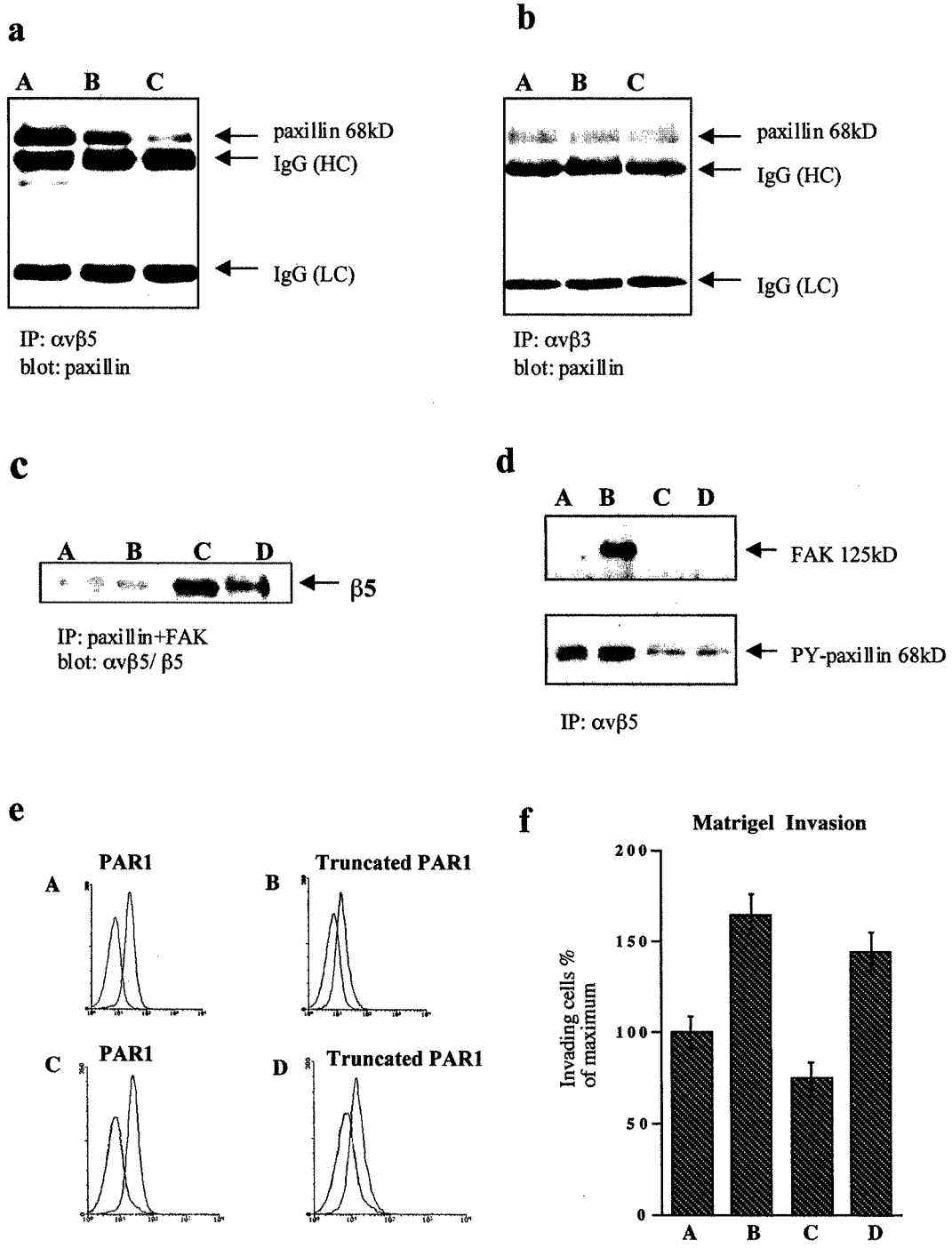


FIG. 5. **Activation of full-length PAR1 but not of truncated PAR1 led to the co-precipitation of $\alpha_v\beta_5$ with paxillin and FAK and reduced invasiveness in the presence of anti-$\alpha_v\beta_5$ antibodies.** Co-precipitation of paxillin with $\alpha_v\beta_5$ (*a*) or with $\alpha_v\beta_3$ (*b*) was measured in cells lysates of naive SB-2 cells (*C*) and of a stable PAR1 transfectant clone 13 that was either thrombin-activated (*A*) or not (*B*). *c*, paxillin and FAK were immunoprecipitated from cell lysates of SB-2 cells that had been thrombin-activated (*A*) or not (*B*) and from the stable PAR1 transfectant clone 13 that was either thrombin-activated (*C*) or not (*D*). The blotted membrane was incubated with anti-$\beta_5$ subunit mAb. *d*, non-invasive MCF7 cells, naturally expressing very low levels of PAR1, were transfected with cDNA expression vectors coding either for PAR1 or for truncated PAR1. In lysates of the PAR1 transfectants, co-precipitation of FAK and paxillin was detected after PAR1 activation by thrombin (*B*) but not without activation (*A*). In lysates of truncated PAR1 transfectants, no co-precipitation of FAK with paxillin with $\alpha_v\beta_5$ was observed regardless of whether the cells were thrombin-activated (*D*) or not (*C*). Tyrosine-phosphorylated paxillin co-precipitated with $\alpha_v\beta_5$ (*lower panel*) in PAR1-transfected cells (*A*); the level of this precipitation increased following thrombin activation of PAR1 (*B*); in truncated PAR1-transfected cells, only minor levels of phosphorylated paxillin were detected with (*D*) or without (*C*) thrombin activation. *e*, PAR1 expression levels were measured by FACS analysis using anti PAR1 mAb (WEDE15, Immunotech, Cedex, France), followed by incubation with FITC-labeled anti-mouse IgG. The analysis was carried out on MCF7 cells following transfection by DNA coding for the full-length PAR1 (*A* and *C*) or for the truncated PAR1 (*B* and *D*). Their levels were compared with non-transfected cells (*first peak*, *B* and *A*). This is true also when PAR1 or truncated PAR1 expression was measured relative to empty vector-transfected cells (*first peak*, *C* and *D*, respectively). *f*, A375SM cells were activated with 1 unit/ml thrombin (*B–D*) or not (*A*). The activated cells were then treated with 20 $\mu$ g/ml either anti-$\alpha_v\beta_5$-blocking mAbs (*C*) or nonspecific IgG (*D*). The treated cells were then subjected to a Matrigel invasion assay. The data presented here are the averages of data from at least three replicate experiments. One hundred percent invasion by the metatastic cells corresponded to 48 ± 3 invading cells as compared with 17 ± 1.5 invading cells by SB-2 non-metastatic cells (data not shown).

pathways is limited, it can be harnessed to integrate the information obtained from multiple receptors for a wide range of cellular responses. Here we have presented evidence showing that the overexpression of PAR1 increases the invasiveness of melanoma cells (Figs. 1*b* and 5*f*) and is also associated with an increase in the adhesion properties of the cell (Fig. 2, *a–c*). The activation of PAR1 resulted in the phosphorylation of the focal adhesion proteins FAK and paxillin that are typical of integrin signaling (Fig. 3*a*). Although the levels of the cell surface integrins were not affected (Fig. 4*a*), there was notable change in their mode of distribution. In particular, in response to PAR1 activation, the integrins $\alpha_v\beta_3$ and $\alpha_5\beta_1$ remained diffusely distributed but, in contrast, we found that the integrin $\alpha_v\beta_5$ was uniquely recruited to the sites of focal adhesion contacts (Fig. 4*b*).

It is well established that there is cooperation between integrins and other cell surface receptors, and further, that this cooperation may operate at several levels (47–50). Physical interactions between the extracellular domains of integrins and non-integrin receptors may result in mutual or sequential activation. For example, the results of several parallel studies demonstrate a physical link of uPAR with the integrin $\alpha_3\beta_1$ in keratinocytes (51), with the $\beta_2$ integrin Mac-1 in leukocytes (52), and with $\alpha_v\beta_5$ in breast cancer (53). The interaction of uPAR with integrin $\beta_1$ has also been shown to involve the functional cooperation of integrins with cell surface receptors via caveolin in a manner dependent on the conformational state of the receptors (54, 55). Alternatively, the activation state of integrins can be modified in an "inside-out" manner. Internal signals conveyed by intersecting cascades react with the cytoplasmic domain of the integrin $\beta$ subunit and thereby increase the affinity to their ligands of the extracellular portion of the integrins. Activation of G-protein-coupled receptor initiates a signal transmission through the C-terminal cytoplasmic domain of the receptor that leads to the assembly of adaptor proteins, non-receptor tyrosine kinases, and small G-proteins. Signals that are transduced in forking pathways, like Ras-Raf-mitogen-activated protein kinase and phosphatidylinositol 3-kinase-Akt/PKB, are also largely shared by integrin and thymidine kinase receptors. In endothelial cells (56), astrocyte cell rounding (57), and nuerite retraction (58), cytoskeletal responses to thrombin are known to involve the activation of the Ras-dependent ERK1/2 mitogen-activated protein kinase pathway during gap formation. These responses have been found to be Rho-dependent and require Rho-specific guanine nucleotide exchange factors (57, 59). More specifically, the Rho-dependent pathway controls barrier maintenance and stress fiber formation while Rac induction and myosin light chain kinase activation are both implicated in barrier dysfunction (56). Together, these facts imply that integrin-related signaling can be intersected by PAR1 signaling at the intracellular level.

Thrombin contains a cryptic RGD epitope that can potentially be recognized by integrins (40). The transient binding of thrombin to its receptor, prior to receptor cleavage, may serve as an RGD-exposing event that enables integrin binding during PAR1 activation. Thus, it seems that, at least theoretically, cooperation between PAR1 and the vitronectin receptor $\alpha_v\beta_5$ may occur at the extracellular level. Using a truncated PAR1 construct that lacks the entire cytoplasmic tail domain, we demonstrated here that it was the cytoplasmic portion of the PAR1 molecule that was responsible for cooperation with the $\alpha_v\beta_5$ integrin. We found that the truncated PAR1 was unable to transmit intracellular signals, and therefore, was unable to recruit $\alpha_v\beta_5$ and to initiate the typical integrin-associated signals. The other vitronectin receptor, $\alpha_v\beta_3$, has been widely implicated in both angiogenesis and melanoma cell invasion and metastasis (60, 61). Nevertheless, many tumor cells that lack $\alpha_v\beta_3$ can still readily metastasize (62). In cells that express both $\alpha_v\beta_5$ and $\alpha_v\beta_3$, $\alpha_v\beta_3$ is constitutively capable of inducing cell spreading and migration, while $\alpha_v\beta_5$ cannot promote cell spreading and migration without an additional exogenous soluble factor (60, 63). Based on our results, we propose that during the invasion process $\alpha_v\beta_5$ is the dominant integrin involved in PAR1-ECM signaling interactions. This is consistent with previous suggestions (64) that $\alpha_v\beta_5$ has a role in mediating human keratinocyte locomotion. Filardo *et al.* (36) also showed that $\alpha_v\beta_5$, as the sole integrin expressed in melanoma cells, could promote cell spreading and migration in cooperation with insulin-like growth factor signaling. It has also been postulated that $\alpha_v\beta_5$-mediated cell migration is protein kinase C $\theta$-dependent (66). Whether, as has been shown for endothelial cell migration (67), PAR1-mediated association of $\alpha_v\beta_5$ during tumor invasion is under the regulation of protein kinase C $\theta$ associated to TAP20 (theta-associated protein) remains to be determined.

The adhesion of tumor cells to the basement membrane is an essential step in the process of invasion. In contrast to the passive, non-active nature of non-malignant cells, the dynamic nature of tumor cell adherence to the underlying ECM precedes matrix degradation and migration. The interactions of the cell matrix involve the activation of integrins as well as the initiation, through focal adhesion structures, of signaling cascades that lead to cytoskeletal reorganization. This has been shown to be the case during tumor progression where TF supports cell adhesion, migration, and spreading through the action of the cytoplasmic portion of the TF molecule (10). The interaction of uPA with its cell surface receptor uPAR is necessary for vitronectin-dependent human pancreatic carcinoma (FG) cell adhesion and migration mediated via the $\alpha_v\beta_5$ integrin (65). The convergence point of the PAR1 and the $\alpha_v\beta_5$ signaling pathways is not yet known and is currently under study in our laboratory. Nevertheless, the data that we have presented here suggest that this unique mode of cooperation specifically promotes the invasive properties of tumor cells. We believe that the PAR1 and the $\alpha_v\beta_5$ signaling pathways that we have studied here may prove to be crucial for other PAR1 functions in vascular biology and embryonic development.

*Acknowledgements*—We thank Prof. Israel Vlodavsky for helpful discussions, Dr. Xiao-Ping (Merck Research Laboratory, West Point, PA) for providing us with the full-length PAR1, and F. R. Warshaw-Dadon for editorial revisions of the text.

REFERENCES

1. Mignatti, P., and Rifkin, D. B. (1993) *Physiol. Rev.* **73,** 161–195
2. Johnsen, M., Lund, L. R., Romer, J., Almholt, K., and Dano, K. (1998) *Curr. Opin. Cell Biol.* **10,** 667–671
3. Even-Ram, S., Uziely, B., Cohen, P., Grisaru-Granovsky, S., Maoz, M., Ginzburg, Y., Reich, R., Vlodavsky, I., and Bar-Shavit, R. (1998) *Nat. Med.* **4,** 909–914
4. Carroll, V. A., and Binder, B. R. (1999) *Semin. Thromb. Hemost.* **25,** 183–197
5. Kurschat, P., Zigrino, P., Nischt, R., Breitkopf, K., Steurer, P., Klein, C. E., Krieg, T., and Mauch. C. (1999) *J. Biol. Chem.* **274,** 21056–21062
6. Al-Mondhiry, H. (1975) *Thromb. Diath. Haemorrh.* **34,** 181–193
7. Shoji, M., Hancock, W. W., Abe, K., Micko, C., Casper, K., Baine, R. M., Wilcox, J. N., Danave, I., Dillehay, D. L., Matthews, E., Contrino, J., Morrissey, J. H., Gordon, S., Edington, T. S., Kudryk, B., Kreutzer, D. L., and Rickles, F. R. (1998) *Am. J. Pathol.* **152,** 399–411
8. Bromberg, M. E., Konigsberg, W. H., Madison, J. F., Pawashe, J. F., and Garen, A. (1995) *Proc. Natl. Acad. Sci. U. S. A.* **92,** 8205–8209
9. Mueller, B. M., and Ruff, W. (1998) *J. Clin. Invest.* **101,** 1372–1378
10. Ott, I., Fischer, E. G., Miyagi, Y., Mueller, B. M., and Ruff, W. (1998) *J. Cell Biol.* **40,** 1241–1253
11. Vassali, J. D., Sappino, A. P., and Belin, D. (1991) *J. Clin. Invest.* **88,** 1067–1072
12. Wei, Y., Lukashev, M., Simon, D. I., Bodary, S. C., Rosenberg, S., Doyle, M. V., and Chapman, H. A. (1996) *Science* **273,** 1551–1555
13. Brooks, P. C., Montgomery, A. M., Rosenfeld, M., Reisfeld, R. A., Hu, T., Klier, G., and Cheresh, D. A. (1994) *Cell* **79,** 1157–1164
14. Kahn, M. L., Hammes, S. R., Botka, C., and Coughlin, S. R. (1998) *J. Biol. Chem.* **273,** 23290–23296

15. Cupit, L. D., Schmidt, V. A., and Bahou, W. F. (1999) *Trends Cardiovasc. Med.* **9,** 42–48
16. Vu, T. K., Hung, D. T., Wheaton, V. I., and Coughlin, S. R. (1991) *Cell* **64,** 1057–1068
17. Nystedt, S., Emilsson, K., Larsson, A. K., Strombeck, B., and Sundelin, J. (1995) *Eur. J. Biochem.* **232,** 84–89
18. Ishihara, H., Connolly, A. J., Zeng, D., Kahn, M. L., Zheng, Y. W., Timmons, C., Tram, T., and Coughlin, S. R. (1997) *Nature* **386,** 502–506
19. Liotta, L. A., Rao, C. N., and Barsky. S. H. (1983) *Lab. Invest.* **49,** 636–649
20. Crowe, D. L., and Shuler, C. F. (1999) *Histol. Histopathol.* **14,** 665–671
21. Giancotti, F. G., and Ruoslahti, E. (1999) *Science* **285,** 1028–1032
22. Bissell, M. J., Weaver, V. M., Lelievre, S. A., Wang, F., Petersen, O. W., and Schmeichel, K. L. (1999) *Cancer Res.* **59,** 1757s–1763s; Discussion 1763s–1764s
23. Hynes, R. O. (1992) *Cell* **69,** 11–25
24. Clark, E. A., and Brugge, J. S. (1995) *Science* **268,** 233–239
25. Schwartz, M. A., Schaller, M. D., and Ginsberg, M. H. (1995) *Annu. Rev. Cell Dev. Biol.* **11,** 549–599
26. Howe, A., Aplin, A. E., Alahari, S. K., and Juliano, R. L. (1998) *Curr. Opin. Cell Biol.* **10,** 220–231
27. Gilmore, A. P., and Burridge, K. (1996) *Structure* **4,** 647–651
28. Wang, N., Butler, J. P., and Ingber, D. E. (1993) *Science* **260,** 1124–1127
29. Felsenfeld, D. P., Choquet, D., and Sheetz, M. P. (1996) *Nature* **383,** 438–440
30. Sheetz, M. P., Felsenfeld, D. P., and Galbraith, C. G. (1998) *Trends Cell Biol.* **8,** 51–54
31. Burridge, K., Turner, C. E., and Romer, L. H. (1992) *J. Cell Biol.* **119,** 893–903
32. Hildebrand, J. D., Schaller, M. D., and Parsons, J. T. (1995) *Mol. Biol. Cell* **6,** 637–647
33. Chen, H. C., Appeddu, P. A., Parsons, J. T., Hildebrand, J. D., Schaller, M. D., and Guan, J. L. (1995) *J. Biol. Chem.* **270,** 16995–16999
34. Schlaepfer, D. D., Hauck, C. R., and Sieg, D. J. (1999) *Prog. Biophys. Mol. Biol.* **71,** 435–478
35. Bockholt, S. M., and Burridge, K. (1993) *J. Biol. Chem.* **268,** 14565–14567
36. Filardo, E. J., Deming, S. L., and Cheresh, D. A. (1996) *J. Cell Sci.* **109,** 1615–1622
37. Ishida, T., Ishida, M., Suero, J., Takahashi, M., and Berk, B. C. (1999) *J. Clin. Invest.* **103,** 789–797
38. Ojaniemi, M., and Vuori, K. (1997) *J. Biol. Chem.* **272,** 25993–25998
39. Albini, A. (1998) *Pathol. Oncol. Res.* **4,** 230–241
40. Bar-Shavit, R., Sabbah, V., Lampugnani, M. G., Marchisio, P. C., Fenton, I. I. J. W., Vlodavsky, I., and Dejana, E. (1991) *J. Cell Biol.* **112,** 335–344
41. Rudiger, M. (1998) *Bioessays* **20,** 733–740
42. Schaphorst, K. L., Pavalko, F. M., Patterson, C. E., and Garcia, J. G. (1997) *Am. J. Respir. Cell Mol. Biol.* **17,** 443–455
43. Ruf, W., and Edgington, T. S. (1994) *FASEB J.* **8,** 385–390
44. Cavanaugh, P. G., Sloane, B. F., and Honn, K. V. (1988) *Haemostasis* **18,** 37–46
45. Zucker, S., Mirza, H., Conner, C. E., Lorenz, A. F., Drews, M. H., Bahou, W. F., and Jesty, J. (1998) *Int. J. Cancer* **75,** 780–786
46. Rickles, F. R., Edwards, R. L., Barb, C., and Cronlund, M. (1983) *Cancer* **51,** 301–307
47. Plopper, G. E., McNamee, H. P., Dike, L. E., Bojanowski, K., and Ingber, D. E. (1995) *Mol. Biol. Cell* **6,** 1349–1365
48. Miyamoto, S., Teramoto, H., Gutkind, J. S., and Yamada, K. M. (1996) *J. Cell Biol.* **135,** 1633–1642
49. Baron, V., Calleja, V., Ferrari, P., Alengrin, F., and Van Obberghen, E. (1998) *J. Biol. Chem.* **273,** 7162–7168
50. Schneller, M., Vuori, K., and Ruoslahti, E. (1997) *EMBO J.* **16,** 5600–5607
51. Ghosh, S., Brown, R., Jones, J. C., Ellerbroek, S. M., and Stack, M. S. (2000) *J. Biol. Chem.* **275,** 23869–23876
52. Simon, D. I., Wei, Y., Zhang, L., Rao, N. K., Xu, H., Chen, Z., Liu, Q., Rosenberg, S., and Chapman, H. A. (2000) *J. Biol. Chem.* **275,** 10228–10234
53. Carriero, M. V., Del Vecchio, S., Capozzoli, M., Franco, P., Fontana, L., Zannetti, A., Botti, G., D'Aiuto, G., Salvatore, M., and Stoppelli, M. P. (1999) *Cancer Res.* **59,** 5307–5314
54. Wei, Y., Yang, X., Liu, Q., Wilkins, J. A., and Chapman, H. A. (1999) *J. Cell Biol.* **144,** 1285–1294
55. Chapman, H. A. (1997) *Curr. Opin. Cell Biol.* **9,** 714–724
56. Vouret-Craviari, V., Boquet, P., Pouyssegur, J., and Van Obberghen-Schilling, E. (1998) *Mol. Biol. Cell* **9,** 2639–2653
57. Majumdar, M., Seasholtz, T. M., Goldstein, D., de Lanerolle, P., and Brown, J. H. (1998) *J. Biol. Chem.* **273,** 10099–10106
58. Jalink, K., van Corven, E. J., Hengeveld, T., Morii, N., Narumiya, S., and Moolenaar, W. H. (1994) *J. Cell Biol.* **126,** 801–810
59. Majumdar, M., Seasholtz, T. M., Buckmaster, C., Toksoz, D., and Brown, J. H. (1999) *J. Biol. Chem.* **274,** 26815–26821
60. Brooks, P. C., Klemke, R. L., Schon, S., Lewis, J. M., Schwartz, M. A., and Cheresh, D. A. (1997) *J. Clin. Invest.* **99,** 1390–1398
61. Seftor, R. E. (1998) *Am. J. Pathol.* **153,** 1347–1351
62. Nip, J., and Brodt, P. (1995) *Cancer Metastasis Rev.* **14,** 241–252
63. Klemke, R. L., Yebra, M., Bayna, E. M., and Cheresh, D. A. (1994) *J. Cell Biol.* **127,** 859–866
64. Kim, J. P., Zhang, K., Chen, J. D., Kramer, R. H., and Woodley, D. T. (1994) *J. Biol. Chem.* **269,** 26926–26932
65. Yebra, M., Goretzki, L., Pfeifer, M., and Mueller, B. M. (1999) *Exp. Cell. Res.* **250,** 231–240
66. Tang, S., Morgan, K. G., Parker, C., and Ware, J. A. (1997) *J. Biol. Chem.* **272,** 28704–28711
67. Tang, S., Gao, Y., and Ware, J. A. (1999) *J. Cell Biol.* **147,** 1073–1084

# Oncogenic transformation induces tumor angiogenesis: A role for PAR1 activation

Yong-Jun Yin,[1] Zaidoun Salah, [1] Myriam Maoz, [1] Sharona Cohen Even Ram, [1] Shalom Ochayon, [1] Gera Neufeld, [2] Shulamit Katzav[3] and Rachel Bar-Shavit[1] *Departments of Oncology[1], The Hubert H. Humphrey Center for Experimental Medicine & Cancer Research[3], The Hebrew University-Hadassah Medical School, Jerusalem 91120 and The Department of Biology[2], Technion, Israel Institute of Technology, Haifa 32000, Israel*

**Running title:** *Par1* induced tumor angiogenesis

**Correspondence Address:**
Rachel Bar-Shavit, Ph.D.
Department of Oncology
Hadassah-University Hospital
POB 12000, Jerusalem 91120
Israel

Phone: 972-2-6777563
Fax: 972-2-6422794
e-mail: barshav@md.huji.ac.il

**ABSTRACT**

The formation of new blood vessels is a critical determinant of tumor progression. We find that *Par1* gene expression plays a central role in blood vessel recruitment in animal models. By *in vivo* injection of either Matrigel plugs containing *Par1*-expressing cells or of rat prostatic carcinoma cells transfected with tetracycline-inducible *par1* expression vectors, we show that *Par1* significantly enhances both angiogenesis and tumor growth. Several VEGF splice forms are induced in cells expressing *Par1*. Activation of PAR1 markedly augments the expression of VEGF mRNAs and of functional VEGFs as determined by *in vitro* assays for endothelial tube alignment and bovine aortic endothelial cell proliferation. Since neutralizing anti-VEGF antibodies potently inhibited *Par1*-induced endothelial cell proliferation, we conclude that *Par1*-induced angiogenesis requires VEGF. Specific inhibitors of PKC, Src and PI3K inhibit *Par1*-induced VEGF expression, suggesting the participation of these kinases in the process. We also show that oncogenic transformation by genes known to be part of PAR1 signaling machinery is sufficient to increase VEGF expression in NIH3T3 cells. These data support the novel notion that initiation of cell signaling either by activating PAR1 or by the activated forms of oncogenes is sufficient to induce VEGF and hence angiogenesis.

**Key words**: Thrombin-receptor, VEGF (vascular endothelial growth factor), invasion, metastasis

## INTRODUCTION

The formation of new blood vessels (vasculogenesis and angiogenesis) involves the coordinated functions of endothelial cell proliferation, migration and tube alignment. The emergence of new blood vessels from pre-existing vasculature is a process that is highly affected by growth factor receptors such as KDR/*flk-1* and *flt-1* and by a spectrum of adhesion molecules, primarily integrins (1,2). Angiogenesis has been designated a hallmark of cancer and determined to be a prerequisite for tumor growth (3, 4) as well as for various ischemic diseases such as retinopathy of prematurity (3). This process takes place as a consequence of an angiogenic genetic switch, which allows the recruitment of blood vessels from neighboring tissues (5). The critical determinants of this angiogenic switch remain to be elucidated.

The relationship between thrombosis and cancer/metastasis was first recognized by the classical observations of Trousseau in 1872 (6). Many studies since have described a systemic activation of the blood coagulation cascade in patients with cancer (7-9). During initiation of the thrombosis/hemostasis cascade, a complex of factors Va and Xa (Va/Xa) acts to convert prothrombin to the serine protease thrombin. Thrombin ligates the Protease Activated Receptor (PAR) family to initiate cellular functions. We have shown previously that PAR1, the first identified member of the PAR family, plays a direct role in both normal (physiological placental implantation) and pathological (malignancy) cell invasion processes (10). Molecular mechanisms underlying PAR1 involvement in tumor invasion and metastasis include increased phosphorylation of focal adhesion complex proteins, cytoskeletal reorganization, and the recruitment of $\alpha v\beta 5$ integrin after PAR1 ligation (11).

PARs are G-coupled cell surface proteins mediating intracellular responses to the serine protease thrombin (12, 13). PAR1 was recently recognized as an oncogene, promoting transformation in NIH 3T3 cells. In addition to its potent focus forming activity, constitutive over-expression of PAR1 in NIH-3T3 cells promoted the loss of anchorage- and serum-dependent growth. PAR1 activity was found to be directly linked to Rho A and inhibited by pertussis toxin and thus mediated via the $G\alpha 13$ subunit (14). The oncogenic function of PAR1 is

especially significant in light of our observation that PAR1 is over-expressed in a series of biopsy specimens of breast tumors (10) as well as in a collection of cell lines exhibiting differential metastatic potentials (11).

Mouse embryos lacking *Par1* or several coagulation factors die with varying frequencies at midgestation, often with signs of bleeding (15-21). Recently (22) it has been shown that *Par1* plays a critical role in endothelial cell embryonic development, rescuing *Par 1* $^{-/-}$ mice from bleeding to death; however, its function in tumor angiogenesis is unknown. It was unclear whether bleeding in embryos lacking *Par1* results from impairment of hemostasis or of blood vessel formation. Griffin *et al* (22) provided elegant evidence demonstrating that loss of *Par1* does not prevent vessel formation but rather impairs the stabilization and maturation of the newly forming vessels, thereby causing abnormal fragility and ruptures in the vessel wall (22, 23). By initiating the PAR1 signaling cascade in endothelial cells, Griffin *et al* were able to rescue *Par1* deficient mouse embryos from bleeding to death. These results demonstrate that activation of PAR1 and its signaling pathway in endothelial cells is essential for vascular integrity. It is interesting to note the phenotypic similarities between *Par1*$^{-/-}$ embryos and various coagulation factor knock out embryos (e.g. factor V$^{-/-}$, tissue factor $^{-/-}$ and prothrombin $^{-/-}$). Most die at midgestation with yolk sac defects and bleeding (16-24).

The major angiogenic factor VEGF acts mainly through two tyrosine kinase receptors present almost exclusively on endothelial cells, VEGF receptor-1 (VEGF-1; also termed *flt*-1) and VEGF receptor-2 (*KDR/flk-1*) ( 25 , 26), and via neuropilins expressed on tumor cells (27). The importance of the VEGF/VEGFR system in angiogenesis is strongly supported by data showing early embryonic lethality in mice either heterozygous or completely deficient in VEGFR (25, 27-31). The crucial biological role of VEGF in angiogenic related functions was shown in studies using targeted gene disruption in mice. Since VEGFR-2 is required for the differentiation of endothelial cells and the recruitment of endothelial cell precursors (31), embryos lacking the VEGFR-2 gene die before birth because the blood vessels do not form (32).

Likewise, inhibition of VEGF activity using neutralizing antibodies or by the introduction of dominant negative VEGF receptors into endothelial cells derived from tumor-associated blood vessels resulted in the inhibition of tumor growth and even in tumor regression. This indicates that VEGF is a major initiator of tumor angiogenesis (32, 33). Furthermore, VEGF expression is potentiated by hypoxia and the induced VEGF production in hypoxic areas of solid tumors contributes significantly to tumor angiogenesis (34-36). VEGF also functions as a survival factor for immature blood vessels. These vessels become VEGF independent once they recruit periendothelial cells and undergo maturation. However, the newly formed vascular network will regress if VEGF is prematurely withdrawn. Thus, VEGF deprivation may lead not only to inhibition of further angiogenesis, but also to regression of already formed, immature, tumor vessels (37).

Several VEGF isoforms are produced from the VEGF gene by alternative splicing. Five human VEGF mRNA splice forms have been identified, encoding VEGFs of various lengths (121, 145, 165, 189 and 206 amino acids; VEGF 121-206) (29-36, 38, 39). They are mainly distinguished by their heparin and heparan sulfate binding ability. While VEGF 121 lacks the amino acids encoded by exons 6 and 7 of the VEGF gene (40) and does not bind heparin or extracellular matrix (41), VEGF165 includes exon 7 and does bind heparin (40, 41) and VEGF145 includes exon 6 and binds tightly to the extracellular matrix (ECM) (42). VEGF189 and VEGF 206 contain the amino acids encoded by both exons 6 and 7 and display a higher affinity for heparin and heparan sulfate than VEGF145 or VEGF165. It is not clear which of these splice forms are involved in VEGF's known effects on angiogenesis and tumor growth. In addition, it is not known whether the effects of VEGF and PAR1 on tumor progression are inter-related in any way. We investigated this question and explored the role of PAR1 in tumor angiogenesis.

## MATERIALS AND METHODS

***Cells-*** SB-2 non-invasive human melanoma (kindly provided by J. Fidler and M. Bar-Eli, Dept. of Cell Biology, University of Texas, M. D. Anderson Cancer Center, Houston) were

grown in 10% FCS-DMEM supplemented with 50 U/ml penicillin and streptomycin (GIBCO-BRL, Gaithersburg, MD, USA) and maintained in a humidified incubator with 8% $CO_2$ at 37°C . The *Par1* stable transfectants, clone 13 and clone MixL, were grown under the same conditions; for long-term maintenance these were supplemented with 200 μg/ml G418 antibiotics (11). MCF-7 (adenocarcinoma) and MDA435 cells (ductal carcinoma) were maintained as previously described (10). NIH 3T3 cells transfected with Vav, Src and Ras were grown in DMEM supplemented with 10% calf serum.

***Cell transfection*** - Cells were grown to 30-40% confluency and then transfected with 0.5-2 μg/ml of plasmid DNA in Fugene 6 transfection reagent (Boehringer Mannheim, Germany) according to the manufacturer's instructions (11). After 10 days of selection, stable, transfected clones were established in medium containing 400 μg/ml G418. Antibiotic resistant cell colonies were transferred to separate culture dishes and were grown in 200 μg/ml G418 medium. Forty-eight hours after transfection, transiently transfected cells were collected and tested ( RNA was extracted either for RT-PCR and/or Northern blot or for preparation of conditioned medium).

***Preparation of conditioned medium***- cells at 90% confluency were fed with fresh medium and incubated either for 30 hours or treated for additional 8 hours with TRAP (100 μM). Conditioned medium was then collected and centrifuged at 1,000 rpm for 5 minutes. The supernatant was either used immediately or stored at $4^0$C prior to use.

***RNA extraction and reverse transcriptase - polymerase chain reaction (RT- PCR)*** Total RNA was prepared, using the *TRI REAGENT* (Molecular Research Center, Inc. Ohio) as described by the manufacturer. One microgram of RNA was used for complementary DNA (cDNA) synthesis, employing M-MLV reverse transcriptase and oligo dT (both from Promega, Heidelberg, Germany). VEGF transcripts were amplified, using Taq polymerase (Bioline, London, UK) for 20ul total PCR reaction. 95°C for 3 minutes for initial melting was followed by 24-30 cycles of 95°C for 1

minute, 59°C for 30 seconds, and 72°C for 1 minute; 7 minutes at 72°C was used for final extension following cycling. PCR primers were as follows: upstream mouse L19, 5'-CTGAAGGTGAAGGGGAATGTG-3'; downstream mouse L19, 5'-GGATAAAGTCTTGATGATCTC-3'(24cycles); upstream human GADPH, 5'-CCACCCATGGCAAATTCCATGGCA-3'; downstream human GADPH, 5'-TCTAGACGGCAGGTCAGGTCCACC(26cycles); upstream VEGF, 5'-TCGGGCCTCCGAAACCATGA-3'; downstream VEGF, 5'-CCTCCTGAGAGATCTGGTTC-3' (30cycles). For VEGF, sequences in the 3' and 5' translated regions were used, allowing the amplification of the known splice variants (516 base pair [bp], 648bp, 720bp, and 771bp) (46). PCR products were separated on a 2% Nusieve (FMC; Rockland , ME) 3:1 agarose gel, stained with ethidium bromide, and visualized under UV light.

***Northern Blot Analysis*** - Total RNA (20μg) was electrophoresed on 1% formaldehyde-agarose gels and transferred to Hybond-$N^+$ membranes (Amersham Pharmacia Biotech UN Limited). The membranes were hybridized (42°C, 18h) with $\alpha$ $^{32}$P-dCTP labelled (Rediprimer II, Amersham Biosciences UK Limited) probe for human $VEGF_{165}$ (690 bp obtained by RT-PCR). After hybridization, membranes were washed and exposed to X-ray films. We used the housekeeping gene β-actin as a control for RNA loading.

***Three dimensional tube forming assay*** - Type I collagen was prepared from the tail tendons of adult Sprague Dawley rats. The collagen matrix gel was obtained by simultaneously raising the pH and ionic strength of the collagen solution. Briefly, collagen was used to coat 24-well cluster plates (0.3 ml/well). After polymerization of the collagen at 37°C for 0.5 h, the BAEC cells (2 X $10^4$/0.5ml/well) were added to each well. Collagen solution (0.4ml) was carefully poured on top of the cells. After the gel was formed, 0.4 ml of conditioned medium from Cl13/*Par1* transfected SB-2 cells, mock transfected SB-2 or control non-transfected cells was added and replaced with fresh medium every other day. Tube formation and alignment of BAEC were visualized by phase microscopy, and photographed at days 8-10 (43).

***BAEC proliferation*** - Cells were seeded in DMEM containing 10% FCS at a density of 2 x$10^3$ cells/16-mm well of a 24-well plate, in triplicate. The medium was replaced with conditioned medium 24 h after seeding, and the cells were cultured for 3 to 14 days in the different conditioned media. Every three days post-seeding, cells (three wells for each condition) were dissociated with trypsin/EDTA and counted with a Coulter counter (Coulter Electronics Ltd.)

***Matrigel plug assay*** - The Matrigel plug assay was performed as previously described (44). Briefly, 300 µl Matrigel (kindly provided by Dr. H. Kleinman, NIDR, NIH, Bethesda, MD) containing $10^6$ *Par1*-transfected SB-2 cells/ml at 4°C were injected, subcutaneously (s.c.) into an abdominal site between the hind limbs of seven-week-old male BALB/c mice (n=6). Injections were performed bilaterally, when always at the right side Matrigel mixed with naïve cells and transfection reagent. Control mice were injected with Matrigel mixed with empty vector transfected SB-2 cells lacking *Par1*. Matrigel plugs were removed after 10 days. The skin of the mouse was easily pulled back to expose the Matrigel plug, which remained intact. After qualitative differences were noted and photographed, the plugs were dissected out of the mouse and fixed with 4% formaldehyde/phosphate-buffered saline and embedded in paraffin for histological evaluation. For vessel density analysis, 5-µm thick sections from paraffin-embedded plugs were stained with H&E and Mallory's staining. Vascular structures were recognized as luminal or slit-like structures that occasionally contained blood cells within them, as described previously (45). The microvessel density was determined in various plug areas. Individual vessels were counted on X200 microscopic fields (0.785$mm^2$). A total of six fields/plug (representative of at least 3 independent Matrigel plugs per condition) were analyzed.

***"Tet-On" system*** - A 1.3 Kb DNA of *hPar1* was cut from PSL-301-PAR1 plasmid by BamH I and Xho I restriction enzymes. This fragment was cloned into the multiple cloning site of pAHygTet1 plasmid between BamH I and Xho I to generate pAHygTet1-*hPar1*.

Cells from a clone of AT2.1/Tet -On (generously provided by Dr. Hua-Quan Miao, Imclone systems, Inc., new York, NY 10014) were transfected with 2μg DNA of either pAHygTet1-*hPar1* or pAHygTet1 using FuGENE 6 transfection reagent (Roche, Mannheim Germany). After 48hr, the medium was changed and cells were selected by 800 μg/ml hygromycin B (Calbiochem, La Jolla, CA). Stable pAHygTet1-*hPar1*-transfected clones were checked for *hPar1* expression by Northern blot analysis after a 48 hr induction with Doxycyclin (Dox) (2μg/ml).

***Tumor growth* in vivo -** 2 month old male Copenhagen rats were anesthetized. Cells (0.3 X $10^6$ / 0.3 ml /rat) were injected subcutaneously at a dorsal site between the hind limbs. The rats (*n*=5, each group) were fed with drinking water containing 1% sucrose. To induce *h*PAR1 expression, 10 μg/ml Dox was added to the drinking water, which was changed every 2 days.

## RESULTS

**PAR1 promotes tumor angiogenesis *in vivo*.** We have previously shown that introducing *Par1* cDNA into non-metastatic melanoma cells induced the invasive and adhesive properties of these cells (11). The molecular mechanisms underlying PAR1-induced tumor invasion include recruitment of αvβ5 integrin, focal adhesion complex formation, and cytoskeletal reorganization. We asked whether PAR1 is also capable of inducing tumor angiogenesis. To address this question, we applied a Matrigel plug assay to evaluate whether *Par1* can recruit blood vessels *in vivo*. Stable *Par1* transfected, non-metastatic SB-2 melanoma cells (C113 cells) were mixed at $4^0$C with Matrigel (reconstituted basement membrane (BM) preparation extracted from EHS mouse sarcoma) and injected *s.c.* into BALB/c mice. Upon injection, the liquid Matrigel rapidly formed a solid gel plug that served not only as an inert vehicle for PAR1 producing cells, but also mimicked the natural interactions that exist between tumor cells and the surrounding extracellular matrix (ECM). Non-transfected SB-2 cells expressing no *Par1* were similarly mixed with Matrigel and injected as a control. In some cases, C113 cells were treated with thrombin receptor activating peptide (TRAP) to activate *Par1* prior to embedding in Matrigel. 10 days after injection, the Matrigel plugs were exposed, examined and photographed. Plugs containing control SB-2 cells were pale, containing few blood vessels; however, those containing *Par1*-expressing C113 cells were reddish, indicative of recruited blood vessels. Plugs containing TRAP-activated C113 cells had the most pronounced red coloration (Fig.1 I). Matrigel plugs were subsequently removed, paraffin-embedded, sectioned, and stained for collagen (Mallory's staining) to allow histological evaluation of blood vessels in the plug. A network of recruited capillary blood vessels is seen in plugs containing C113 cells while few vessels appear in plugs containing non transfected cells (Fig. 1 II). The difference in angiogenesis induced by activated PAR1-transfected cells as compared to non transfected either treated by thrombin or not is particularly striking (Fig 1 II).

Quantification of blood vessels in Matrigel sections indicated that these differences are statistically significant (Fig. 1 III). An average of 22.33±3.01 blood vessels were found in unactivated SB-2-containing plugs and 90.00±15.00 in TRAP-activated SB-2 plugs. For Cl13-containing plugs before and after TRAP activation the numbers were 40.40±9.55 and 327±26.5, respectively.

**Inducible *Par1* expression in rat prostatic carcinoma increases tumor mass and angiogenesis.** Differential expression of *Par1* in the Dunning rat prostate carcinoma cell variants was observed by RT-PCR. The AT2.1 variant expressed low levels of *Par1*, while AT3.1, which is more motile and tumorigenic than AT2.1 (47), expressed high levels (Fig. 2 IA). In order to establish the exclusive effect of *Par1* expression on prostate tumor progression, AT2.1 cells were transfected with human *Par1* cDNA under the control of a tetracycline-inducible promoter (Fig. 2II). Two clones (AT2.1/Tet-On/ *hPar1* clones 1 and 4) were isolated, in which *hPar1* expression was strongly induced by the tetracycline analog Dox as determined by Northern blot analysis. *Par1* expression was nearly undetectable in the absence of Dox. Following addition of Dox, the levels of the 4.1 kb *Par1* mRNA were increased substantially (Fig. 2II, D & F). The optimal dose of Dox necessary to induce *Par1* expression was 1-2 μg/ml (not shown). *Par1* mRNA could be detected as early as 4-6 h, and reached maximum levels at 20-24 h after Dox treatment (not shown). AT2.1 cells transfected with the pTet-On vector without the *Par1* gene did not express any detectable *Par1* mRNA levels either in the presence (Fig. 2II, lane B) or in the absence (Fig. 2II, lane A) of Dox.

To assess the effect of PAR1 on tumor growth *in vivo,* AT2.1/Tet-On/*hPar1* clone 4 cells or control transfected cells were injected *s.c.* into rats. Rats were then maintained for 2 weeks with either regular drinking water (supplemented with 1% sucrose) or drinking water containing Dox

(and 1% sucrose) to induce *Par1*. In all injected rats, marked tumor growth occurred during this time period. In the absence of Dox the mean mass of AT2.1 clone 4 tumors was 0.35±0.1 gr (Fig. 2 III, B). When PAR1 expression was induced by Dox in the drinking water, mean AT2.1 clone 4 tumor mass increased 3.7 fold to 1.30 ± 0.14 gr. This increase was statistically significant. In addition to being larger, tumors in these Dox –treated animals had a very reddish appearance (Fig. 2III, C) compared to the pale appearance of tumors from untreated animals (Fig. 2 III, B). In comparison, tumors from control-transfected and non-transfected AT2.1 tumors were significantly smaller and did not increase in mass or change in color when Dox was delivered in their drinking water (Fig. 2 IV). We conclude, therefore, that the regulated induction of the *Par1* gene markedly enhanced two critical determinants of tumor progression: tumor size and angiogenesis.

***Par1* expressing cells induce functional VEGF.** Next we analyzed the expression levels of VEGF165 in the stably *Par1*-transfected melanoma cells (Cl13 and Mix L) using Northern blot analysis (Fig. 3I). Parental SB-2 or control transfected cells (Fig. 3I, A&B respectively) showed no detectable levels of VEGF, but both Cl13 and MixL had significant levels of VEGF165 mRNA (Fig. 3I, C&D respectively). A probe for the house keeping gene, β-actin, was used as a control for loading. Activation of PAR1 by thrombin or TRAP further increased levels of VEGF165 mRNA (Fig. 3II). Maximal induction was obtained after 8 h of TRAP treatment (Fig. 3II, lane G), at concentrations of 100μM and 50 μM and was reduced markedly with lower concentrations (Fig. 3III, lanes B-F). When control SB-2 cells were treated with 100 μM of TRAP for 8 h there was no detectable change in VEGF mRNA levels compared to untreated SB-2 cells (data not shown). A similar pattern was obtained for VEGF145 but not for VEGF 189, which was slightly expressed only after 8h of TRAP treatment (Fig. 3IV). Using RT-PCR with

primers targeting the start site (exon 1) and the end point (exon 8) of the VEGF gene, we could detect all the different splice forms induced by *Par1*. *Par1* markedly induced VEGF 121, VEGF 145, and VEGF 165; it induced only very low levels of VEGF 189 and VEGF 206 was not detected at all. No VEGF isoforms were detected in the absence of *Par1* in SB-2 parental cells, control-transfected SB-2 cells, or non metastatic cells (MCF7) (Fig. 3 IV). Activation of PAR1 (TRAP; 8h) increased substantially the level of VEGF189, similar to the pattern obtained in the highly metastatic cells (MDA 435).

To determine whether the increased levels of VEGF mRNA induced by *Par1* gene correspond to increases in functional VEGF protein, we collected conditioned medium from untreated or TRAP activated Cl13 cells as well as from control transfected and non transfected SB-2 cells. We used an endothelial tube forming assay to assess VEGF activity: BAEC cells were embedded in a 3 dimensional collagen (type I) mesh and the extent of tube-forming network was evaluated following application of the various conditioned media. While low vascular branching activity was obtained with untreated control conditioned medium, either treated with thrombin or not (Fig. 4I A-C), a more complex appearing network was obtained with activated PAR1 conditioned medium obtained from *Par1*-transfected cells (Fig. 4I, D-F). We also examined the effect of *Par1* transfected cell conditioned media on the rate of bovine aortic endothelial cell (BAEC) proliferation *in vitro*. BAEC proliferation was found to be maximal using conditioned medium from Cl13 cells activated with TRAP (8 hours) and was comparable to proliferation seen using conditioned medium from the highly invasive MDA 435 cell line (Fig. 4II). When neutralizing anti-VEGF antibodies were applied during the proliferation assay, a significant inhibition was obtained. Nearly complete inhibition is seen at a 1:100 dilution of the antibodies; the effect decreases in a dose-dependent manner at greater

dilutions (Fig. 4 III). These data demonstrate that activated PAR1 expressing cells secrete high levels of functional VEGF.

**VEGF induction by *Par1* is mediated via PKC, PI3K and Src.** The phorbol ester PMA increased VEGF mRNA levels in Cl13 cells in a dose-dependent manner, with maximum induction achieved between 1 and 500 ng/ml (Fig. 5I). To determine whether PKC might play a role in PAR1-induced increases in VEGF, we used the potent PKC inhibitor, calphostin C. At concentrations of 500 ng/ml and higher, calphostin C potently blocked the TRAP-induced increase in VEGF mRNA in Cl13 cells (Fig. 5II). No effect was observed at a lower concentration (50 ng/ml). These data suggest that PKC plays a role in the induction of VEGF by PAR1. Specific inhibitors of two other kinases also inhibited the PAR1-dependent increase in VEGF expression in Cl13 cells. Wortmannin, a PI3K inhibitor, inhibited TRAP-induced increases in VEGF mRNA levels (Fig. 5III). In addition, PP-2, a potent Src inhibitor, also inhibited VEGF induction (Fig. 5IV ). These data point to essential roles for PKC, Src and PI3K in the molecular mechanisms underlying VEGF induction by PAR1.

**Transformation of NIH 3T3 cells by the oncogenes v-Ha-Ras, V-Src, or VavK49 induces VEGF mRNA.** To determine the effect of oncogenic transformation on VEGF expression, mRNA from transformed and control NIH3T3 cells was examined for VEGF transcripts (Fig. 6I). NIH3T3 cells were transfected with the active forms of *ras*, *src* or *vav*(K49) oncogenes, wild type (wt) *vav* protooncogene, or two different SH2 domain mutants of *vav* (W622R and R647L). *Ras, src,* and the oncogenic *vav* all have potent transforming capability. While the full-length *vav* proto-oncogene and the W622R *vav* mutant exhibit greatly reduced transforming

potential, the R647L *vav* mutant retains the transforming potential of the oncogene. As shown in Fig. 6I, a marked induction in VEGF mRNA expression was observed in the NIH3T3 cells transfected with *src* or the *vav* oncogene. However, only low levels of VEGF mRNA are induced in cells transfected with *ras* or the proto-oncogene *vav*, and no VEGF is detected when cells are transfected with *vav* W622R, the SH2 mutant with reduced transforming ability (Fig. 6I). Low levels of VEGF mRNA were present in cells transfected with vav R647L, which maintains its transforming capability (data not shown). These results suggest that cell transformation is sufficient to induce VEGF.

By performing RT-PCR with primers directed to exons 1 and 8 of the VEGF gene, we examined which VEGF splice forms are expressed in transformed cells. While control NIH 3T3 cells do not express any of the VEGF splice variants, *src*-transfected NIH 3T3 cells express VEGF121, 145, 165, and 189 but not VEGF 206 (Fig. 6III). The VEGF forms present in *src*-transformed NIH3T3 were similar to those found in activated (8 hours of TRAP) Cl13 cells.

## DISCUSSION

We have previously shown that *Par1* is a critical gene involved in tumor invasion and metastasis (10, 11). Here we wished to determine the involvement of PAR1 in tumor angiogenesis. Although the association between the protease thrombin and angiogenesis has been previously documented (49-51), dissection of the role of PAR1 in tumor angiogenesis and its mechanism of activation are largely unknown.

Our results provide a comprehensive analysis of PAR1 involvement in tumor angiogenesis. We demonstrate here the ability of *Par1* to elicit tumor angiogenesis both *in vivo* in animal models and *in vitro* (as shown by the endothelial tube forming assay and cell proliferation). In addition, *Par1* expression induces VEGF mRNA. The data indicate that while the expression of *Par1* is sufficient to induce VEGF levels, activation of the PAR1 protein and initiation of the cell signaling machinery greatly enhance expression of 4 VEGF splice forms; VEGF121, VEGF145, VEGF165 and VEGF189 but not VEGF 206. This correlates with an increase in effects on angiogenesis in the Matrigel plug assay and on endothelial tube formation and cell proliferation following activation of PAR1. The fact that a greater angiogenic response is seen in Matrigel plugs containing pre-activated *Par1*- expressing cells indicates that active recruitment of blood vessels take place early on, immediately following the introduction of the Matrigel plugs. These findings, together with our previous results on the increased invasion potential of *Par1*-overexpressing cells, strongly support a significant role for *Par1* in the two critical events in tumor progression, tumor invasion and angiogenesis (10,11).

Activation of PAR1 leads to synthesis and secretion of functional VEGF protein as indicated by our observation that conditioned medium from *Par1*-overexpressing cells increases BAEC proliferation and 3 dimensional tube forming assay *in vitro*. The growth promoting

activity of activated PAR1 is mediated by VEGF as demonstrated by the dramatic inhibition of *PAR1*-induced endothelial cell proliferation in the presence of neutralizing anti-VEGF antibodies. *Par1* expression induces 4 VEGF splice forms (VEGF121, VEGF145, VEGF165, VEGF189), which are markedly further induced following activation of PAR1 by thrombin or TRAP. This increase in VEGF mRNA is most likely due to stabilization of VEGF mRNA rather than enhanced transcription as documented recently by Haung and S. Karpatkin (51) and our data (not shown). It appears therefore, that *Par1* plays a dual role in the control of blood vessel formation. The expression of *Par1* in tumor cells is sufficient to induce VEGF expression levels, leading to endothelial cell proliferation and sprouting. In addition, *Par1* is required in endothelial cells for maturation and stabilization of the blood vessels (22).

Previous studies have shown that thrombin activates PKC, Src, PI3K, and MAPK (52-54). Our studies show the involvement of these signaling enzymes in PAR1-induced angiogenesis, since PP-2, a Src inhibitor, Wortmannin-a PI3K inhibitor and Calphostin C, a PKC inhibitor, all potently inhibited VEGF165 mRNA induction. Furthermore, oncogenic transformation of NIH3T3 cells with genes which participate in PAR1 signaling (e.g. *ras, src* or *vav;* 55-59) is sufficient to induce the same 4 VEGF splice forms seen in *Par1*-transfected tumor cells. PAR1 couples to different G-proteins and activates the tyrosine kinases Src and Fyn (56, 57, 60). Thrombin has been shown to induce tyrosine phosphorylation of the adaptor protein Shc, which is then recruited to Grb2 (60). It has been reported that a dominant negative Shc that is deficient in Grb2 binding capability suppresses thrombin-mediated activation of p44 MAP kinase and cell growth, highlighting out the importance of Shc in this pathway. In CCL-39 fibroblasts, thrombin activates p21 *ras* in a manner that is inhibited by pertussis toxin and the tyrosine kinase inhibitor genistein suggesting that activation of Ras involves both G-proteins and activation of protein

tyrosine kinases (61). Although the mechanism by which PAR1 couples to Ras is still unclear, it is likely that Src and Fyn activate Ras through the adaptor protein Shc in complex with Grb2 and SOSRas exchange factor (56, 57). It has been documented previously that activated forms of Ras induce VEGF gene expression in NIH 3T3 cells and primary endothelial cells ( 62, 63) - our results confirm and support these data. Vav activates GTP-binding proteins and is part of the PAR1 signaling cascade (64, 65); we now show that it also induces low levels of VEGF. The oncogenic form of *vav* induces high levels of VEGF. The fact that two SH2 mutants of Vav (R647L and W622R), both shown to be defective in their tyrosine phosphorylation properties, had different abilities to induce VEGF suggests a correlation between VEGF production and transforming potential (48, 66). The W622R mutant, which is defective in transforming properties, does not induce VEGF expression while R647L, which maintains its transforming potential, does.

Together, these data strongly support the notion that PAR1 expression and, more importantly, the initiation of the PAR1 signaling cascade are highly significant in eliciting tumor angiogenesis.

## REFERENCES

1. Ferrara, N., and Alitalo, K. (1999) Clinical application of angiogenic growth factor and their inhibitors. *Nature Med.* **5**, 1359-1364

2. Hynes, R.O., Bader, B.L., and Hodivala-Dilke, K.(1999) Integrins in vascular development. *Braz. J. Med. Biol.* Res. **32,** 501-510

3. Carmeliet, P., and Jain, R.K. (2000) Angiogenesis in cancer and other diseases. *Nature* **407**, 249-257

4. Folkman, J. (1971) Tumor angiogenic therapoeitic implications. *N. Engl. J. Med.* **285,** 1182-1186

5. Hanahan, D., and Folkman, J. (1996) Pattern and emerging mechanisms of angiogenic switch during tumorigenesis. *Cell* **86,** 353-364

6. Trousscau, A. (1872) *Lectures in Clinical Medicine, Delivered in Hotel-Dieu, paris. Pp 281-295. New Sydenham Society. London*

7. Rickles, F.R., and Edwards, R.L. (1983) Activation of blood coagulation in cancer: Trousseau's syndrome revisited. *Blood* **62**,14-31

8. Sloan, B.F., Rozhin, J., Johnson, K., Taylor, H., Crissman, J.D., and Honn, K.V. (1986) Cathepsin B: association with plasma membrane in metastatic tumors. *Proc. Natl. Acad. Sci. USA* **83,** 2483-2487

9. Zacharsky, L.R., Memoli, V.A., Morian, W.D., Schlaeppi, J.M., and Rousscau, S.M. (1995) Cellular localization of enzymatically active thrombin in intact human tissues by hirudin binding *Throm Haemostasis* **73,** 793-797

10. Even-Ram, S., Uziely, B., Cohen, P., Ginzburg, Y., Reich, R. Vlodavsky, I. and Bar-Shavit, R. (1998) Thrombin receptor overexpression in physiological and malignant invasion process. *Nature Medicine* **4,** 909-914

11. Cohen Even-Ram, S., Maoz, M., Pokroy, E., Reich, R. Katz, B-Z., Gutwein, P., Altevogt, P., and Bar-Shavit, R. (2001) Tumor cell invasion is promoted by activation of protease activated Receptor-1 in cooperation with $\alpha v\beta 5$ integrin. *J. Biol. Chem* **276,** 10952-10962

12. Vu, T-K., Hung, H.D.T., Wheaton V.I., and Coughlin, S.R. (1991) Molecular cloning of a functional thrombin receptor reveals a novel proteolytic mechanism of receptor activation. *Cell* **64,** 1057-1068

13. Rasmussen, U.B., Vouret-Craviari. V, Jallat, S., Schlesinger, Y., Pages, G., Pavirani, A., Lecocq, J.P., Pouyssegur, J., and Van Obberghen-Schilling, E. (1991) cDNA cloning and expression of a hamster $\alpha$-thrombin receptor coupled to $Ca^{+2}$ mobilization. *FEBS Lett* **288,** 123-128

14. Martin, C.B., Mahon, G.M., Klinger, M.B., Kay, R.J., Symons, M., Der, C.J., and Whitehead, I.P. (2001) The thrombin receptor, PAR-1, causes transformation by activation of Rho-mediated signaling pathways. *Oncogene* **20,** 1953-1963

15. Connolly, A.J., Ishihara, H., Kahn, M.L.,Fares,Jr. R.V., and Coughlin, S.R. (1996) Role of the thrombin receptor in development and evidence for a second receptor. *Nature* **381,** 516-519

16. Bugge, T.H., Xiao, Q., Kombrinck, K.W., Flick, M.J., Holmback, K., Danton, M.J., Colbert, M.C., Witte, D.P., Fujikawa, K., Davie, E.W., and Degen, J.L. (1996) Fatal

embryonic bleeding events in mice lacking tissue factor, the cell-associated initiator of blood coagulation. *Proc. Natl. Acad. Sci. USA* **93,** 6258-6263

17. Carmeliet, P., Ferreira, V., Breier, G., Pollefeyt, S., Kieckens, L., Gertsenstein, M., Fahrig, M., Vandenhoeck, A., Harpal, K., Eberhardt, C., Declercq, C., Pawling, J., Moons, L., Collen, D., Risau,, W., and Nagy, A. (1996) Abnormal blood vessel development and lethality in embryos lacking a single VEGF allele. *Nature* **380,** 435-439

18. Toomey, J.R., Kratzer, K.E., Lasky, N.M., Stanton, J.J., and Broze, Jr. G.J. (1996) Targeted disruption of the murine tissue factor gene results in embryonic lethality. *Blood* **88,** 1583-1587

19. Cui, J., O'Shea, K.S.M., Purkayastha, A., Saunders, T.L, and Ginsburg, D. (1996) Fatal haemorrhage and incomplete block to embryogenesis in mice lacking coagulation factor V. *Nature* **384,** 66-68

20. Sun, W.Y., Witte, D.P., Degen, J.L., Colbert, M.C., Burkart, M.C., Holmback K, Xiao Q, Bugge TH, and Degen SJ. (1998) Prothrombin deficiency results in embryonic and neonatal lethality in mice.*Proc. Natl. Acad. Sci. USA*. **95,** 7597-7602

21. Xue, J., Wu, Q., Westfield, L.A., Tuley, E.A., Lu, D., Zhang, Q., Shim, K., Zheng, X., and Sadler, J.E. (1998) Incomplete embryonic lethality and fatal neonatal hemorrhage caused by prothrombin deficiency in mice. *Proc. Natl Acad. Sci.* USA **95**, 7603-7607

22. Griffin, C.T., Snirivasan, Y., Zheng, Y-W., Haung, W., and Coughlin, S.R. (2001) A role for thrombin receptor signaling in endothelial cells during embryonic development. *Nature* **293,** 1666-1670

23. Preissner, K.T., Nawroth, P.P., and Kanse, S.M. (2000) Vascular protease receptors: integrating haemostasis and endothelial cell functions. *J. Pathol.* **190,** 360-372

24. Carmeliet, P. ( 2001) Clotting factors build blood vessels. *Science* **293,** 1602-1604

25. Shibuya, M., Yamaguchi, S., Yamane, A., Ikeda, T., Tojo, A., Matsushime, H., and Sato, M. (1990) Nucleotide sequence and expression of a novel human receptor-type tyrosine kinase gene (flt) closely related to the fms family. *Oncogene* **5,** 519-524

26. Terman, B.I., Carrion, M.E., Kovacs, E., rasmussen, B.A., Eddy, R.L., and Shows, T.B. (1991) Identification of a new endothelial cell growth factor receptor tyrosine kinase. *Oncogene* **6,** 1677-1683

27. Neufeld, G., Cohen, T., Gengrinovitch, S., and Poltorak, Z. (1999) Vascular endothelial growth factor (VEGF) and its receptors. *FASEB J* **13,** 9-22.

28. Kim, K.J., Li, B., Winer, J., Armanini, M., Gillett, N., Phillips, H.S., and Ferrara, N. (1993) Inhibition of vascular endothelial growth factor-induced angiogenesis suppresses tumour growth in vivo. *Nature* **362,** 841-844

29. Millauer, B., Shawver, L.K., Plate, K.H., Risau, W., and Ullrich, A. (1994) Glioblastoma growth inhibited in vivo by a dominant-negative Flk-1 mutant. *Nature* **367,** 576-579

30. Carmeliet, P., Ferreira, V., Breier, G., Pollefeyt, S., Kieckens, L., Gertsenstein, M., Fahrig, M., Vandenhoeck, A., Harpal, K., Eberhardt, C., Declercq, C., Pawling, J., Moons, L., Collen, D., Risau, W., and Nagy, A. (1996) Abnormal blood vessel development and letality in embryos lacking a single VEGF allele. *Nature* **380,** 435-439

31. Shalaby, F., Ho, J., Stanford, W.L., Fischer, K.D., Schuh, A.C,, Schwartz, L., Bernstein, A., and Rossant, J. (1997) A requirement for Flk1 in primitive and definitive hematopoiesis and vasculogenesis. *Cell* **89**, 981-90

32. Fong, G.H., Rossant, J., Gertsenstein, M., and Breitman, M.L. (1995) Role of Flt-1 receptor tyrosine kinase in regulating the assembly of vascular endothelium. *Nature* **376,** 66-70

33. Shweiki, D., Itin, A., Soffer, D., and Keshet, E. (1992) Vascular endothelial growth factor induced by hypoxia may mediate hypoxia-initiated angiogenesis. *Nature* **359**, 843-845

34. Plate, K.H., Breier, G., Weich, H.A., and Risau, W. (1992) Vascular endothelial growth factor is a potent tumor angiogenesis factor in human gliomas *in vivo*. *Nature* **359**, 845-848

35. Leung, D.W., Cachianes, G., Kuang, W.J., Goddel, D.V., and Ferrara, N. (1989) Vascular endothelial growth factor is a secreted angiogenic mitogen. *Science* **246**,1306-1309

36. Tischer, E., Gospadorowicz, D., Mitchell, R., Silva, M., Schilling, J., Lau, K., Crisp, T., Fiddes, J.C., and Abraham, J.A. (1989) Vascular endothelial growth factor: a new member of the platelet - derived growth gene family. *Bichem. Biophys. Res. Commun.* **165,** 1198-1206

37. Benjamin, L.E., Golijanin, D., Itin, A., Pode, D., and Keshet, E. (1999) Selective ablation of immature blood vessels in established human tumors follows vascular endothelial growth factor withdrawal. *J Clin Invest* **103,** 157-8

38. Keck, P. J., Hauser, S,D., Krivi, G., Sanzo, K., warren, T., Feder, J., and Connolly, D.T. (1989) Vascular permeability factor, an endothelial cell mitogen related to PDGF. *Science* **246**, 1309-1312

39. Houck, K.A., Ferrara, N., Winer, J., Cachiaes, G., Li, B., and Leung, D.W. (1991) The vascular endothelial growth factor family-identification of a fourth molecular species and characterization of a alternative splicing RNA. *Mol Endocrinol.* **5,** 1806-1814

40. Cohen, T., Gitay-Goren, H., Sharon, R., Shibuya, M., Halaban, R., Levi, B., and Nefeld, G. (1995) VEGF121, a vascular endothelial growth factor isoform lacking heparin binding ability, requires cell surface heparan sulfates for efficient binding to the VEGF receptors of human melanoma cells. *J. Biol. Chem.* **270,** 11322-11326

41. Park, J.E., Keller, G.A., and Ferrara, N. (1993) Vascular endothelial growth factor (VEGF) isoforms - differential deposition into the subepithelial eextracellular matrix and bioactivity of extracellular matrix –bound VEGF. *Mol. Biol. Cell* **4,**1317-1326

42. Poltorak, Z., Cohen, T., Sivan, R., Kandelis, Y., Spira, G., Vlodavsky, I., Keshet, E., and Neufeld, G. (1997) VEGF 145: a secreted VEGF form that binds to extracellular matrix. *J. Biol. Chem.* **272,** 7151-7158

43. Schnaper, H.W., Grant, D.S., Stetler-Stevenson, W.G., Fridman, R., D'Orazi, G., Murphy, A.N., Bird, R.E., Hoytha, M., Fuerst, T. R., French, D.L., et al. (1993) type IV collagenase(s) and TIMPs modulate endothelial cell morphogenesis in vitro. *J Cell. Physiol.* **156,** 235-246

44. Passaniti, A., Taylor, R.M., Pili, R., Guo, Y., Long, P.V., Haney, J.A., Pauly, R. R., Grants, D.S., and Martin, G.R. (1992) A simple, quantitative method for assessing angiogenesis and antiangiogenic agents using reconstituted basement membrane, heparin, and fibroblast growth factor. *Lab Invest.* **67**, 519-528

45. Itoh, T., Tanioka, M., Yoshida, H., Yoshioka, T., Nishimoto, H., and Itohara, S. (1998) Reduced angiogenesis and tumor progression in gelatinase A-deficient mice. Cancer Res. **58**,1048-1051

46. Fiedler, W., Graeven, U., Ergun, S., Verago, S., Kilic, N., Stockschlader, M., Hossfeld, D. K. (1997) Vascular endothelial growth factor, a possible paracrine growth factor in human acute myeloid leukemia. *Blood* **89,** 1870-1875

47. Miao, H-Q., Lee, P., Lin, H., Soker, S., and Klagsbrun, M. (2000) Neuropilin-1 expression by tumor cells promotes tumor angiogenesis and progression. *FASEB J* **14,** 2532-2539

48. Katzav, S. (1993) single point mutation in the SH2 domain impair the transforming potential of *vav* and fail to activate proto-*vav*. *Oncogene* ***8,*** 1757-1763

49. Tsopanoglou, N.E., and Maragoudakis, M.E. (1999) On the mechanism of thrombin-induced angiogenesis. *J. Biol Chem.* **274,** 23969-23976

50. Richard, D.E., Vouret-Craviari, V., and Pouyssegur, J. (2001) Angiogenesis and G-protein coupled receptors:signals and bridge the gap. *Oncogene* **20,**1556-1562

51. Huang, Y-Q., Li, J-J., Hu, L., Lee, M., and Karpatkin, S. (2001) Thrombin induces increased expression and secretion of VEGF from human FS4 fibroblasts, DU145 prostate cells and CHRF megakaryocytes. *Throm. Haemst.* **86,** 1094-1098

52. Carter, A.N., Haung, R., Sorisk, A., Downes, C.P., and Rittenhouse, S.E., (1994) Phosphatidylinositol 3,4,5-triphosphate is formed from phosphatidylinositol 4,5-bis-phosphate in thrombin –stimulated platelets. *Biocem J* **310,** 415-420

53. Gutkind, J.S., Lacal, P.M., and Robbins, K.C. (1990) Thrombin-dependent association of phosphatidylinositol –3-kinase with p60c-src and p59fyn in human platelets. *Mol. Cell. Biol.* **10,** 3806-3809

54. Leach, K., L., Ruff, V.A., Jarpe, M.B., Adams, L.D., Fabbro, D., and Raben, D.M., (1992) Alpha thrombin stimulates nuclear localization of protein kinse C isozyme in IIC9 cells. *J. Biol. Chem.* **267,** 21816-21822

*55.* Cichowsky, K., Brugge, J.S., and Brass, L.F. (1996) Thrombin receptor activation and integrin engagement stimulate tyrosine phosphorylation of the proto-oncogene product, p95vav, in platelets. *J. Biol. Chem.* **271,** 7544-7550

56. Chen, Y-H., Pouyssegur, J., Coutridge, S.A., and van Obberghen-Schilling, E. (1994) Activation of Src family kinase activity by the G protein-coupled thrombin receptor in growth-responsive fibroblasts. *J. Biol. Chem.* **269,** 27372-27377

57. Chen, Y., Grall, D., Salcini, A.E., Pelicci, P.G., Pouyssegur, J., and Van Obberghen-Schilling, E. (1996) Shc adaptor proteins are key transducers of mitogenic signaling mediated by the G protein-coupled thrombin receptor. *EMBO J* **15,** 1037-1044

58. Shock, D.D., He, K., Wencel-Drake, J.D., and Parise, L.V (1997) Ras activation in platelets after stimulation of the thrombin receptor, thromboxane A2 receptor or prote. *Biochem J* **321**, 526-530

*59.* Collins, L.R., Rickets, W. A., Olefsky, J. M., and Brown, J.H. (1997) The G12 coupled thrombin receptor stimulates mitogenesis through the Shc SH2 domain. *Oncogene* **15,** 595-600

60. Maulon, L., Mari, B., Bertolotto, C., Ricci, J.E., Luciano, F., Belhacene, N., Deckert, M, Baier, G., and Auberger, P. (2001) Differential requirements for ERK1/2 and P38 MAPK activation by thrombin in T cells. Role of P59Fyn and PKC epsilon. *Oncogene* **20,** 1964-1972

61. Ricketts, W., Brown, J.H., and Olefsky, J. M. (1999) Pertussis toxin-sensitive and -insensitive thrombin stimulation of Shc phosphorylation and mitogenesis are mediated through distinct pathways. *Mol. Endocrinol.* **13,** 1988-2001

62. Grugel, S., Finkenzeller, G., Weindel, K., Barleon, B. and Marme, D. (1995) Endothelial Growth factor in NIH 3T3 cells. *J Biol. Chem.* **270,** 25915-25919

63. Meadows, K.N., Bryant, P., and Pumiglia, K. (2001) Vascular endothelial growth factor induction of the angiogenic phenotype requires Ras activation. *J. Biol. Chem.* **276,** 49289-4929

64. Bar-Shavit, R,, Maoz, M., Yongjun, Y., Groysman, M., Dekel, I. And Katzav, S. (2000) Signalling pathways induced by protease-activated receptors and integrins in T cells. *Immunology* **105,** 35-46

65. Landau E, Tirosh R, Pinson A, Banai S, Even-Ram S, Maoz M, Katzav S, Bar-Shavit R.(2000) Protection of thrombin receptor expression under hypoxia. *J Biol Chem* **275(4),** 2281-7

*66.* Katzav, S., Packham, G., Sutherland, M., Aroca,P., Santos, E., and Cleavland, J.L. (1995) Vav and ras induce fibroblast transformation by overlapping signaling pathways which require c-Myc function. *Oncogene* **11,** 1079-1088

**LEGENDS**

**Figure 1. *Par1* induces angiogenesis *in vivo*.** Matrigel plugs containing Cl13 (SB-2 cells stably transfected with *Par1)* or non-transfected SB-2 cells were injected *s.c.* into the peritoneal cavity of BALB/c mice in a bilateral fashion. Mice were divided into four groups dependent on the nature of the injected cells: Group A (n=9) untreated SB-2 cells; Group B (n=8) SB-2 cells treated with TRAP (100μM, 8 hours); Group C (n=11) untreated Cl13 cells; and Group D (n=12) Cl13 cells treated with TRAP (100μM, 8 hours). **I. Matrigel plugs under phase microscopy.** 10 days after *in vivo* implantation, Matrigel plugs were removed and examined. Matrigel containing SB-2 cells remained pale (A). The appearance of the Matrigel plugs containing SB-2 cells pretreated with TRAP was not significantly different (B). Matrigel plugs containing Cl13 cells exhibited a reddish color (C), which was more pronounced in Cl13 cells pretreated with TRAP (D). Magnification 5X. **II. Histolgical evaluation of Matrigel plugs.** Serial sections were prepared from Matrigel plugs, and processed with Mallory's stain. A. Untreated SB-2 cells B. SB-2 cells pretreated with TRAP C. Untreated Cl13 cells D. Cl13 cells pretreated with TRAP. Magnification X 20.

**III. Quantification of capillary vessels in Matrigel plugs.** Six separate fields of each Matrigel plug stained with H&E and Mallory's' Stain were examined under phase microscopy and capillary vessels were counted. Data shown are representative of at least 3 independent Matrigel plug sets of experiments.

**Figure 2. Inducible *Par1* expression in rat prostatic carcinoma increases tumor mass and angiogenesis. I.** Differential expression of *Par1* in the Dunning rat prostate carcinoma cell variants was observed by RT-PCR using primers specific for PAR1. Primers for L19 were used as a loading control. **II.** Inducible *Par1* expression in a rat prostatic carcinoma cell line - AT2.1. AT2.1 cells were transfected with a plasmid containing the human *Par1* coding sequence under the control of a tet-inducible promoter. Two stably transfected clones, AT2.1/Tet-On/*hPar1* clones 4 and 1, were tested for the inducibility of human *Par1* expression by the tetracycline analog, Dox as evaluated by Northern blot analysis. **III.** AT2.1/Tet-On/*hPar1* clone 4 cells and

control transfected (vector only) cells were injected into rats *s.c.* Animals were maintained for 2 weeks with regular drinking water or drinking water supplemented with Dox. After 2 weeks, the tumors were excised and examined. Tumors shown were from animals injected with: A. control transfected cells; B. AT2.1/Tet-On/*hPar1*, clone 4; C. AT2.1/Tet-On/*hPar1* clone 4, fed with Dox for 2 weeks. **VI**. Tumor weight. Data shown are the mean at least 3 independent sets of experiments.

**Figure 3. Expression of VEGF isoforms by stable *Par1*-transfected clones. I. Northern blot analysis of VEGF expression**. Total RNA was prepared from SB-2 cells (A), SB-2 cells transfected with an empty expression vector (B), and two clones stably expressing PAR1: Cl13 (C) and MixL(D). The Northern blot was hybridized with a probe specific for $VEGF_{165}$. The bottom panel shows hybridization to the housekeeping gene L32, as a control for RNA loading. **II. Kinetics of VEGF165 mRNA induction following activation of PAR1.** Cl13 or SB-2 cells were treated with Thrombin (1u/ml) or TRAP (100μM) for the indicated times and RNA levels were analyzed by Northern blot. **III. Dose response of VEGF165 mRNA induction by TRAP.** Cl13 cells were treated with the indicated doses of TRAP for 8 hours. RNA was analyzed by Northern blot. **IV. RT-PCR for the detection of VEGF splice forms in *Par1* transfected cells.** RT-PCR was performed using primers directed to exons 1 and 8 to detect all splice forms. Four different splice forms are detected in Cl13 cells: $VEGF_{121}$, $VEGF_{145}$, $VEGF_{165}$, and $VEGF_{189}$. None, or very little, is seen in non- transfected (SB-2) cells, cells transfected with empty vector (SB-2 Vector) and non-metastatic cells (MCF7). The pattern of expression of *Par1* splice forms in TRAP- or thrombin-activated Cl13 cells is similar to that in highly metastatic cells (MDA435).

**Figure 4. PAR1 activity induces functional VEGF. I. Conditioned medium from Cl13 cells increases the complexity of cell tube formation**. Cultures of endothelial cells in a three-dimensional collagen type I matrix were grown with conditioned media from: A) Non metastatic MCF7 cells transfected with an empty vector; B) Non metastatic MCF7 cells /empty vector cells

treated with thrombin; C) control, non metastatic MCF7 cells; D) *Par1* transfected MCF7 cells; E) *Par1* transfected MCF7 cells treated with thrombin; or F) highly metastatic MDA435 cells. **II.**

**Conditioned media from *Par1* transfected cells induce the proliferation of BAEC.** BAEC cells were cultured in the presence of conditioned medium from the indicated cells. Cultures were refed with fresh conditioned medium every two days. At each indicated time point, cells were removed from plates with trypsin/EDTA and counted. The data exhibit a typical experiment representing triplicates. **III. Anti-VEGF antibodies inhibit the effects of activated *PAR1* cell conditioned medium on BAEC proliferation.** BAECs were cultured in the presence of conditioned medium from activated Cl13 cells (TRAP, 8 hours) Anti-VEGF antibodies were added to cultures at varying concentrations as indicated and were present for the entire period of the assay. The effects of conditioned medium from control SB-2 cells and the highly metastatic MDA435 line are shown for comparison.

**Figure 5. Induction of VEGF by PAR1 is mediated by PKC, PI3K and Src.**
**I. Dose response of VEGF mRNA induction by PMA.** Various concentrations of PMA were added to cultures of Cl13 cells and VEGF mRNA levels were determined by Northern blot. RNA from non-transfected, non-metastatic cells was included as a control (lane A). **II. Calphostin C inhibits PAR1-induced increases in VEGF mRNA.** Calphostin C was added to Cl13 cultures at the indicated concentrations 30 minutes prior to addition of TRAP. Cells were harvested after 8 hours of TRAP/ calphostin treatment and VEGF mRNA levels were determined by Northen blot. **III. Wortmannin , a PI3K inhibitor, blocks PAR1-induced increases in VEGF mRNA .** Inhbition by Wortmannin is observed at 1μM (F) and up to 10 μM (G) but not at 0.1 μM (E). **IV. PP-2, an inhibitor of Src, blocks PAR1-induced increases inVEGF mRNA.** Inhbition of VEGF is observed at 10 μM (B), 1 μM (C) as compared to *Par1* transfected cells (A) and parental non transfected cells (G).

**Figure 6. Expression of VEGF mRNA splice forms in *ras*-, *src* -and *vav*-transformed NIH3T3 cells. I. Northern blot analysis of transformed NIH 3T3.** NIH 3T3 cells were

transfected with activated *ras* or *src* oncogenes, wild type (w.t.) *vav* proto-oncogene, oncogenic *vav* or an SH2 mutant of *vav*. Total RNA was isolated and 15μg were analyzed by Northern blotting using a probe for $VEGF_{165}$. **II. Quantitation of changes in VEGF mRNA levels in transformed cells.** Photoimage was used to quantitate VEGF165 mRNA levels from Northern blots. VEGF165 mRNA levels were normalized to β-actin mRNA levels to control for loading differences. Data shown are representative of 3 independent experiments. **III. RT-PCR analysis of VEGF splice forms.** A representative RT-PCR experiment shows elevated levels of $VEGF_{121}$, $VEGF_{145}$, $VEGF_{165}$ and $VEGF_{189}$ splice forms in *src*-transformed NIH3T3 cells. *Par1* transfected/activated cells (Cl13/TRAP/8h) and non-transfected SB-2 cells are included as positive and negative controls.

**ACKNOWLEDGEMENTS**

We are grateful to Dr. H. Kleinman (NIDR, NIH, Bethesda, MD) for kindly providing Matrigel and Dr. Hua-Quan Miao (Imclone systems, Inc., new York, NY 10014) for the AT2.1/Tet – On clone. This work was supported by grants from the Israel Science Foundation founded by the Israel Academy of Sciences and Humanities and by the U.S. Army Medical Research (R.B.S.).

**Fig. 1**

**I.**

**II.**

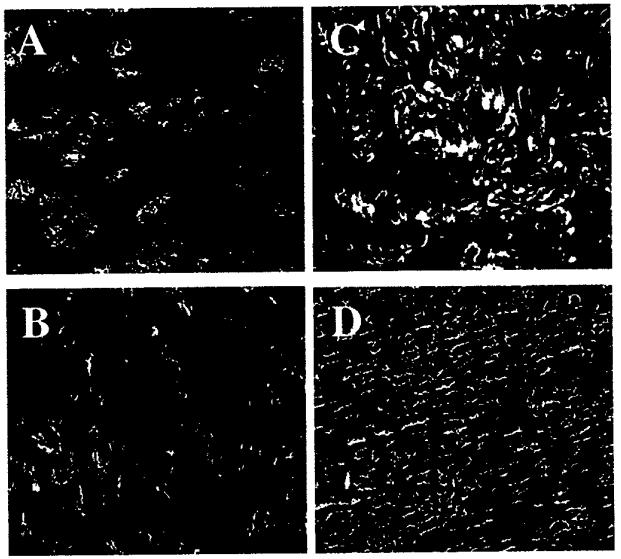


**III.**

**Vessel density analysis in Matrigel micropocket experiment**

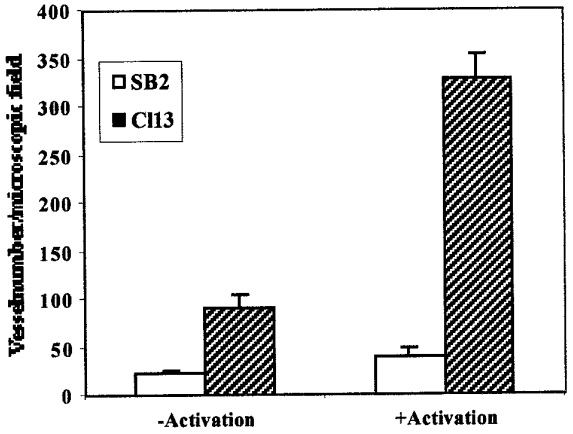

Fig. 2

I.

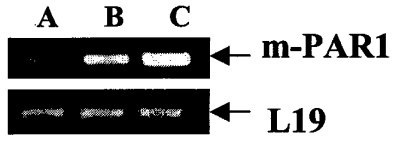


A- AT2.1
B- AT3.1
C- Baf 210

III.

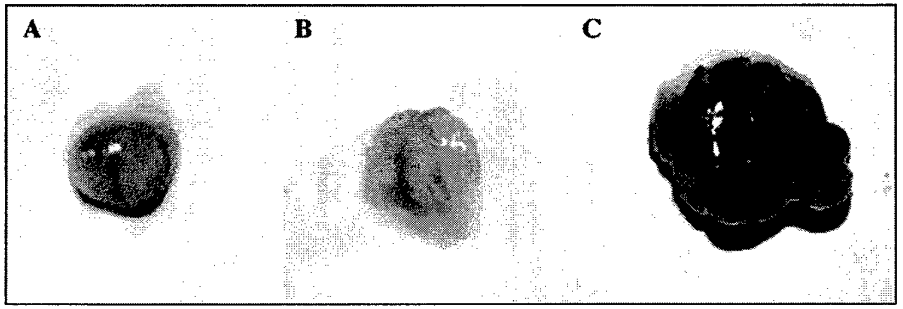


II.

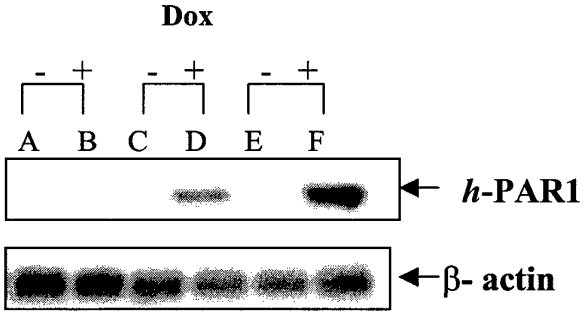


A- AT2.1/cont/ non induced
B- AT2.1/cont/ induced by Dox
C- Clone 1/PAR1/ non induced
D- Clone 1 /PAR1/ induced by Dox
E- Clone 4 /PAR1/ non induced
F- Clone 4 /PAR1/ induced by Dox

IV.

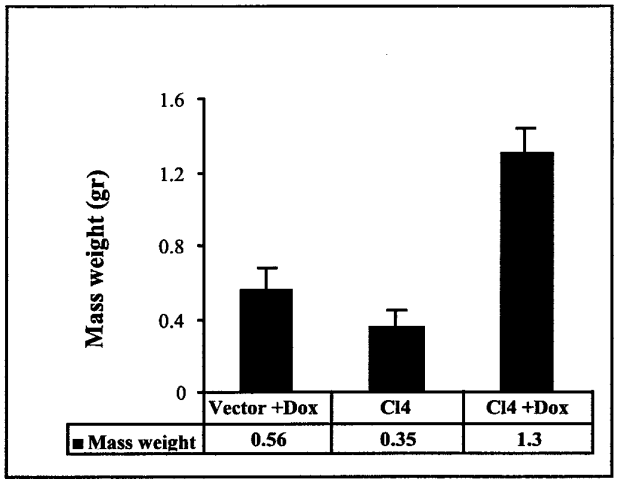

Fig. 3

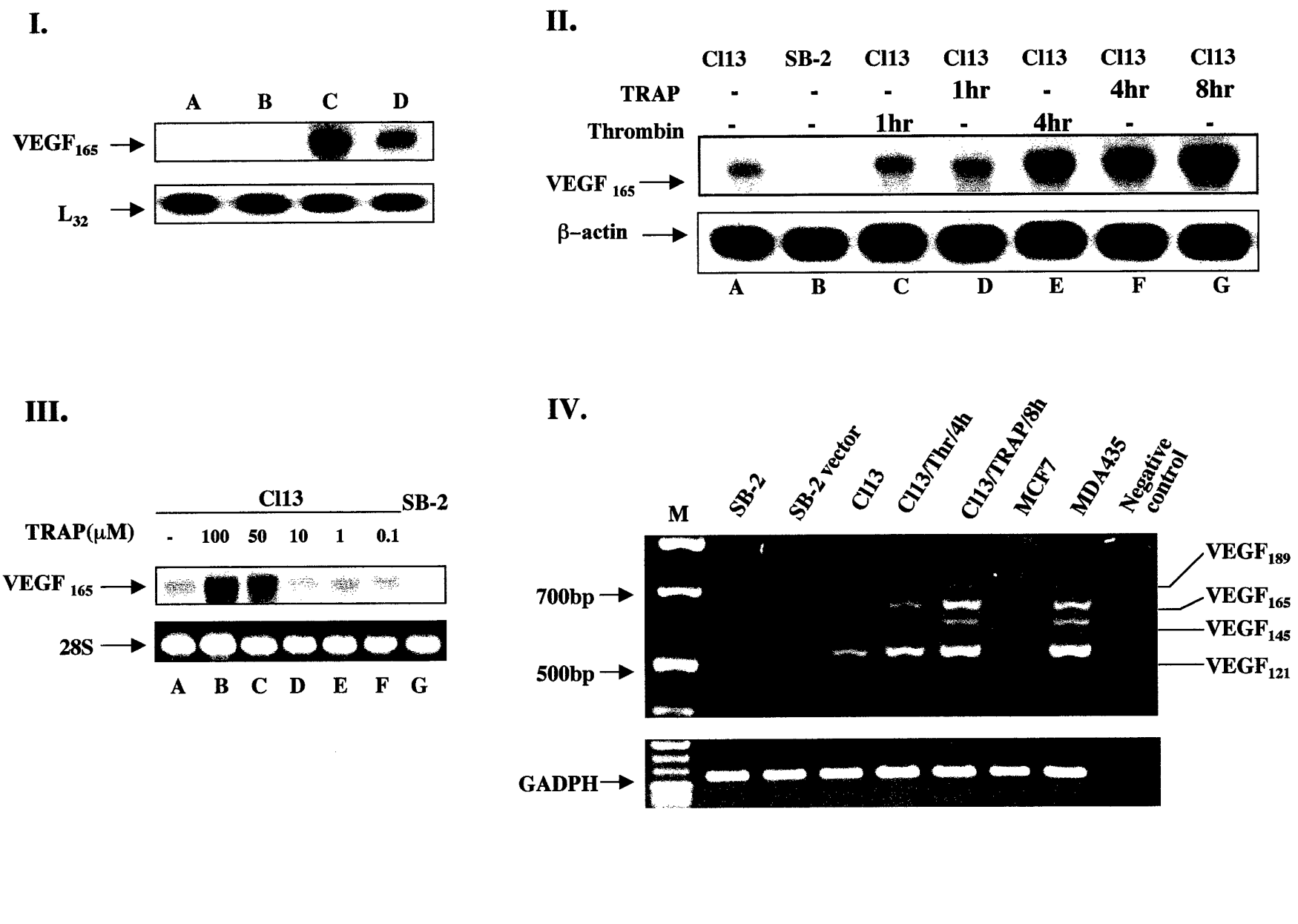
I.
A
B
C
D
VEGF165
L32
II.
Cl13
SB-2
Cl13
Cl13
Cl13
Cl13
Cl13
TRAP
-
-
-
1hr
-
4hr
8hr
Thrombin
-
-
1hr
-
4hr
-
-
VEGF 165
β-actin
A
B
C
D
E
F
G
III.
Cl13
SB-2
TRAP(μM)
-
100
50
10
1
0.1
VEGF 165
28S
A
B
C
D
E
F
G
IV.
M
SB-2
SB-2 vector
Cl13
Cl13/Thr/4h
Cl13/TRAP/8h
MCF7
MDA435
Negative control
700bp
500bp
GADPH
VEGF189
VEGF165
VEGF145
VEGF121

**Fig. 4**

**I.**

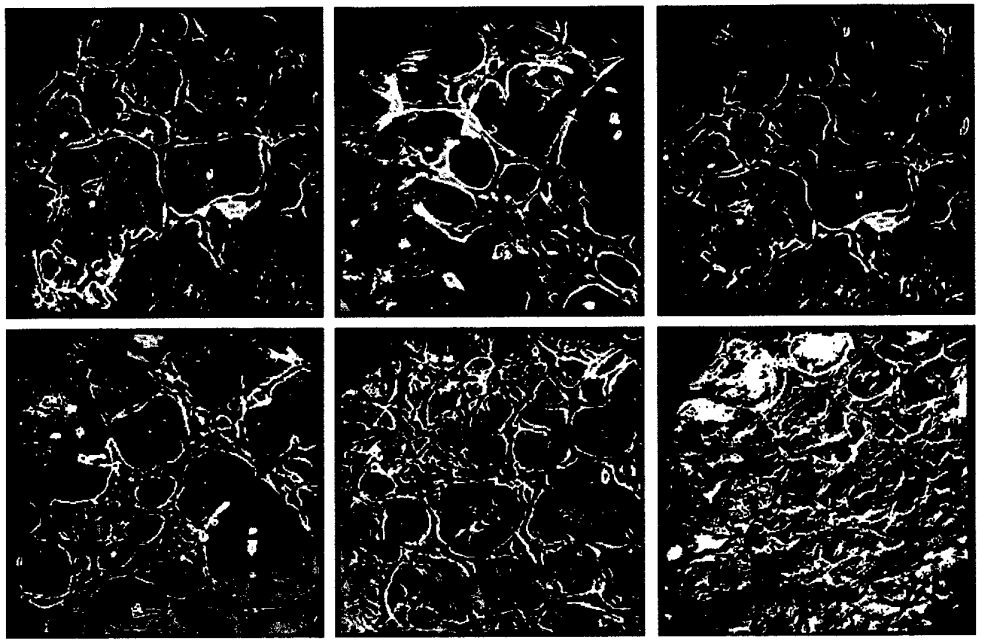

A. CM-Vector

B. CM-Vector+Thr

C. CM-non metastic MCF7

D. CM-MCF7 F.L

E. CM- MCF7 F.L+Thr

F. CM-highly metastic MDA435

**II.**

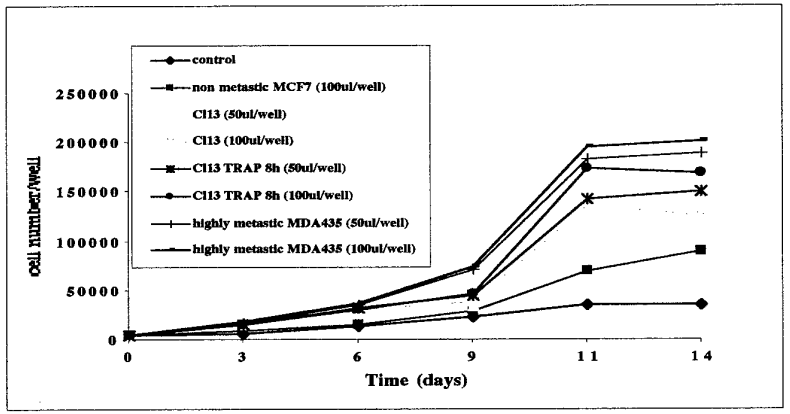


**III.**

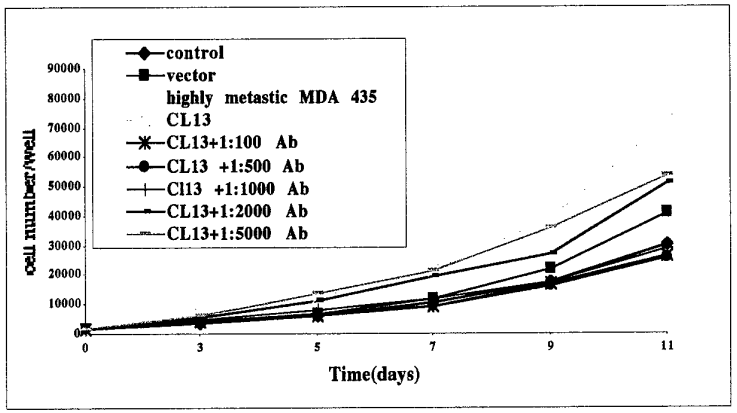

Fig. 5

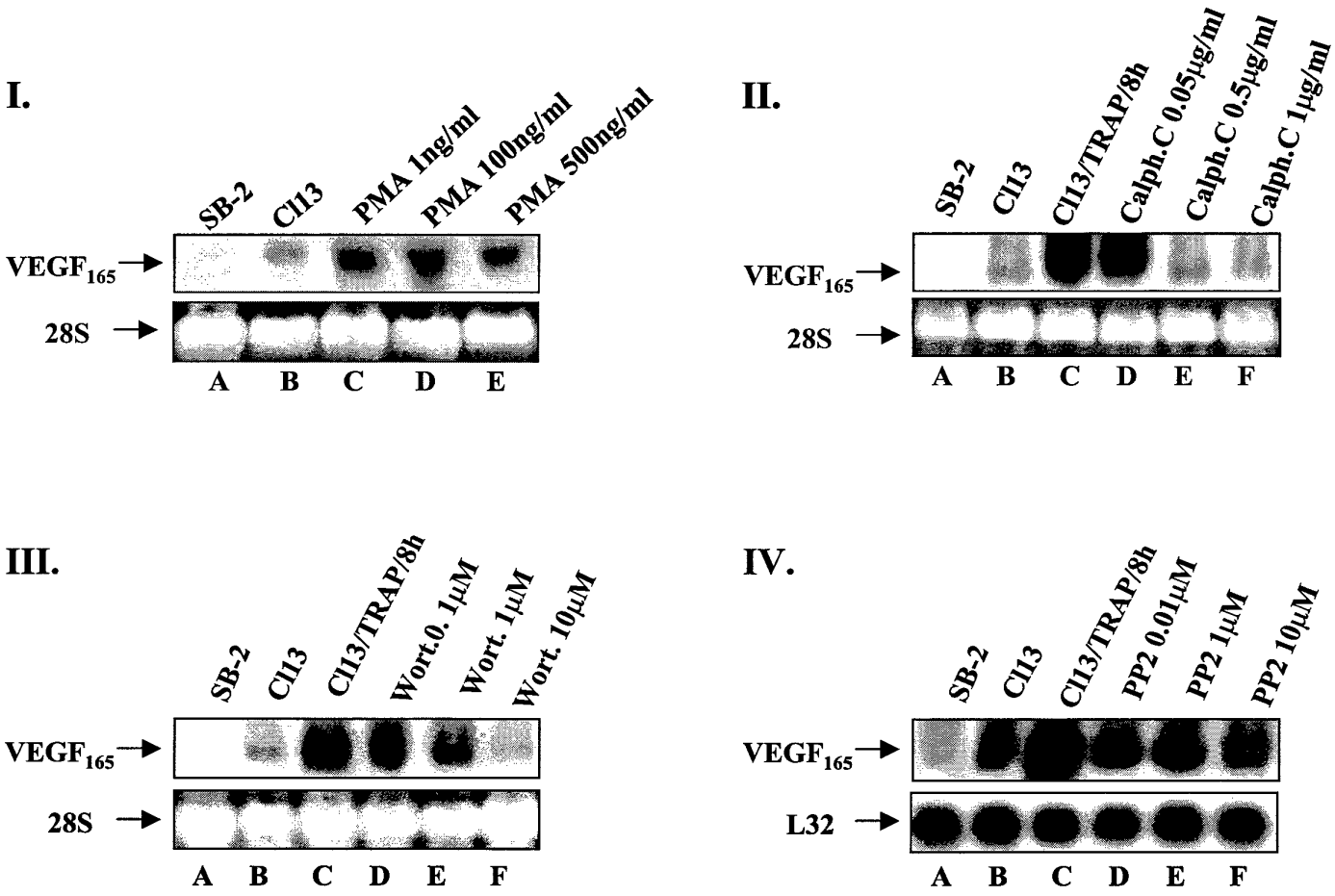
I.
SB-2
Cl13
PMA 1ng/ml
PMA 100ng/ml
PMA 500ng/ml
VEGF165
28S
A B C D E
II.
SB-2
Cl13
Cl13/TRAP/8h
Calph.C 0.05μg/ml
Calph.C 0.5μg/ml
Calph.C 1μg/ml
VEGF165
28S
A B C D E F
III.
SB-2
Cl13
Cl13/TRAP/8h
Wort.0. 1μM
Wort. 1μM
Wort. 10μM
VEGF165
28S
A B C D E F
IV.
SB-2
Cl13
Cl13/TRAP/8h
PP2 0.01μM
PP2 1μM
PP2 10μM
VEGF165
L32
A B C D E F

Fig. 6

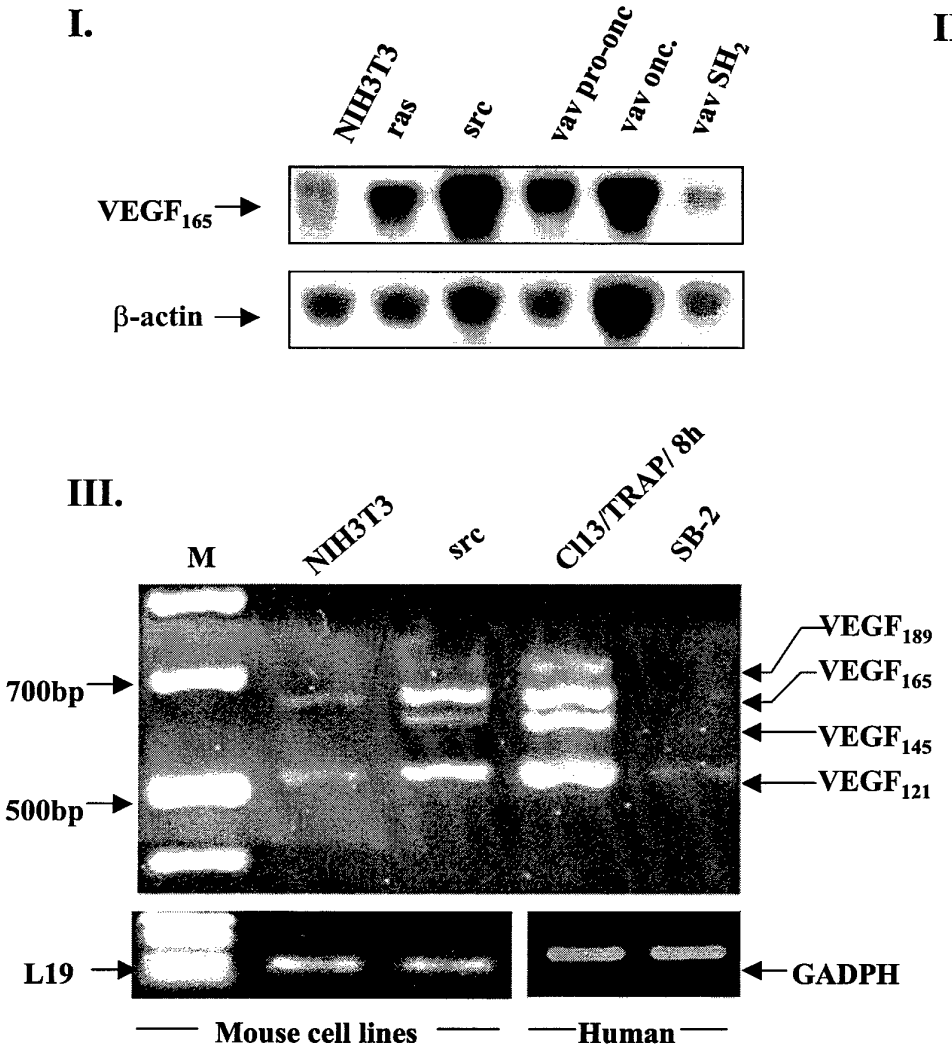
I.
NIH3T3
ras
src
vav pro-onc
vav onc.
vav SH2
VEGF165
β-actin
III.
M
NIH3T3
src
Cl13/TRAP/8h
SB-2
700bp
500bp
VEGF189
VEGF165
VEGF145
VEGF121
L19
GADPH
Mouse cell lines
Human

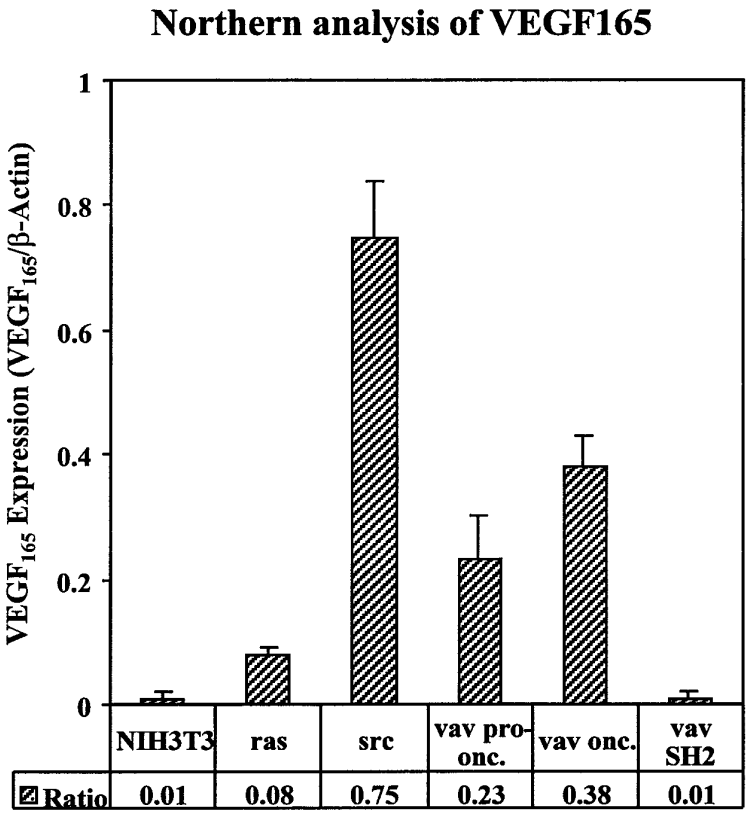
II.
Northern analysis of VEGF165
VEGF165 Expression (VEGF165/β-Actin)
1
0.8
0.6
0.4
0.2
0
NIH3T3
ras
src
vav pro-onc.
vav onc.
vav SH2
Ratio
0.01
0.08
0.75
0.23
0.38
0.01